THESIS SUBMITTED FOR THE DEGREE OF DOCTOR OF COMPUTER ENGINEERING, AUTOMATION AND SIGNAL PROCESSING

From Lille University

Multi-level risk and collective perception for high quality of service automated mobility in a highly dynamic V2X connected environment

Presented and defended by

Sabrine BELMEKKI

03/04/2023

Reviewers:
Sebastien Glaser, jury president, Full Professor, Queensland University-QUT
Redouane Khemmar, Associate professor, ESIGELEC and IRSEEM

Examiners:
Léo Mendiboure , Researcher, University of Gustave Eiffel
Lylia Alouache, Associate professor, CY Cergy Paris University

Supervisors:
Charles TATKEU, Research Director, University of Gustave Eiffel
Dominique GRUYER, Research Director, University of Gustave Eiffel

Doctoral school: MADIS doctoral school

Reasearch units :
LEOST Laboratory - COSYS unit - Gustave Eiffel University
PICS-L Laboratory - COSYS unit - Gustave Eiffel University

Thèse présentée en vue de l'obtention du diplôme de docteur en génie informatique, automatique et traitement du signal

De l'Université de Lille

Risque multi-niveaux et perception collective pour une mobilité automatisée à haute qualité de service dans un environnement connecté V2X dynamique

Présentée et soutenue par

Sabrine BELMEKKI

03/04/2023

Rapporteurs:
Sebastien Glaser, président du jury, Professeur, Université du Queensland
Redouane Khemmar, Enseignant-Chercheur, ESIGELEC et IRSEEM

Examinateurs:
Léo Mendiboure , Chargé de recherche, Université de Gustave Eiffel
Lylia Alouache, Enseignante-Chercheure, CY Cergy Paris Université

Directeurs:
Charles TATKEU, Directeur de recherche, Université Gustave Eiffel
Dominique GRUYER, Directeur de recherche, Université Gustave Eiffel

École doctorale: École doctorale MADIS

Unités de recherche :
Laboratoire LEOST - Unité COSYS - Université Gustave Eiffel
Laboratoire PICS-L - Unité COSYS - Université Gustave Eiffel

Remerciements

Je suis remplie d'une profonde reconnaissance envers Dieu pour m'avoir accordé la patience, la persévérance et la force nécessaires pour surmonter les obstacles et atteindre mes objectifs. Chaque jour, je suis reconnaissante pour les bénédictions innombrables qu'il a généreusement répandues dans ma vie, même à travers les défis qui m'ont aidé à grandir et à apprendre.

Yuri Milner a si justement dit: *"Nous ne sommes pas seuls dans nos succès et nous ne sommes pas seuls dans nos échecs."*

Cette citation résonne profondément en moi, et je souhaite exprimer ma profonde gratitude envers ceux qui ont contribué à mon parcours.
C'est pour cela que je tiens à exprimer ma profonde gratitude, tout d'abord au laboratoire LEOST de l'unité de recherche COSYS à l'université Gustave Eiffel qui a financé mes recherches. Merci à mes directeurs de recherche, Charles Tatkeu et Dominique Gruyer, d'avoir porté un regard critique et constructif sur mon travail et de m'avoir fait bénéficier de leur expérience en recherche académique.
Je souhaite également exprimer ma reconnaissance envers les membres de mon comité de thèse, Sébastien Glaser, Redouane Khemmar, Léo Mendiboure et Lylia Alouache. Leur temps précieux, leurs commentaires constructifs et leurs suggestions éclairées ont grandement contribué à l'excellence de ce travail.
Le soutien familial que j'ai reçu a été d'une importance capitale dans la réussite de ce travail. Je tiens à exprimer ma profonde gratitude envers ma mère, **ZAARATTE Fatima Zohra**, qui est mon pilier, mon roc inébranlable. Sans elle, je n'aurais jamais pu accomplir ce travail. Je lui dois tout, et mes mots ne suffisent pas pour exprimer l'amour et la reconnaissance infinis que j'ai pour elle. Je suis également reconnaissante envers mon frère **Mehdi**, dont le soutien indéfectible m'a donné la force de persévérer lorsque les défis semblaient insurmontables. Je leur dédie mes plus profonds sentiments d'amour et de gratitude.
À ma seconde mère, **Hadja Habiba**, partie trop tôt, je souhaite du fond du cœur dédier cette thèse de doctorat en souvenir ému de son âme aimante. Sa bienveillance infinie, sa sagesse réconfortante et son amour inconditionnel ont illuminé ma vie et ont été une source inestimable d'inspiration. Sa présence chaleureuse et ses encouragements constants me manquent profondément. En lui dédiant cette thèse, je souhaite rendre hommage à l'impact indélébile qu'elle a eu sur ma vie. C'est un modeste témoignage de ma reconnaissance et de mon amour éternels envers elle. Que son âme repose en paix, sachant qu'elle a laissé une empreinte durable dans mon cœur et dans cette réalisation académique.
J'aimerai également exprimer ma gratitude envers toute **la famille ZAARATTE**, votre soutien inlassable a été un pilier solide sur lequel je me suis appuyée tout au long de cette expérience, et mes chers amis, qui ont été présents à chaque étape

de ce voyage.
Enfin, je tiens à remercier chaleureusement toutes les personnes qui m'ont soutenue tout au long de cette aventure de recherche, que ce soit de près ou de loin. Votre présence, vos encouragements et votre soutien inconditionnel ont été des sources d'inspiration et de motivation inestimables. Je vous adresse mes plus sincères remerciements pour votre générosité, votre bienveillance et votre soutien tout au long de ce parcours qui a façonné ma vie.
Que mes mots traduisent fidèlement la profondeur de ma gratitude envers chacune de ces personnes qui ont contribué à mon succès. Je vous suis profondément reconnaissante pour votre impact positif dans ma vie et votre contribution à la réalisation de mes aspirations.

Sabrine.

Contents

List of Figures

Glossary

ADAS Advanced Driver Assistance System. 38

AV Autonomous Vehicles. 52

C-ITS Cooperative Intelligent Transportation Systems. 25

CAV Cooperative Automated vehicle. 48

CBL Chain Branch Leaf. 52

CBL-G Chain Branch Leaf extended with Gateway. 78

CBL-I Chain Branch Leaf Extended with Infrastructure. 59

CTT Cumulative Travel Time. 94

CVPL Connected Vehicles With Platooning. 95

CVWPL Connected Vehicles Without Platooning. 95

DBSCAN Density-Based Spatial Clustering of Applications with Noise. 31

DG Distance of Gruyer. 117

DRAC Deceleration Rate to Avoid Accident. 42

EES Equivalent Energy Speed. 113

ETSI European Telecommunications Standards Institute. 23

FSD Full Self Driving. 21

ICRI Integrated Conflict Risk Index. 42

ITS Intelligent Transportation System. 22

LiDAR Light Detection and Ranging. 128

LoA Level of Automatization. 9, 21

LOS Line-of-Sight. 61

MOBIC Mobile Oriented Broadcasting for Inter-Vehicle Communication. 30

MTTC Modified Time-to-Collision. 45

New-ALM New Approach for Load Balancing in Mobile Ad hoc Networks. 30

NHTSA The National Highway Traffic Safety Administration. 20

OBU On Board Unit. 22, 25

PICUD Possibility Index for Collision with Urgent Deceleration. 46

PSD Passing Sight Distance. 45

Qos Quality of service. 34

RCRI Rear-end Crash Risk Index. 95

RIMUM Risk Estimator with Uncertainties and Multidimensional Model. 120

RoI Regions of Interest. 42

RSS Responsibility Sensitive Safety. 46

RSU Roadside Unit. 23, 35, 59

SAE Society of Automotive Engineers. 20

SCRP Stable CDS-Based Routing Protocol. 30

SSAM Surrogate Safety Assessment Model. 94

SSD Stopping Sight Distance. 41

TET Time Exposed Time-to-Collision. 45

TH Time Headway. 112

TIT Time Integrated Time-to-Collision. 45

TransAID Transition Areas for Infrastructure-Assisted Driving. 95

TTC Time to Collision. 110

TTCE Time-To- Closest-Encounter. 45

UC Use Case. 62

UNECE United Nations Economic Commission for Europe. 20

V2I Vehicle-to-Infrastructure. 27

V2V Vehicle-to-Vehicle. 25, 27

V2X Vehicle-to-Everything. 25

VANET Vehicular Ad-Hoc Network. 22

VISSIM Vienna SIMulation Model. 94

General Introduction

Automated vehicles are vehicles that are able to navigate and operate without human input. They use a combination of sensors, cameras, and machine learning algorithms to perceive their environment and take good decisions about where to go and how to avoid obstacles.
One important aspect of automated vehicles is their ability to communicate with one hand, other vehicles Vehicle-to-Vehicle (V2V) and on the other hand with infrastructure Vehicle-to-Infrastructure (V2I) communication. This allows vehicles to share information such as their location, speed, and other important data, which can be used to improve safety and reduce the risk of collisions with others. However, the implementation of these technologies also brings new challenges, especially related to assure continuity of communication despite the very dynamic environment and collision risk. Overall, while automated vehicles have the potential to greatly improve safety and efficiency on the road, it is important to carefully consider the potential risks and challenges associated with their use. ITS addresses critical life issues such as road safety since they are dedicated to automated vehicles. Their design has attracted significant interest from the research sector and industry in recent years, but it also comes with many problems.
Indeed, the increase in road accidents and driving fatalities have urged authorities to look for ways to improve road safety and anticipate dangerous situations. Many research projects have been conducted in recent years with the goal of proposing new and innovative mobility solutions that address current societal challenges such as safety, sustainability, and mobility accessibility. Questions about the impact of these systems and their real benefit of automated driving and decision systems in terms of safety remain. Even more when a human operator is increasingly removed from the driving task, it is critical to be able to ensure that automated driving systems strictly respect the safety constraints, of the vehicle's passengers and other road users.
Autonomous vehicles (AVs) have the potential to greatly assure communication between the vehicle and Roadside Unit (RSU) through the use of various technologies such as V2X (vehicle-to-everything) communication, GPS, and LIDAR sensors. This communication allows AVs to access remote information from mobile objects or fixed infrastructures, which in turn extends the range of perception and improves its quality. This expanded perception can also help AVs to anticipate and to predict remote driving behavior and potential risk situations, allowing for safer and more efficient driving. By connecting AVs with RSU, the overall transportation system can become more efficient, reliable, and safer for all road users.
The focus of our research is on structural analysis and evaluation of the road environment through the incorporation of a communication infrastructure via RSUs.

This thesis is organized as follows: Chapter 1 provides an overview of the background and research topic, followed by a review of the current state of the art. In chapter 2, we conduct an examination of the structure of the communication-based localization (CBL) system to determine its suitability for communication interoperability, specifically in regard to V2V and V2I communications. Taking advantage that offer the RSUs, i.e the potential to improve deficiencies of ad-hoc networks and enhance network performance in vehicular ad-hoc networks (VANETs). And given the limitations of relying solely on V2I communications in real-world road environments, we have studied CBL-infrastructure communication in various node distributions.
In chapter 3, we present our study's results and introduce the novel concept of CBL-Gateway Clustering (Chain Branch Leaf Gateway) and the computation used to achieve an optimal topology of RSUs, which ensures a high-quality and continuity of service while addressing isolated nodes and modeling the frame loss probability.
Furthermore, chapter 4 is dedicated to the examination of local multi-level perception, which is extended to the cluster level.
In chapter 5, we integrate these extended perceptions into our CBL-G communication structure and system and use them to estimate four collision risks. We first evaluate the most relevant metrics (TTC, TH, DG, R, RIMUM) which we evaluate under scenarios of perfect localization and perception, as well as perception uncertainty and perfect localization.
In chapter 6, the research work is concluded with an examination of the author's research, perspectives, contributions, and scientific impact.

Chapter 1

State of the art

Contents

1.1 Background

1.1.1 Automated vehicle

Automated vehicles are vehicles that use a combination of advanced technologies such as sensors, cameras, radars, and artificial intelligence algorithms to perceive the environment, take decisions, and navigate roads safely. Automated vehicles have the potential to revolutionize the way we travel and transport goods by reducing traffic congestion, improving safety, and providing more efficient and sustainable mobility solutions. However, there are also challenges that need to be addressed, such as ensuring the security and privacy of data generated by automated vehicles, developing effective regulations and policies, and building public trust in this technology. Despite these challenges, automated vehicles are poised to play an increasingly important role in shaping the future of transportation.
Many studies, including (Hallerbach et al., 2018; Rahman et al., 2018), have endeavored to prove the effectiveness of connected vehicles (CVs) in improving traffic safety. The concept of connected vehicle is defined by the U.S. government's: The National Highway Traffic Safety Administration (NHTSA) in the paper of (National Highway Traffic Safety Administration, 2019) and according to the Society of Automotive Engineers (SAE), vehicles containing connected vehicle technologies allows them to be more autonomous, productive, efficient and responsive to consumer demand.

1.1.1.1 Automation levels for AV (LoA)

To define autonomous vehicle automation, the SAE categorized the spectrum ranges from level 0 to 5 (from no automation to fully autonomous vehicles).
Autonomous vehicles are classified into 6 levels of automation illustrated in Figure 1.1, from level 0 (no automation) to level 5 (in research, complete self-driving); the level currently available is level 2 (partial automation with drivers who keep control).
France has announced that it will amend its highway code to reflect (United Nations Economic Commission for Europe (UNECE) changes, while the United Kingdom says Level 3 applications will be allowed on the road by the end of 2021. All countries will comply with the rules listed above.
In the US, the main problem is achieving consistency across all states, with each state and city taking its position on autonomous testing. It is unlikely that the deployment of Level 3 applications can be controlled by individual states, as customers would find it unacceptable if a major selling point of the vehicle were unavailable in their state. This would also cause problems if the car's operation had to be changed when it crossed state lines. Harmony is required to bring Level

3 applications to the US. However, NHTSA does not indicates that this is on the

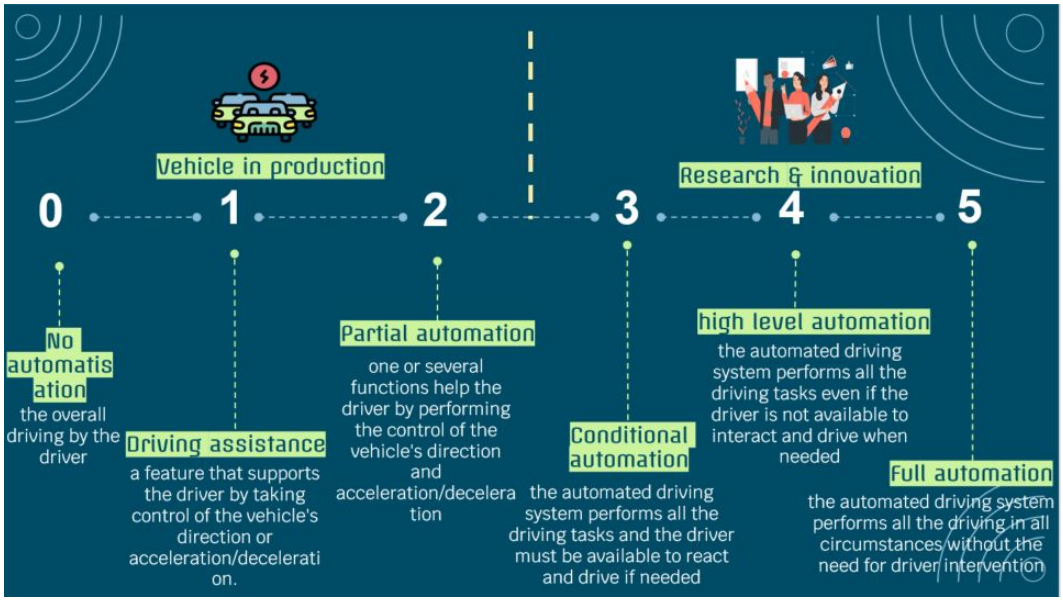

Figure 1.1: The Level of Automatization (LoA) of AVs defined by NTSHA

near horizon. Highway autopilot (a Level 3 technology) will be permitted on the roads starting in "2025+," along with fully automated safety features. Thus, it is unlikely that the U.S. will see high levels of private autonomy on the road anytime soon. This is also reflected in IDTechEx's "Autonomous Cars, Robotaxis and Sensors 2022-2042" forecast, with the U.S. not entering the market until 2025, up to 3 years behind other regions (Jeffs, 2021).
Tesla's Full Self Driving (FSD) is particularly sophisticated and advanced. The latest FSD update warns that the driver must always maintain control of the vehicle with his or her hands on the wheel. Tesla's FSD is an example of a Level 3 vehicle in waiting. It might be technically capable of achieving these levels of operation, but current legislation prevents it from doing so (Jeffs, Sep 17, 2021).
As a result, numerous research projects such as "CarTALK2000" (Borgonovo et al., 2003), "COOPERS" (Frotscher, 2008) and "SAFESPOT" (AZIONI, 2007) rise up from this need to study issues related to safety and design of cooperative systems for optimized road traffic. This projects took advantage of the rapid advances in wireless technologies that enable vehicular communications.
Thus, the exchange of data between nearby vehicles is made possible by the short distance of the links created spontaneously as the need arises. Vehicles in motion can form networks on the fly without pre-installation of infrastructure (Sharma and Nidhi, 2019).
These self-organizing networks known as vehicular ad hoc networks or VANETs

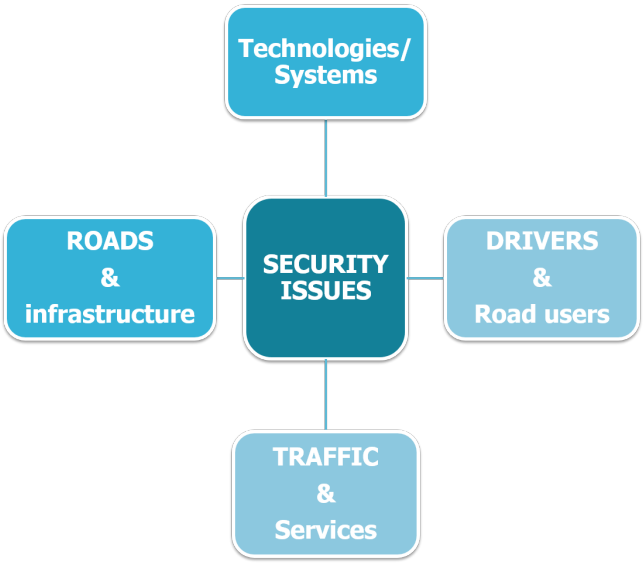

Figure 1.2: A Vanet elements environment presentation

have emerged as a specialization of MANETs. Their flexibility and low deployment cost make them attractive. In addition, VANETs offer the possibility of innovative applications that will ensure road safety and improve the lives of drivers and passengers.

1.1.2 Vehicular AdHoc Network

Vehicular Ad-Hoc Network (VANET) are part of Intelligent Transportation System (ITS). The VANET environment is made up of drivers, traffic, roads and technologies and the problems we find are related to safety and traffic. We illustrated it in figure 1.2. Their mobile nodes, also called On Board Unit (OBU), are embedded in vehicles that move in a road network. They are, therefore, subject to mobility constraints: the configuration of the road network, its traffic rules, and the characteristics of the road traffic (Um, 2020). The authors of (Gerla et al., 2006), defined VANET that allows inter-vehicular communication in a continuous way in a mobile environment whose topology is dynamic.
According to (Parrado and Donoso, 2015; Sathya Narayanan and Joice, 2019; Wang, Liu, and Kato, 2019; Tripp-Barba et al., 2019; Zekri and Jia, 2018), a VANET is characterized by:

1. A very dynamic topology: Speed and path choice define this.
2. Frequent disconnection from the network: every 5 seconds or so, nodes require another link.

3. Interaction with built-in sensors: Sensors help to find nodes and the nature of their movement.

4. Mobility prediction: the need to know the position of other nodes and their movements to stay connected with them, which is very difficult to predict when nodes are moving.

1.1.3 Inter-vehicle communication technologies

Automated driving goes hand in hand with improved communications between the entities that make up the system: (cooperative vehicles, equipped highways). For Inter-vehicle communication technologies, DSRC and LTE-V are already two major standards in the automotive network community. On one hand, DSRC has the characteristics of short distance and low delay. Still, it has limitations in the high-speed autonomous driving scenario, and it is necessary to add Roadside Unit (RSU). It supports communication between nodes with a distance of up to 1000 meters with a speed of 200 km/h.
In the United States, a frequency band (5.850 - 5.925 GHz) was reserved for vehicle-to-vehicle communications in 1999. In Europe European Telecommunications Standards Institute (ETSI), has allocated a similar frequency band (5.855 - 5.925 GHz) since 1990 (DTR/ITS, 2009; RTS/ITS, 2015). We present a summary of the characteristics of the most used technologies in table 1.1.

The integration of automated driving with improved communication among various entities, including cooperative vehicles and equipped highways, is a crucial aspect of the autonomous vehicle system. There are two major standards in the automotive network community, namely DSRC and LTE-V, that are used for Inter-vehicle communication(Frenzel, 2017). DSRC has the advantage of short distance and low delay, but it has limitations in high-speed autonomous driving and requires the use of Road Side Units (RSUs). On the other hand, LTE-V utilizes existing cellular infrastructure for broader coverage and better support for high-speed travel(Cecchini et al., 2017; Zekri and Jia, 2018). LTE-V2X, which stands for Long-Term Evolution for Vehicle-to-Everything, does not require the use of RSU. Unlike DSRC (Dedicated Short-Range Communications), which has limitations in high-speed autonomous driving scenarios and requires the addition of RSUs to support communication between nodes, LTE-V2X has the advantage of reusing existing cellular infrastructure and offering broader coverage and better support for high-speed travel. This enables direct one-hop communication from mobile to mobile without the need for RSUs.
The future of which communication technology will dominate the autonomous vehicle network is uncertain and depends on the roles of governments, telecom operators, and car manufacturers, as well as regional differences. The NHTSA is

Table 1.1: Comparison table of existing communication technologies for V2X communication.

Technology	Frequency Band	Communicatio Range	Communicatio Mode	Data Rate	Latency	Reliability	Security
DSRC	5.9 GHz	300-1000 meters	Broadcast	Up to 27 Mbps	10-50 ms	High	Basic
C-V2X	LTE	Up to 10 km	Direct communication	Up to 1 Gbps	<10 ms	High	Advanced
Wi-Fi 6	2.4 GHz, 5 GHz	100-200 meters	Direct communication	Up to 9.6 Gbps	<1 ms	Medium	Advanced
5G	Various	Up to several km	Direct communication	Up to 20 Gbps	<1 ms	High	Advanced

encouraging the use of IEEE 802.11p WIFI, but the telecommunications industry is proposing solutions based on centralized cellular systems with subscription fees (UIT, 2020). The battle between these technologies is ongoing, and it is recommended to have approaches that can be implemented regardless of the technology used. We present a summary of the characteristics of the most used technologies in table 1.1
ITS technologies enable communication between vehicles, infrastructure, and pedestrians to provide Cooperative Intelligent Transportation Systems (C-ITS) services. However, the increasing demand for connectivity can negatively impact the reliability of these services, which is crucial for road safety events. A comprehensive analysis model, as proposed by (Maaloul et al., 2022), can be used to evaluate and compare the performance of different vehicular communication technologies, such as LTE-V2X and IEEE 802.11p/ITS-G5, under various environmental conditions. The findings of the analysis show the trade-offs and limitations of the considered technologies and highlight the need for understanding their behavior in realistic environments. The authors recommend the use of adaptive reconfiguration and density sharing to limit these trade-offs, but further research is needed to improve this concept. The recent introduction of 5G technology has added more flexibility in resource allocation, but its impact on Vehicle-to-Everything (V2X) applications needs to be evaluated.

1.1.4 Communication architectures between vehicles

1.1.4.1 Vehicle to Vehicle (V2V) communication

Vehicle-to-Vehicle (V2V) communication architecture is based on communication links between OBUs. OBUs work together in a decentralized manner to form an ad hoc network. As a result, the V2V architecture is modular and adaptable. The V2V architecture can tolerate the failure of a network node but requires a sufficient number of nodes on the communication port for communication to occur. This number of nodes depends on the traffic penetration rate of the communication system. To operate effectively, the V2V architecture also necessitates the use of high-performing distributed routing algorithms.
According to the authors of (Zekri and Jia, 2018), the V2V system enables short and medium range communications between vehicle users, with low deployment costs and short message transmission with low latency as shown in figure1.3. It should be noted that the number of nodes directly correlates to the communication system's penetration rate in the traffic. Furthermore, the implementation of the V2V architecture necessitates distributed routing algorithms, the performance of which is by definition more difficult to predict than that of a centralized architecture.

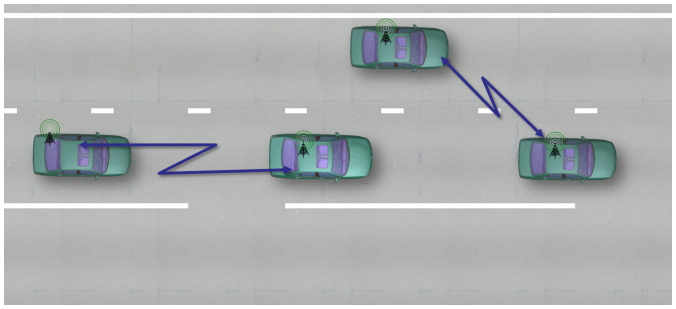

Figure 1.3: Vehicle-to-vehicle (V2V) communication architecture

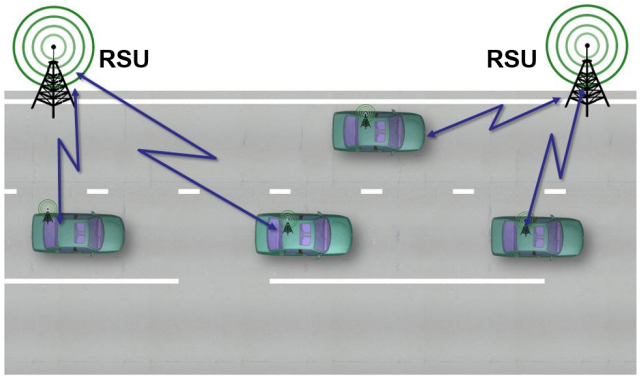

Figure 1.4: Vehicle-to-infrastructure (V2I) communication architecture

Finally, as with the previous V2I solution, the V2V solution will be confronted with technological evolution and, as a result, with the organization of upgrades of a fleet of technologically heterogeneous communicating vehicles.

1.1.4.2 Vehicle to infrastructure (V2I) communication

RSUs are used at regular intervals along the road in the Vehicle to Infrastructure (V2I) communication architecture to communicate with both the infrastructure and the vehicles. As depicted in Figure 1.4. The central network architecture, managed by the road manager, optimizes the communication traffic between connected devices.
The deployment cost of RSUs in the V2I architecture is substantial, with installation costs estimated at approximately 5000$ per terminal (Zhu et al., 2014). In addition to installation costs, maintenance expenses must also be considered throughout the life cycle. Authors (Alouache et al., 2017) defines the Communica-

tion Barriers and among them we find the lack of RSU terminals, the rapid change of the network topology and the network topology, the variation of the density of vehicles.
From a communication perspective, a centralized architecture may seem simpler to establish and operate. However, the management of hardware obsolescence over large distances is a significant challenge (Silva et al., 2017). Logistical difficulties such as managing equipment errors and failures, ensuring compatibility between various ITS applications, ensuring interoperability between older and newer equipment, and maintaining continuous V2I communication services in the event of RSU failure, all pose challenges to making a centralized architecture feasible (Zekri and Jia, 2018).

1.1.4.3 Vehicle to everything communication (V2X)

Vehicle to Everything or Vehicle-to-All is a vehicular communication system that will allow vehicles to exchange information with each other, with infrastructure and with pedestrians. V2X includes other more specific types of communication such as: V2V, vehicle to device (V2D), Vehicle-to-Infrastructure (V2I), vehicle to network (V2N), vehicle to pedestrian (V2P), and vehicle to grid (V2G).
V2I communications only may be inappropriate in some contexts and ineffective at times in the presence of occasional degraded conditions. While a centralized approach has the advantage of accuracy and capacity, it requires an infrastructure with radio access points at regular intervals. It is clear that this could not be guaranteed, if only for reasons of return on investment, especially in sections of roads that are generally not very busy.
Moreover, the information passing through the infrastructure may present a risk of obsolescence compared to a direct V2V communication when the vehicles involved are close (Zekri and Jia, 2018). In our case, we're interested in combining the two systems, V2I and V2V as shown in figure 1.5. In this mode of operation, the two systems must complement and collaborate in order to ensure service continuity. The goal is to use the information received from ground infrastructure or neighboring vehicles to refine and improve their own localization, and in some cases, the V2V system could be an alternative in areas not covered by RSUs.

1.1.5 Nodes organization and road topology

VANETs are decentralized and self-organizing networks that lack a centralized management and coordination entity in charge of bandwidth management and contention operations. Furthermore, because VANET nodes are mobile End-to-end, communication cannot be guaranteed particularly in highway scenarios. An intermittent connection can cause issues such as packet loss and compromise traffic

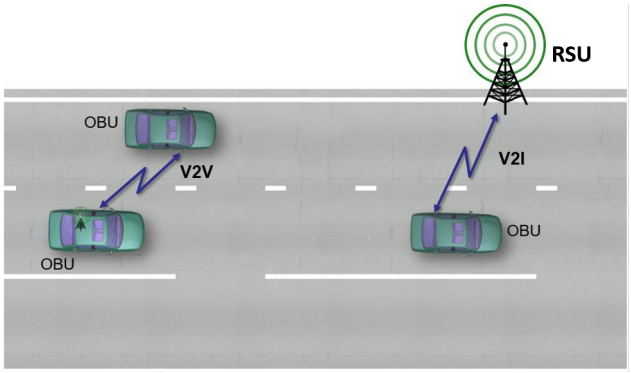

Figure 1.5: Illustration of the Vehicular Communication Architecture showing the two forms of communication: V2V and V2I

safety. In addition, VANETs is a large-scale network, however, the communication range of a vehicle is limited, which may also result in a weak connection between nodes (Bali, Kumar, and Rodrigues, 2014).
Therefore, maintaining a global network topology is essential for a node. Thus, a flat network topology is no longer efficient for information transmission in VANETs. To solve this problem, a hierarchical network topology, called clustering, has been proposed for VANETs. VANET routing protocols are generally categorized into, V2V and V2I based on the VANET architecture. V2V is categorized on the basis of information routing and transmission strategies based on topology, position, and uni-cast, and multi-cast. The literature categorizes routing protocols as either proactive, reactive, or hybrid.
Another classification is power-sensitive routing protocols and predictive mobility protocols designed for efficient use of limited resources and improved quality of service. For centralized control, clustering-based routing (Senouci, Aliouat, and Harous, 2019; Bao et al., 2020) Topology-based or position-based protocols are designed for efficient routing with low latency and no congestion (Wahid et al., 2018).

1.1.5.1 Overview of Clustering Algorithms for VANET Communications

In self-organizing networks, clustering consists in dividing the network into a set of geographically close nodes(Sethi and Chand, 2017). Indeed, the authors of (Wang, Liu, and Kato, 2019) claim that clustering is necessary to achieve the distributed formation of the VANET hierarchical structure and improve its evolution and reliability. Moreover, as a traffic management scheme, the cluster can be used to reduce traffic congestion, improve road safety, save road space, and make traffic

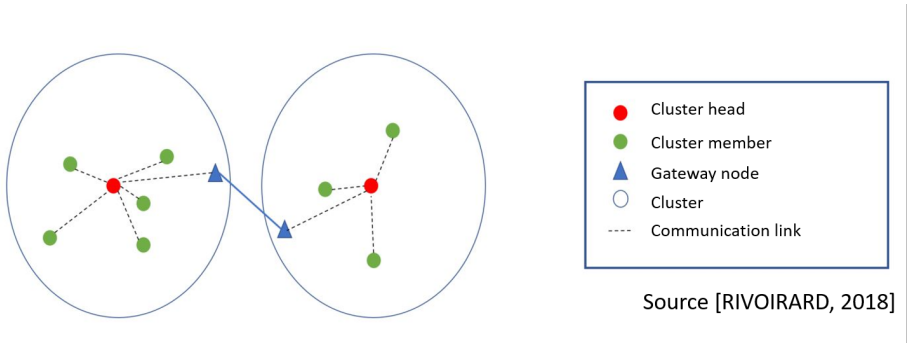

Figure 1.6: A cluster type configuration :Diagram of Cluster's members

more orderly (Louazani, Senouci, and Bendaoud, 2014).
The illustration in figure 1.6, depicts the actors of a cluster: the formation of a cluster is generally carried out around a node called the cluster head, the other members of the cluster are considered ordinary nodes (cluster members).
In some cases, there is an intermediate node called a gateway, which is characterized by its membership in several clusters and this is used to transmit information between the clusters of which it is a part. This is an interesting solution for simplifying and optimizing the functions and services deployed in figure 1.6.
According to (Ramakrishnan et al., 2011; Guizani, 2012; Sathya Narayanan and Joice, 2019), it allows the routing protocol to operate more effectively by reducing control traffic in the network and simplifying the data routing process. Several clustering algorithms have been proposed and evaluated (Cooper et al., 2016). However Clustering algorithms can be limited in their ability to handle high-dimensional data. It can be challenging to determine the optimal number of clusters for a given data set. These algorithms have different characteristics. They are designed to satisfy certain objectives depending on the context in which the clustering is deployed (routing, security, energy conservation, etc.) that are summarized in table 1.2.
A classification of existing clustering approaches has been established by several studies, including (Boyinbode et al., 2010; Liu, 2012; Dua, Kumar, and Bawa, 2014; Cooper et al., 2016).
In (Kakkasageri and Manvi, 2014), the authors break down clustering into 3 steps:

1. Division into groups (cluster).
2. Distribution according to mobility, direction, etc.
3. The election of the Cluster Head (CH) according to the used metric.

Clustering protocols for VANETs have been classified into various categories, including Hierarchical Clustering, Density-Based Clustering, Fuzzy Clustering,

Position-Based Clustering, ID-based such as DMAC, and energy-based such as HEED, LEACH, and EECS (Ramakrishnan et al., 2011; Maslekar et al., 2011; Sathya Narayanan and Joice, 2019; Debnath et al., 2021).
Speed-based clustering algorithms, such as CODE (Zheng, Tong, and Wu, 2017), use direction and relative speed to select CHs. However, this algorithm may not be suitable for highly dynamic environments. The ECHS (Banikhalaf and Khder, 2020) introduces conditions such as cluster centralization based and connection time with its neighbors. However, this algorithm relies solely on CH stability, which may not be sufficient in highly dynamic vehicle environments.
Distance-based algorithms like D-jump or D allow for flexible clusters, but reliability of estimated distance can be affected by other factors besides signal strength (Debnath et al., 2021). MC-DRIVE (Maslekar et al., 2011) is a direction-based clustering algorithm suitable for intersections, but only for simple road topologies.
Several energy-based algorithms have been proposed for balancing the energy consumption and increasing the lifetime of nodes in VANETs (Ramakrishnan et al., 2011).
LEACH is a distributed proactive protocol with nodes choosing CHs based on minimum energy spent during communication. TEEN is a hierarchical protocol with high energy consumption for message transmission. UCS balances energy consumption but may not be usable in large networks.
Intelligent clustering based on driving patterns is proposed to solve frequent interruptions (Chang and Ning, 2021). CBVANET and AODV-CV are among the best-known algorithms (Ramakrishnan et al., 2011; Bali, Kumar, and Rodrigues, 2014).
(Guizani, 2012) shows that Clustering is the best strategy to reduce overhead. AES-based cluster security routing is also proposed (Sharma, Vidwans, and Gupta, 2016).
Mobile Oriented Broadcasting for Inter-Vehicle Communication (MOBIC) and New Approach for Load Balancing in Mobile Ad hoc Networks (New-ALM) choose nodes with low global mobility or variance as CHs (Basu, Khan, and Little, 2001; Souza, Nikolaidis, and Gburzynski, 2010).
K-Means Clustering is a popular clustering algorithm that uses a centralized approach to form clusters based on the proximity of nodes, K-hop clustering improves stability (Zhang, Boukerche, and Pazzi, 2011). Stable CDS-Based Routing Protocol (SCRP) uses the dominate set to form a stable backbone (Togou, Senhaji Hafid, and Khoukhi, 2016).
CBL (RIVOIRARD, 2018) is a novel approach for routing in ad hoc VANETs, providing the application layer with a dynamic and stable virtual infrastructure. CBL enables close communication for data and alert message exchange and management of the road network.

Clustering algorithms are an important aspect of VANET communication, as they help in grouping vehicles with similar characteristics to improve communication efficiency.
The choice of the best clustering algorithm depends on various factors, such as the network topology, communication range, traffic pattern, and mobility model.
Some of the most commonly used clustering algorithms for VANETs are the Density-Based Spatial Clustering of Applications with Noise (DBSCAN), K-Means, and Hierarchical Clustering. The DBSCAN algorithm is popular for its ability to identify dense clusters of vehicles, while K-Means is widely used due to its simplicity and efficiency. Hierarchical Clustering is used when the number of clusters is not known in advance and the relationships between the clusters are important.
Ultimately, the best clustering algorithm for a VANET communication system will depend on the specific requirements and constraints of the system. It is important to evaluate and compare different clustering algorithms to determine the one that best fits the system's needs.

1.2 Problematic & Research Questions

The present thesis aims to make a significant contribution to the field of cooperative systems and traffic responses by investigating the interplay between traditional vehicles with human drivers and automated vehicles with automated driving. The research, conducted in collaboration between the COSYS department of Gustave Eiffel University and the Laboratory on Perception, Interactions, Behaviours, and Simulation of Road and Street Users (PICS-L), seeks to answer the following specific questions:

1. Can the clustering V2V communication model be adapted for use in vehicle-to-infrastructure (V2I) communications and if so, how can the CBL structure be adapted to support both V2V and V2I communications? Is the CBL model appropriate for hybrid (V2V/V2I) communications?

2. In the context of using infrastructure, what role will RSUs play in enhancing the CBL algorithm when used in a clustering method?

3. How can the CBL vehicular communication structure be used to mitigate distant risks?

4. Can local perception captured by the onboard sensors of the nodes lead to a multi-level perception?

5. How will the nodes in the communication system use this data to estimate collision risk at various levels (local, local extended, branch extended, and

Table 1.2: Clustering Protocols for VANET Networks

Type	**Clustering Protocols**	**Description**	**Advantages**	**Disadvantages**
Energy-based	HEED, LEACH, EECS	Energy-based protocols to balance energy consumption and increase the nodes' lifetime	Increase nodes' lifetime	May not be suitable for large-scale networks
Hierarchical	TEEN	high energy consumption for message transmission	Can be effective in networks with hierarchical clusters	High energy consumption
Direction-based	MC-DRIVE	based on the direction of nodes	Suitable for intersections with simple road topologies	May not be suitable for highly dynamic environments
Speed-based	CODE	based on the relative speed of nodes	Uses relative speed to select Cluster Heads	May not be suitable for highly dynamic environments
Distance-based	D-jump or D	based on the estimated distance between nodes	Allows for flexible clusters	Reliability of estimated distance can be affected by factors other than signal strength
Dominate Set-based	SCRP	use the Dominate Set to form a stable network infrastructure	Enables stable network infrastructure	May not be suitable for highly dynamic environments
Hybrid (Routing)	CBVANET, AODV-CV, CBL	combining clustering and intelligent routing techniques for improved communication efficiency	Can improve communication efficiency	complexity

global)?

6. Which risk indicator is most suitable for multi-level risk estimation when taking into account all the attributes of the vehicles in question?

The purpose of this research is to understand the adaptability and suitability of the CBL communication model in cooperative systems and traffic responses, as well as to identify the role of RSUs and the use of multi-level perception for risk mitigation. The potential impact of the research is to enhance communication and collaboration between traditional and automated vehicles for safer and more efficient traffic flow.

1.3 Literature Review

Before developing a new method, it is necessary to review the existing methods proposed by the scientific community in the current literature, to understand their mechanisms and identify their flaws so we can propose a more complete solution that covers a broader spectrum.
In this chapter's section, we establish a the state of the art solutions recently proposed in the field of vehicular networks, beginning with the types of vehicular communications, then moving on to infrastructure, collective perception and its use for collision risk estimation, risk indicators and finally the risk estimation indicators.

1.3.1 V2V and V2I Communications Approach VANET

Several researches have addressed the issue of hybrid aspect in communications between connected vehicles, indeed the authors (Huang, Lin, and Wu, 2020) proposes to combine V2V communications with V2I communications for the purpose of offloading VANET data from the base station (BS) of the cellular network to the RSU using the multi-hop V2V path that can connect with the front or rear RSU to increase the possibility of offloading VANET data.
In contrast to traditional offloading methods, in which data is only transmitted when a vehicle is within the range of a RSU signal coverage, the volume of data offloaded is significantly increased through the use of a vehicle-to-vehicle-to-infrastructure (V2V2I) offloading approach. The stability of the V2V2I offloading path is measured by the average path lifetime and the average session time, and can be improved through the utilization of a path recovery mechanism.
However, it should be noted that this study only considers the scenario of a single RSU and does not take into account the presence of multiple RSUs, including overlapping or non-overlapping front/rear RSUs, or the issue of when to switch

between RSU A and RSU B when a vehicle is situated between them. Additionally, the study does not address the lifetime and Quality of service (Qos) of the path, such as delay time, in the selection of a V2V2I offloading path.
Critical urban events, which occur randomly and require prompt handling by public authorities to maintain the smooth functioning of cities, can benefit from the use of cooperative localization techniques. However, these techniques, which rely on inter-vehicle communications, can be hindered by the presence of hidden vehicles and limited detection/communication range. Recently, GPS-free localization based on V2V communication with roadside infrastructure has emerged as a more accurate alternative. However, existing techniques necessitate communication with two RSUs to achieve high location accuracy.
The study presented in (Khattab, Fahmy, and Wahab, 2015) proposes a GPS-free localization framework that utilizes bi-directional time of arrival to localize vehicles through communication with a single RSU. The authors employ onboard inertial navigation system (INS) data to enhance the accuracy of vehicle localization using Kalman filters. The results demonstrate that the proposed framework yields a localization error of 1.8 meters, which represents an improvement of 65% and 47.5% in comparison respectively to GPS-based techniques without and with the utilization of INS, respectively. Additionally, this accuracy gain reaches 73.3% when compared to existing RSU-based techniques.
(Kassir et al., 2020) examines a network architecture in which vehicles use V2V links to form relay network clusters, which in turn connect to one or more RSUs through V2I links. This cluster-based multi-homing approach offers improved performance in terms of coverage and sharing rate per user, however, it is dependent on the penetration of V2V-V2I capable vehicles and potential blockages cause by legacy vehicles that impede line-of-sight based V2V links, such as those based on millimeter wave and visible light technologies. The study conducts an analysis of the connection and throughput performance of a typical vehicle on a highway in free-flowing traffic, investigating its dependence on vehicle density, blockage sensitivity, number of lanes, and inter-lane heterogeneity. The results show that even with moderate vehicle densities and penetration of V2V-V2I capable vehicles, such architectures provide significant connection improvements and reduced per-user rate variability compared to V2I-based networks. It is also shown that the performance of a typical vehicle improves significantly on a multi-lane highway compared to a single-lane road. This paper also highlights how network performance is affected when vehicles can control their relative positions, by characterizing the connection-rate trade-off faced by groups of vehicles.

1.3.2 Exploring the RSU Role and Challenges in V2X Communication Systems

RSUs play a crucial role in V2X communication systems, as they act as intermediaries between vehicles and the infrastructure. Over the years, the RSU have shown their efficiency and relevance in vehicular communication. Indeed scientists have been able to highlight the importance of RSU incorporation into a connected vehicle communication environment since RSU does a variety of jobs, including:

- Multi-hop communication (Zhang et al., 2012; Borsetti and Gozalvez, 2010a).
- Downloading content (Yang, Jia, and Xie, 2018; Liu et al., 2013).
- Data management and broadcasting (Viriyasitavat, Bai, and Tonguz, 2010; Lochert et al., 2007)
- Data aggregation (Bruno and Nurchis, 2013)
- Gaming and streaming (Ferretti and Roccetti, 2009)
- Gateway (Liang and Zhuang, 2012; Marchang, Sanders, and Joy, 2018)
- Vehicle location (Ansari et al., 2013; Khattab, Fahmy, and Wahab, 2015; Borsetti and Gozalvez, 2010a)
- QoS (Silva et al., 2016; Saleem, Mitton, and Loscri, 2021)
- Real-time assistance (Korkmaz, Ekici, and Özgüner, 2010)
- Routing (Mershad, Artail, and Gerla, 2012; Annese et al., 2011; Borsetti and Gozalvez, 2010b)
- Security (Lu, Qu, and Liu, 2019; Liao et al., 2013)

In this section we provide and discuss the importance of transforming physical infrastructure before deploying connected and automated vehicles (CAVs), and the various roadway infrastructures and issues they pose. It also references various research studies and articles on the topic, including works by (Rana and Hossain, 2021), (Ansari et al., 2018), (Ou, 2014), (Jeong et al., 2021), and (Wang et al., 2018).
With the current transportation network, one of the main challenges they highlight is the deployment of RSUs which are required to support communication and data exchange between CAVs and the infrastructure. However, the deployment of RSUs is complex and expensive, and their maintenance and upgrade require continuous investments. Additionally, the authors (Rana and Hossain, 2021) mention

the limitations of RSU coverage, as vehicles moving out of the RSU coverage area may experience communication disruption and loss of information. To overcome these challenges, the authors suggest the integration of CAVs with advanced communication technologies such as 5G and the development of hybrid RSU-vehicle communication systems to ensure reliable and continuous communication.
The authors in (Ou, 2014), proposed a VANETs localization scheme that utilizes RSUs for accurate positioning of vehicles. Vehicles passing within the range of an RSU communicate with it using beacon signals, and their position is estimated using either Time of Arrival (TOA) or Time Difference of Arrival (TDOA) measurements. This approach heavily relies on the availability and functionality of RSUs for accurate localization, which can be a potential limitation. The survey by (Jeong et al., 2021), found that there are several security and privacy issues in vehicular networks. They studied and discussed three key areas, including vehicular network architecture, vehicular address auto-configuration, and vehicular mobility management. The study also discussed the role of the RSU in key management and privacy, highlighting the potential use of edge computing to perform public key and certificate operations. For example, an ECD near a RSU could obtain the public keys of the vehicles in advance, allowing for secure communication. However, despite these efforts to address security and privacy issues, there is still a need for further research and development to ensure the secure and private operation of vehicular networks.
In the work of (Wang et al., 2018), the authors propose a method for improving the data service mechanism for vehicles outside the coverage area of RSUs. The authors suggest that when vehicles travel through the RSU's coverage area, they can retrieve and cache some of the data elements using Vehicle-to-Infrastructure (V2I) communication.
However, due to the limited time that vehicles spend within the RSU coverage, the authors plan to design an efficient data service mechanism for vehicles outside the RSU coverage using V2V communication. To achieve this, RSUs will assist by dividing vehicles into different groups, in order to reduce the interference caused by multiple vehicles broadcasting data items at the same time.
This approach has the potential to improve data services for vehicles outside the RSU coverage, but it also has certain limitations, such as the need for a well-designed group division mechanism and the potential for increased communication overhead due to the division of vehicles into different groups.
In conclusion, despite these limitations, RSUs are still considered an important component of V2X communication systems, and research is ongoing to overcome these limitations and improve the effectiveness and reliability of RSUs.

1.3.3 The Collective Perception in Connected and Automated Vehicles

The perception of autonomous vehicles is primarily determined by the capability of their onboard equipment. These equipment are equipped with various sensors, such as cameras, lidars, and radars, that collect data about the surrounding environment. The collected data, such as images and other sensory information, is used by the autonomous vehicle to construct a 3D representation of the environment. The onboard computer then processes this information to make decisions regarding the vehicle's movements, such as braking, accelerating, and steering. According to the authors (Trabelsi et al., 2022), the quality and accuracy of the sensory data collected by the onboard equipment is crucial for the effective performance of these functions. They present a recent survey on Vision-Based On-Road Behaviors Understanding. Perception is of great importance for security concerns in road environments, and connected and automated vehicles (CAVs) can enhance their perception by exchanging information through V2X communication. This is known as collaborative or collective perception, which involves using a range of on-board sensors to detect the environment.
Collective perception provides a more comprehensive view of the surrounding environment, which improves the safety and efficiency of CAVs. In a cooperative intelligent transportation system, sharing sensor data, also called cooperative perception, is essential for protecting vulnerable road users. However, limitations such as limited perception range and restrictions in specific conditions, require future autonomous vehicles to form an inter-vehicle network to enhance information interaction, perception, and planning capability.
Collective Perception Service (CPS) is a V2X service offered by an ITS station that enables the sharing of information about its environment with other ITS stations. This involves providing data about perceived objects and available free space for safe allocation (European Telecommunications Standards Institute (ETSI), 2020). However, the exchange of sensor data representations in C-ITS use cases will lead to increased radio channel load with the increasing bandwidth demand.
Collective perception improves a vehicle's awareness of its surroundings by extending its field of view beyond its line of sight. For example, in figure 1.7 Vehicle A is informed of the presence of Vehicle D through the inter-vehicle communication network (communication with vehicle B and C), even though Vehicle A cannot perceive Vehicle D directly through its onboard sensors. vehicle C, B, and A, by sharing perceived objects among communications, collective perception increases vehicle's A awareness of objects out of its vicinity. According to ETSI, collective perception messages should be generated by vehicles following set rules. The timing and content of these messages are important for improving CAV perception. However, excessive message generation could clog communication channels.

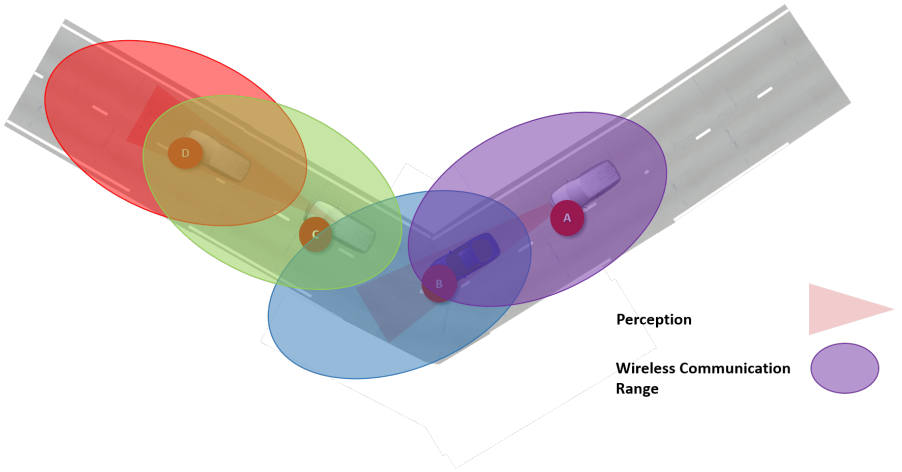

Figure 1.7: Explanatory example of a scenario where extended perception between vehicles in a V2V communications environment is beneficial

Research of (Thandavarayan, Sepulcre, and Gozalvez, 2020) showed that current rules result in a high number of CPMs containing information about a small number of objects, making the communication channel inefficient. The authors proposed a solution to reduce the number of CPMs and improve the reliability of V2X communication and perception for CAVs. The authors found that reducing the number of CPMs would lead to more efficient use of the communication channel.
However, research by (Herbert, Varadi, and Bokor, 2020) showed that running multiple services on the same channel can negatively impact the quality of the CP service, suggesting that multi-channel solutions should be explored.
The research by (Shan et al., 2021) showed that a connected vehicle (CV) can "see" a pedestrian around corners through CPMs received from a RSU. The authors also discussed the processing of CPMs and the trajectory planning within CAVs. The study highlights the importance of collective perception in enhancing the perception and safety of CAVs.
However, the limitations of collective perception must also be considered. One such limitation is the limited perception range of individual sensors, which requires inter-vehicle communication to enhance information exchange, perception, and planning capabilities.

1.3.4 Safety indicators

The development and deployment of technologies for Advanced Driver Assistance System (ADAS), and more recently autonomous driving systems and connected

and automated vehicle applications, necessitates the detection and analysis of the road environment in its full complexities. Because of the mixed traffic and vehicle interactions, assessing the level of safety associated with a road situation using local and dynamic perception maps that include five key components and their attributes (obstacles, road, ego vehicle, environment, and driver) is insufficient. It is necessary to construct information and indicators from these perception data and key components in order to evaluate the risk level of a situation.
The recent survey of (Westhofen et al., 2022), has established a review on the state of the art of criticality measures, their properties, and their applications in the context of automated driving. According to (Pinnow et al., 2021) due to limited movement at the approach level, rear-end collisions are the most predominant type. It is therefore important to distinguish between internal and approach conflicts when considering which indicator is more appropriate.
According to (Ma et al., 2020) the accident types in the Chinese highway are due to lane change (62%) and rear-end collision (38%). According to Canada, (37%) rear-end collisions and (18%) vehicle side-slip. Human-driven vehicles, unlike automated vehicles (which have a perfectly defined perception by sensors), have a variable perception of the environment due to their cognitive, psychological, and physiological states. These driver states also influence decision-making.
Communications for AV complete their knowledge of the environment and therefore allow for better decision-making with possible anticipation. We rely on the general definition of risk that is published in the (Monkhouse, Habli, and McDermid, 2020) paper. It presents an improved vehicle control model based on the definition provided by the ISO 26262.0 standard. The automotive risk matrix describes risk (R) as follows:

$$R = F(f, C, S) \tag{1.1}$$

Where f is the frequency of occurrence of a hazardous event, C is the control capability of the system, and S is the severity of the event. For the risk related to road situations, the frequency of occurrence of a hazardous event corresponds to the probability of collision, the control capacity is the existence of avoidance manoeuvers and the severity is the mortality rate estimated from the Equivalent Energy Speed (EES).
Existing risk estimates can be broken down into two families: distance-based estimates and probabilistic estimates, we will be discussing them in the two following sections.

1.3.4.1 Distance-based indicators

The most widely used and well-known safety indicators applied to traffic management and collision risk assessment are distance-based indicators. They are defined by the distance between the vehicles. Among them, the time to collision (TTC)

and the time headway (TH) is the most frequently used in the literature and are described as follows:
The time to collision, as it was defined by (Minderhoud and Bovy, 2001) :

$$TTC(i,j) = \frac{Xj - Xi - Lj}{Vi - Vj} \tag{1.2}$$

Time to a headway (TH), can be referred to in some scientific papers as inter-vehicular time (TIV):

$$TH(i,j) = \frac{Xj - Xi - Lj}{Vi} \tag{1.3}$$

With Xi (respectively Xj) the positions and Vi (respectively Vj) the speed of the following vehicle (respectively leader), and Lj the length of the leader.
The authors proposed a comprehensive literature review of proximity risk estimates in (Mahmud et al., 2017). They reviewed the exhaustive list of estimates based on distance, speed, and acceleration in (Muzahid, Fauzi, and Rahim, 2021). However, these estimates did not account for crash severity due to the relative dynamics of vehicles.
(Labayrade et al., 2010) proposed a dedicated distance, Dij, to compute the distance between measurements and clusters in road obstacle detection using multi-sensor data fusion. According to (Gruyer et al., 2017), this distance considers uncertainties and headings of uncertainty ellipsoids .
The authors of (Wang et al., 2021) conducted a comprehensive review of surrogate safety measures, building on previous work (Mahmud et al., 2017; Md Muzahid, Kamarulzaman, and Rahim, 2020). They also reviewed the use of surrogate safety measures (SSMs) in various studies to assess the safety of VAs, focusing on finding specific SSMs for mixed human-driven traffic scenarios.
Additionally, (Mammar et al., 2004) describes The Time-to-Line-Crossing (TLC) lateral risk estimator is a method used to estimate the risk of a vehicle deviating from its lane and potentially colliding with another vehicle or an obstacle. It differs from longitudinal risk estimators, which estimate the risk of a collision based on the time difference between two vehicles.
The TLC can be either obstacle-oriented or road-oriented. Obstacle-oriented TLC estimates the risk of collision based on the time it would take for the vehicle to cross a line marking the boundary of the lane, in relation to a fixed obstacle in the adjacent lane.
Road-oriented TLC estimates the risk of collision based on the time it would take for the vehicle to cross a line marking the boundary of the lane, in relation to the road's curvature. However, it only provides information about the risk of lateral collision and does not take into account other factors such as the speed of the vehicle or the presence of other vehicles. Moreover, it is usually designed for two-dimensional applications and lacks adaptability to various road and vehicle

types, which might necessitate customization for each scenario. This could result in significant expenses and time consumption. Also, it may not be suitable for high-speed objects, as it assumes that the object's speed remains constant throughout the measurement. The TLC equation is given as follow:

$$TLC(Y_h, v) = \frac{\sqrt{(R_x)}}{v}.\sqrt{(W - y_H).(2 + \frac{(y_H = W}{Rr})} \tag{1.4}$$

where yH is the distance from the left (right) front tire to the left (right) lane boundary, v is the vehicle speed, W is the lane width (typically 3.5 on highways), and Rr is the radius of curvature of the road.
A human-centered risk assessment algorithm is proposed by (Shin and Yi, 2018) By considering the human reaction time, the algorithm provides a more realistic assessment of the risk of collision. And taking into account the vehicle uncertainty boundary, the algorithm provides a more comprehensive assessment of the risk of collision. By using V2V communication, the algorithm can more effectively assess the risk of collision in real time and perform active safety control interventions if necessary. However, the accuracy of the algorithm depends on the reliability of V2V communication, which can be affected by a variety of factors, including range, interference, and network congestion. The accuracy of the algorithm depends on the accuracy of the vehicle position information, which can be affected by a variety of factors, including GPS accuracy and sensor errors, and it may not be suitable for all driving scenarios, such as low-speed urban driving or high-speed highway driving.
The Stopping Sight Distance (SSD) takes into account the reaction time of the driver, which is the time it takes for the driver to perceive the obstacle and initiate the braking process. It also takes into account the braking distance, which is the distance traveled by the vehicle while the brakes are applied. The braking distance depends on the speed of the vehicle, the road conditions, and the braking capability of the vehicle.
The SSD is used in road design and engineering to ensure that the visibility and clearance distances are adequate for safe vehicle operation and to identify potential hazards on the road. By knowing the SSD for different speeds, engineers can determine the safe design speeds for a road, the required stopping sight distances for intersections and driveways, and the minimum sight distances for curves and hills. However, it may not accurately reflect actual driving conditions, as it is based on theoretical calculations and does not take into account real-world variables such as road slope and tire wear. And SSD only takes into account the driver's reaction time and the braking capability of the vehicle. It also does not take into account other factors such as road conditions, vehicle speed, or the presence of other vehicles. SSDs are estimated as a function of vehicle speed (V), friction coefficient (f), and drivers' reaction time (t), (Chen and Chen, 2019) as shown in

Eq 1.5:

$$SSD = \frac{Vt}{3.6} + \frac{V^2}{254f} \tag{1.5}$$

Where: V denotes vehicle speed; t denotes drivers' reaction time; f denotes the friction coefficient of the pavement.
The first term on the right-hand side of the equation, $\frac{Vt}{3.6}$, calculates the distance traveled by the vehicle during the driver's reaction time. The value of 3.6 is a conversion factor that is used to convert the vehicle speed, which is usually given in kilometers per hour (km/h), into meters per second (m/s). So, dividing V by 3.6 gives the speed of the vehicle in meters per second. Multiplying this by t gives the distance the vehicle will travel during the driver's reaction time t.

The second term on the right-hand side of the equation, $\frac{V^2}{254f}$, calculates the distance required for the vehicle to come to a complete stop based on the friction coefficient f and the vehicle speed V. The value of 254 is a conversion factor used to convert the friction coefficient f from units of pounds per ton to units of Newtons per kilogram. This term increases as the square of the vehicle speed V and decreases as the friction coefficient f increases. Therefore, a higher speed or a lower friction coefficient will increase the SSD. In (Labayrade et al., 2010), a dedicated Dij distance is presented to compute the distance between measurements and clusters in a multi-sensor data fusion process for road obstacle detection.
This distance is similar to a special case of the generic Bhattacharyya distance. While both Bhattacharyya distance and Gruyer distance are used to compare the similarity of two probability distributions, they are defined differently and can give different results when used to compare the same sets of data. Bhattacharyya distance is known for its ability to measure the similarity of two probability distributions, while Gruyer distance is known for its ability to capture the spatial distribution of data points. However, the main advantage of this Gruyer distance is that it takes into account uncertainties and directions of the uncertainty ellipsoids. The demonstration of this distance is provided in the article of (Gruyer, 2017).
The distance of (Gruyer and Rahal, 2019) is applied in a global perception architecture with adaptive detection and tracking of static and dynamic obstacles. This perception step is shared in a set of dedicated Regions of Interest (RoI) surrounding an ego-vehicle. In this architecture, inaccuracies and uncertainties in the data are taken into account.
While a summary of various surrogate estimators is proposed by (Li, Lu, and Xu, 2017) such as TTC, Deceleration Rate to Avoid Accident (DRAC), and Integrated Conflict Risk Index (ICRI). The latter indicator is used in predictive modeling in the following cases of lane change maneuvers with intersecting trajectories. These indicators are calculated as follows:

Deceleration rate to avoid accident (DRAC):

$$DRAC_{ij} = \frac{(v_i - V_j)^2}{2(X_j - X_i - L_j)} \tag{1.6}$$

Integrated Conflict Risk Index (ICRI) :

$$ICRI = \sqrt{TTC^2 - DRAC^2} \tag{1.7}$$

However, they applied indicators designed in a one-dimensional way to two-dimensional situations, translated into a single channel. The choice of these estimators does not seem to be the most appropriate for the situation.

1.3.4.2 Probabilistic based collision estimation methods

Probabilistic collision estimation methods assess the probability of collision and its severity based on statistical analysis. (Glaser et al., 2010b) proposed a risk assessment method for autonomous vehicles that calculated total risk as the sum of normalized probability functions applied to both Time-to-Collision (TTC) and Time-to-Intersection-of-Vehicles (TIV). The proposed method provides a useful tool for autonomous vehicles, as it helps to ensure that they operate safely and make appropriate decisions in real-world driving scenarios. The method has the potential to improve road safety and reduce the risk of accidents involving autonomous vehicles, as it takes into account multiple factors that can impact the risk of collision. However, it is important to note that this method is based on theoretical calculations and may not accurately reflect actual driving conditions. Further research and testing may be required to validate its effectiveness and reliability in real-world scenarios.
(Demmel, Gruyer, and Rakotonirainy, 2013) used collision probability and severity functions to evaluate the level of risk in a car-following scenario. The method focuses on car-following scenarios but does not consider other types of collision scenarios that may occur on the road. This limits the usefulness of the method in more complex driving situations.
(Leroy et al., 2021) introduced an adapted risk assessment method based on the Gruyer distance, considering positional uncertainties due to accelerations. The Gruyer distance is a well-established longitudinal risk assessment method that calculates the distance between two vehicles as a function of time and speed. In this adapted risk assessment method, the positional uncertainties due to accelerations are taken into account when calculating the Gruyer distance. This helps to more accurately reflect the actual risk of collision in a driving scenario, taking into account the variability in the acceleration and speed of road users. This method provides a more comprehensive and accurate approach to risk assessment

for autonomous vehicles, as it takes into account the effects of positional uncertainties due to accelerations. This can help to better identify and mitigate potential collision risks, making the method a promising approach for use in real-world scenarios. However, RIMUM is inadequate for assessing the risk between vehicles in specific two-dimensional configurations such as road intersections, highway insertions, highway exits, and traffic circles. Its predictive ability is also limited at the prediction level. The fatality risk calculated from RIMUM remains at a sufficient level for non-collision situations while the risks based on TTC and TH are too high given the configurations.

The proposed method by (Katrakazas, Quddus, and Chen, 2017) provides a comprehensive and interaction-aware assessment of the risk of collision based on dynamic Bayesian networks (DBNs), considering the motion and behavior of multiple road users such as vehicles, bicycles, and pedestrians, taking into account their interactions and dependencies. The results of the risk assessment can be used to inform decision-making by autonomous vehicles or to support driver warnings and interventions. It is a promising approach to collision risk modeling for autonomous vehicles. However, it requires significant computational resources and may be difficult to implement in real-world scenarios. It requires large amounts of data to train the DBNs, which can be difficult to obtain in practice and may not be suitable for real-time implementation.

The proposed method of (Philipp and Goehring, 2019), calculates the collision risk by considering the distances between the octagonal representation of the vehicle and the octagonal representations of surrounding road users and obstacles. The collision risk is then calculated based on the minimum distance between the vehicle and the surrounding road users and obstacles, taking into account the velocity and direction of each road user.

The analytical approach proposed by (Philipp and Goehring, 2019) provides a computationally efficient way to assess collision risk, as it only requires simple geometric calculations and does not require extensive computations. This makes it suitable for real-time implementation in autonomous vehicles. However, the method may have limitations in accurately representing the surrounding space, especially in complex and dynamic road environments with multiple road users and obstacles. The method also assumes that road users and obstacles follow a linear motion, which may not always be the case in real-world scenarios.

The adapted risk from Gruyer distance, considering positional uncertainties due to accelerations, was introduced in (Leroy et al., 2021).

1.3.5 Discussion of the literature on risk estimation indicators

The Time-To-Collision (TTC) metric is widely used in risk estimation due to its ability to combine spatial proximity and speed, and is considered reliable. However, it is only effective in congested environments and unsuitable for measuring lane change conflicts (Mattas et al., 2020). In low congestion periods like overnight, it's inadequate (Charly and Mathew, 2019). In simple two-vehicle scenarios, it can be used directly from the following vehicle's perspective (Demmel, 2012). However, complex representations of driving risk are possible with extended perception (Eggert and Puphal, 2017).
Limitations of TTC in complex scenes have led to proposed alternatives Time-To-Closest-Encounter (TTCE), an improved version of TTC that takes into account factors such as occlusion and dynamic objects. Gaussian and spatial occupancy probability approach, and survival analysis (Eggert and Puphal, 2017).
Modified Time-to-Collision (MTTC) is the mean time it takes for two objects to collide, considering various scenarios and conditions. It provides a more comprehensive view of the likelihood of a collision over time and is used to evaluate the performance of collision avoidance systems. On the other hand, TTC is the time elapsed between the detection of a potential collision and the actual impact. It is a measure of the immediacy of a potential collision and provides a snapshot of the situation at a specific point in time.
In summary, while both TTC and MTTC are used to evaluate the risk of a collision, TTC focuses on the immediacy of a potential collision at a specific point in time, while MTTC considers the average time it takes for a collision to occur, considering various scenarios and conditions.
Time Integrated Time-to-Collision (TIT), Time Exposed Time-to-Collision (TET) have the same drawback (Shi et al., 2018). Rear free-flow zone studies also provide insights (Shi et al., 2018). Indicators for connecting lanes should account for increased risk near ramps (Shi et al., 2018).
TIT is a measure of the time elapsed between the detection of a potential collision and the actual impact. In the field of autonomous driving, TIT is used as a critical metric to evaluate the performance of collision avoidance systems. A low TIT indicates that a collision avoidance system has detected a potential collision early and has had enough time to take appropriate action to avoid the impact. The faster the system can detect the potential collision and take action, the lower the TIT and the higher the level of safety. It shows a good ability to capture individual crash risk, but only under congested highway conditions (Shi et al., 2018). TET is unreliable due to advanced video processing/simulation (Yuan et al., 2019; Shi et al., 2018).
Passing Sight Distance (PSD) and DRAC perform well in free-flow areas. PSD

takes into account the uncertainty and variability in vehicle speeds and driver reaction times, while DRAC represents the Deceleration rate to avoid accidents in a given scenario. DRAC provides a clear and concise measure of the risk of a collision, which can be used to make informed decisions about how to best avoid an accident. However, it is only applicable in situations where both vehicles have the ability to detect and respond to each other, which may not always be the case in real-world scenarios.

Possibility Index for Collision with Urgent Deceleration (PICUD) considers the safety margins of a road and the vehicle's ability to decelerate, providing a more accurate estimate of the collision risk compared to methods that only consider relative velocity. However, one of its limitations is that it requires accurate and real-time information on the vehicle's velocity and acceleration, which may not always be available in a vehicular network which makes it not that widely used and its robustness is questionable (Shi et al., 2018; Kuang, Qu, and Wang, 2015).

The Time-To-Accident (TA) metric is a useful avoidance-based indicator for measuring various conflict types (Ma et al., 2020).

Passage time (H) is a measure of traffic severity, applicable in all traffic environments (Mahmud et al., 2017). However, most indicators have mainly focused on end-of-line or right-angle collisions, with limited studies considering intersection and diverging collisions (Yang, Ozbay, and Bartin, 2010; Bin, Uno, and Iida, 2003; St-Aubin, 2012). Head-on collisions are rarely measured using this conflict indicator. (Johnsson, Laureshyn, and Ceunynck, 2018; Tarko, 2018) suggest integrating important aspects of different environments in an indicator. According to the conflict model proposed by (Davis et al., 2011), conflicts are caused by initial conditions and avoidance maneuvers that vary depending on road geometry. For example, rear-end collisions can occur in a traffic circle, merging on-ramps, or turning at an intersection. The correlation between observed and estimated conflicts depends on road geometry, with freeways having the largest variety of indicators. Indicators for rear-end collisions from similar studies can be used to determine appropriate indicators.

Responsibility Sensitive Safety (RSS), is a mathematical formulation of the duty of care in autonomous vehicle (AV) safety. It defines safe and potentially dangerous inter-vehicle distances and classifies the responsibility in case of an accident. Developed by Intel Mobileye(Mobileye, 2018), it considers factors such as reaction time and maximum acceleration to determine a vehicle's ability to avoid a collision. The safe longitudinal distance formulation of RSS can be used as a proactive safety measure, classifying safe and potentially dangerous situations. One of the key advantages of RSS is its consideration of additional factors such as the state of the ego-vehicle, road geometry, and environmental parameters(Chai et al., 2019; Koopman, Osyk, and Weast, 2019). This makes it a more complete indicator in

terms of key elements present in a driving scenario. However, it is important to note that there may be limitations to the implementation of the RSS indicator, such as the need for precise data input or the potential for it to add complexity to the driving experience.

1.4 Research Scope & Objectives

The objective of this research is to enhance the communication among entities in the road ecosystem, such as cooperative vehicles, RSUs, road users, and infrastructure managers, to facilitate the deployment of automated mobility services. The thesis focuses on the application of vehicular clustering communication architecture, in the context of autonomous vehicles operating in highway environments.
The aim of enhancing communications among the entities that constitute the road ecosystem, such as (cooperative vehicles, RSUs, road users, and infrastructure managers) is to facilitate the robust and efficient deployment of automated mobility services. The access to remote information obtained from mobile objects or fixed infrastructures and their exploitation can extend the perception range and thus enhance its quality. Furthermore, this extended perception can contribute to anticipating and predicting remote behaviors and potentially hazardous situations. In order to enable the deployment of automated mobility in critical situations and functions, the estimation of the attributes of three essential "actors" is crucial. These actors include obstacles, road conditions, and the current state of the ego-vehicle.
This thesis presents a study on the application of vehicular clustering communication architecture in the context of autonomous vehicles operating in highway environments. The objective is to improve the performance of Vehicle Ad-hoc Network (VANET) networks by efficiently utilizing the Chain branch leaf (CBL) communication model. The adaptability and suitability of CBL in cooperative systems are evaluated with respect to their impact on traffic responses. Initially, the CBL model is limited to V2V communications. However, the proposed work extends the CBL model by incorporating Vehicle-to-Infrastructure (V2I) communications through the use of RSUs. The integration of both V2V and V2I communications into a single architecture enables the development of a complementary relationship that leverages the strengths of both communication modes. V2V communication allows for direct information exchange between vehicles, enabling them to sense and respond to situations beyond the range of their onboard perception systems. V2I communication, on the other hand, enables vehicles to receive information from the surrounding infrastructure, such as traffic signals, road signs, and other fixed road elements. The combination of V2V and V2I communications results in a more comprehensive understanding of the road environment and potential

hazards, leading to a more robust and reliable system for ensuring the safety and efficiency of autonomous vehicles.
The primary goal of the proposed work, is to evaluate the adaptability of the CBL-I model to different route configurations in the context of vehicular clustering communication architecture for autonomous vehicles in highway environments. The objective is to ensure that the CBL-I model can be integrated into real-world routes, including the presence of RSUs, in different cases (such as lack of RSu's deployment or malfunction on some RSU) while maintaining communication between nodes. The objective is to maintain the transmission of relevant information for various applications, such as location tracking and security. The evaluation of the adaptability of the CBL-I model will provide insights into its suitability for deployment in real-world scenarios, thereby contributing to the development of a robust and effective vehicular clustering communication architecture for autonomous vehicles.
Another goal of the proposed work is to address the issue of isolated nodes that were not considered in the original Chain branch leaf (CBL) communication model for vehicular clustering communication architecture for autonomous vehicles in highway environments. This is achieved by introducing a new type of node and implementing a new incremental algorithm, referred to as the CBL-G model. The new algorithm and node type are designed to address the limitations of the original CBL model in handling isolated nodes, thereby enhancing the coverage performance of the CBL-I model. The improvement in handling isolated nodes is expected to contribute to a more effective vehicular clustering communication architecture for autonomous vehicles operating in highway environments and guarantee a high in term of accuracy, certainty, accessibility, availability, and continuity. Moreover, the quality aspect also is related to the capability to send messages and data in a constrained time (low delay and latency).
Furthermore, we want to use the resulting architecture and communication strategies that take into account the information of surrounding vehicles, in order to extend perception and a global risk calculation approach.
In order to effectively implement our proposed solutions, it is essential to have access to data pertaining to obstacle detection, road configuration (such as lanes and markings), and potentially the environment (such as degraded conditions caused by weather or infrastructure). If this information is limited to a local range, as obtained from on-board perception systems, then Cooperative Automated vehicle (CAV) will only be able to perform reactive functions, such as vehicle spacing regulation and emergency braking. To effectively anticipate and estimate dangerous situations, it is necessary to consider the concept of global risk, which encompasses both near and far risks.
To achieve this, different levels of risk will be addressed: (i) the local risk of the

vehicle, as determined by its onboard perception systems; (ii) the extended local risk, estimated by the cluster head using the perception of cluster members; (iii) the extended branch risk, estimated by the branch using the perception of adjacent branches (upstream and downstream); and (iv) the global risk, which considers most of the available information, and is calculated by the branch nodes using information collected from communications outside the clusters. We use different risk estimators in different scenarios. The use of these metrics will allow us to quantify and compare the collision risks in different scenarios, providing a comprehensive evaluation of the performance of the proposed CBL-G in terms of anticipation and real-time accuracy.

Chapter 2

Adaptive Communication in VANETs: An Improved CBL Algorithm with RSU Integration

Contents

2.1 Introduction

The widespread adoption of Autonomous Vehicles (AV)s requires the users (drivers) to have confidence in their safety, reliability, and compliance. To gain this trust, it is important for AVs to provide clear explanations for their actions and decisions. In this Chapter, we aim to address this issue by proposing a solution for effective V2X communication coordination in critical data routing for cooperative driving automation applications. We focus on improving both V2V and V2I communications, through an adaptive and multi-modal approach.
Our solution involves refining the clustering concept originally introduced in CBL (RIVOIRARD, 2018), to incorporate both V2V communications already present in the CBL algorithm, and V2I communications enabled through the use of RSUs along the road side.

2.2 Chain branch leaf model for routing protocol

2.2.1 Chain branch leaf presentation (CBL)

Chain Branch Leaf (CBL) is a highly decentralized algorithm proposed and detailed in the work of (RIVOIRARD, 2018). CBL follows the principle of creating a hierarchy between communication nodes to build clusters so that each "cluster member" node in a cluster can communicate directly with a "cluster head" node through one hop without the need to go through an intermediate node. Each clus-

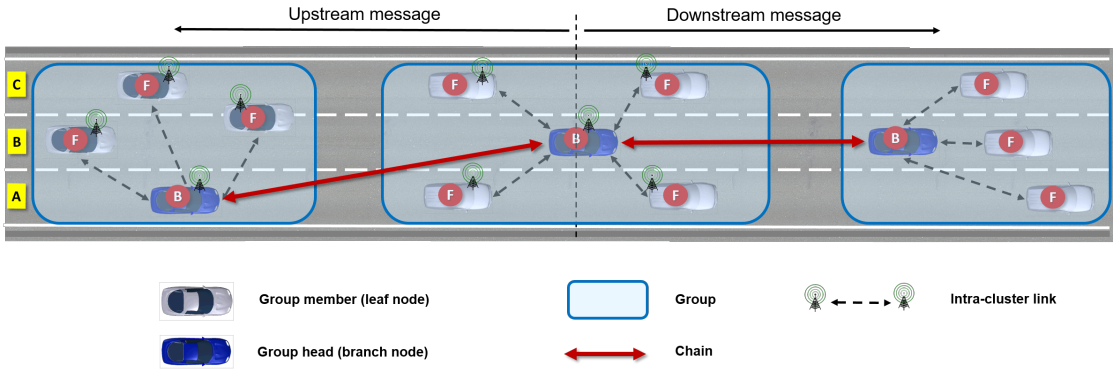

Figure 2.1: Representation of the functional model of CBL on a three-lane highway

ter in CBL has a centralized architecture, with only the branch node being able to communicate with other clusters. As a result, CBL distinguishes two types of nodes: "branch" nodes and "leaf" nodes.

Both types of nodes send periodic HELLO messages to dynamically build a structure called a "chain," which connects the "branch" nodes, and thus the clusters, in each direction, as shown in Figure 2.1 (RIVOIRARD, 2018). The node's communication range is related to the HELLO message range which is represented in Figure 2.2. CBL employs a metric known as connection time to construct stable

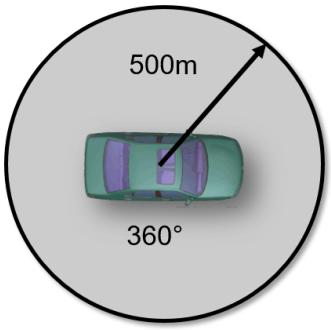

Figure 2.2: The vehicle communication range representation

chains (CT). This metric measures the time it takes for nodes in the network to connect and allows nodes to manage the selection of their branch node.
The following are the definitions of "branch" nodes, "leaf" nodes, chain, and connection time:

1. The "branch" node is the cluster head that is elected by the other nodes (branch or leaf) in its 1-hop neighborhood. It sends HELLO messages like every other node, but it is the only one allowed to send a Topology Control (TC) message, transmit request messages, and participate in the chain construction. By relaying a message, based on the request specified in the header fields, a "branch" node can send it to :

   - Its own leaf nodes;
   - Its own upstream branch ;
   - Its own downstream branch ;
   - Its own branch (in another direction of traffic).

2. A leaf node is an ordinary node that must connect itself to the nearest branch node. If no branch node is detected, the leaf node elects the neighbor that is moving with the lowest speed and in the same direction of travel as its branch. A leaf node generates and transmits only HELLO messages and application traffic data.

3. The resulting CBL Structure (one chain per direction) is comparable to a virtual spinal structure, which could be obtained with the infrastructure. It is maintained through the links that are made between the nodes.
   Each node contains the following parameters:

   - BranchChoice: the address of a branch node selected by a leaf node, BranchChoice is null if its type is the branch ;
   - ChainUP: the address of the branch node chosen to relay information to upstream traffic. The ChainUP field is empty if the node is a leaf node;
   - ChainDO: the address of the branch node chosen to relay information to downstream traffic. The ChainDO field is empty if the node is a leaf node;
   - Connexion time (CT) : is the expected duration of the communication between two nodes Ni and Nj when they keep the same speed.

2.2.2 The periodic control structure

CBL is a proactive algorithm that utilizes a regular "Hello" message transmission to discover its neighboring nodes. The Hello Interval refers to the frequency of the transmission of these messages. The messages sent by node Ni contain information about the neighboring nodes Nj within one hop and the type of link between them. The messages must include eight attributes:

- @Adress, the address of the message-sending node Ni;
- Type, the current type of node Ni (branch or leaf);
- Position, the absolute position of node Ni (Xi, Yi);
- Speed (Vj), in meters per second, of the average vehicle speed of the neighboring node Nj over one second;
- Steering angle in degrees of the average steering angle of the vehicle of the neighboring node over a second;
- @ChainUP, the address of the downstream node;
- @ChainDO, the address of the upstream branch node ;
- @BranchChoice, the address of the node chosen as the relay branch node number.

2.2.3 Chain branch leaf (CBL) algorithm

The CBL strategy is composed of 5 different algorithms explained with more details by (RIVOIRARD, 2018). The general architecture of CBL with the 5 functions is presented in figure 2.3:

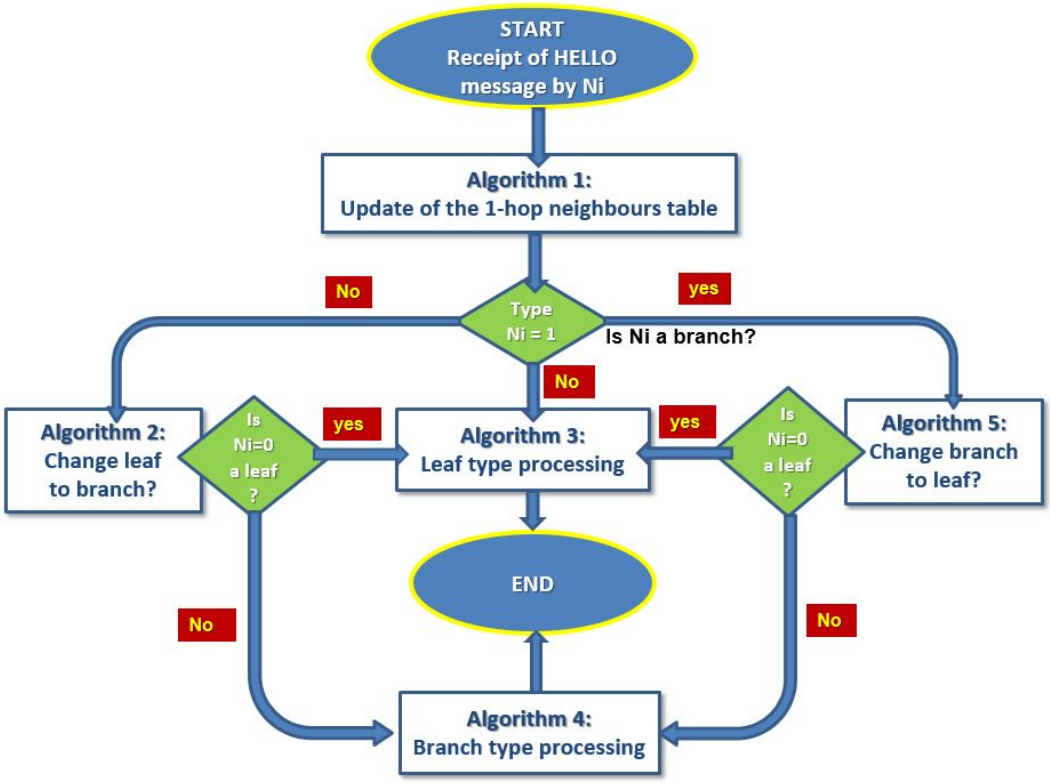

Figure 2.3: CBL algorithm with the 5 different functions. This algorithm is run at the reception of a Hello message

2.2.4 Chain Branch Leaf (CBL) functional diagram

CBL follows a set of steps during its operation. The first step concerns the initialization of the Branch. When a node enters a specific area, it is initially in the leaf state, which means that it must perform certain tasks such as electing the branch node to which it will be linked/attached. The address of this node is stored in its "Branch Choice" variable and this information is then shared with its one-hop neighbours through the "HELLO" messages it sends (RIVOIRARD, 2018).

A leaf node attaches to the first detected branch node. However, it may detect more than one branch node or, conversely, it may not detect any:

- If more than one branch node is detected, the selection is made following these criteria: the branch node is moving in the same direction, the branch node is part of a chain (set of connected branch nodes), and the branch node has the longest connection time. These three selection criteria guarantee that the relay node elected at a given date from among several detected branch nodes will be the one that has the longest radio link time with the electing leaf node. This strategy is applied in order to optimize the stability of a cluster.

- If none is detected, after a waiting period, the leaf node chooses the neighboring leaf node that travels in the same direction and whose relative speed is the lowest, as the relaying leaf node. This election of a leaf node as a branch node initiates the creation of a chain structure and starts the initialization of a new cluster.

The process by which a leaf node transforms into a branch node is as follows:

- Firstly, the node *Ni* checks if it has been designated as both a branch and a leaf node for a duration greater than *C3*HELLO INTERVAL*, as defined in the study conducted by (RIVOIRARD, 2018).

- Secondly, if these criteria is met, Ni examines its own @Ni address within the fields *@HELLO.BranchChoice*, *@HELLO.ChainUP*, or *@HELLO.ChainDO* contained within the *HELLO* message.

- Thirdly, if *Ni's* address is present within one of these fields, it indicates that the node has been elected as a branch node by its neighboring nodes. The node will subsequently update its local variables and record the fact that it has been elected as a branch node by this specific neighbour in its table of one-hop neighbours.

- Finally, if, however, the neighboring node is itself a branch node and has elected Ni as an upstream node, Ni will record the address of this neighbour in its local variable *@ChainUP* and update its local variables accordingly.

A branch node also plays a role in the formation of the chain by electing both an upstream and downstream branch node among its neighboring branch nodes that move in the same direction, if it has elected them. The addresses of these nodes are recorded in the local variables *@ChainDO* and *@ChainUP*, respectively,

and this information is subsequently shared with the node's one-hop neighbours through the *HELLO* messages it transmits. The strategy proposed by the CBL protocol is for a branch node to attach to the first branch node detected upstream of its position. Nevertheless, several types of situations can be met:

- If it detects several of them and has not yet notified its choice to its neighbours, then the branch node moving in the same direction, that is part of a chain, that offers the longest chain time, and whose degree is the highest is elected. The degree of node Nj at a hop of Ni is the number of neighbouring nodes of Nj after excluding the node Ni and the neighbouring nodes at a hop of Ni, this metric is used to identify the neighbouring nodes at a hop that bring the knowledge of new neighbouring nodes.

- If none is detected, after a waiting period of *C2 * HELLO INTERVAL*, the node elects, as upstream branch node, the leaf node which meets the same criteria as before. This election of a leaf node as a branch node extends the chain size with an additional link.

- Once the branch node has added a link to its chain, it does not change its choice until the spatial ordering of the upstream and downstream vehicles with respect to this branch node has undergone permutations.

On the other hand, a transformation of the node from branch type to leaf type is possible if one of the following conditions is fulfilled:

- The validity time elapsed since the date of the last reception of a *HELLO* message from a node having elected it is exceeded

- If it has just passed the node it had chosen as a branch node at the front of its chain

- If it has detected that a branch node downstream from its position has already elected another branch node that is upstream from its position

The neighbourhood table is updated when a *HELLO* message is received from a neighbour.

Despite CBL having demonstrated its ability to effectively handle node communications in different densities, it still has certain limitations. The structure of CBL can be complex, in the event of a node failure, the whole network can be affected, causing communications disturbance.
As a result, the CBL strategy is currently limited to a V2V configuration, but it

can be extended to a V2I configuration in highway areas to ensure a Vehicle-to-Everything (V2X) architecture. This extension would allow for better communication between vehicles and the surrounding infrastructure, enhancing the safety and efficiency of vehicular networks.

2.3 Improving VANET Performance with Roadside Units

Roadside units (RSUs) have been shown to mitigate the limitations of ad-hoc networks and improve performance in a vehicle-to-vehicle communications. Research conducted in (Nguyen et al., 2019) has demonstrated that VANET networks, which facilitate wireless communication between vehicles equipped with communication capabilities and between Roadside Units (RSUs) provide the advantage of low transmission time and high processing density in terms of accounting for mobile nodes, particularly in scenarios of high vehicle density in the coverage area.
CBL has demonstrated its ability to effectively manage communications and nodes in different densities, however it still has some limitations. The structure of CBL can be complex, if one node fails, the whole network can be affected, causing communications disruption/disturbance.
We propose an extension to the Chain Branch Leaf (CBL) routing scheme, introduced in (Rivoirard et al., 2018), by involving fixed communication nodes called Road Side Units (RSUs) to improve its functionality as shown in figure 2.4. The RSUs serve as additional communication points in the network and can potentially enhance the efficiency and reliability of the CBL routing scheme.

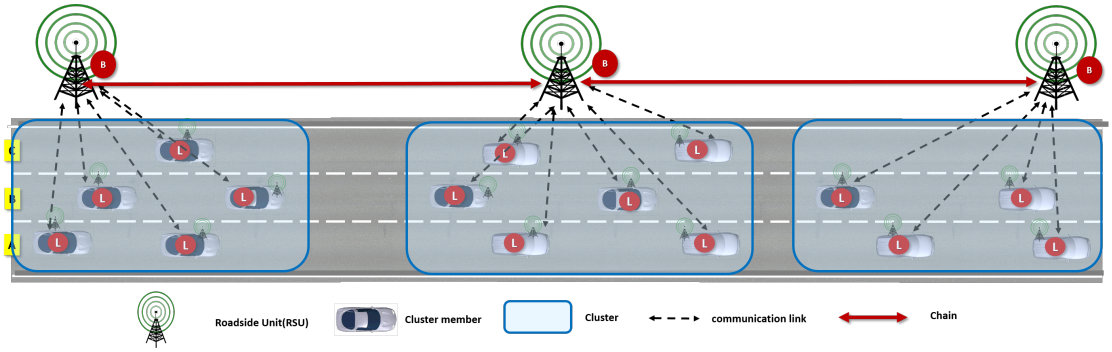

Figure 2.4: The CBL-Infrastructure representation of vehicles on tree lanes high way and full deployment of Road side unit

2.3.1 A Study on CBL-I Routing and RSUs

The exploitation of RSUs in the development of Chain Branch Leaf (CBL) routing scheme is addressed through two different configurations or use cases. The first use case is "free RSUs," where RSUs are placed freely in the network without specific constraint which correspond to the actual RSU state in the physical road which makes it usable in sustainable context. The second use case is "branch RSUs," where RSUs are positioned at specific locations to create branches in the network. In other words, the flexibility of using RSUs in different configurations provides a solution to the challenges of routing and maintaining communication connection in a VANET. And provide a more comprehensive solution to the routing challenges and specially service continuity i.e, maintaining communication connection between mobiles nodes in vehicular ad hoc networks. This can address the issues of limited availability of vehicles equipped with communication capabilities and incomplete infrastructure deployment.

2.3.1.1 First use case (UC1)

We have incorporated RSU nodes into the CBL architecture by using the existing architecture, without any specific requirements for them to act as a "leaf" or "branch" of the CBL, as illustrated in Figure 2.4. In other words, these RSU nodes can be thought as static vehicles parked along the roadside. They do not have a predetermined role in the network and can be used in either a "leaf" or "branch" capacity, depending on the needs of the network at any given time. The goal of introducing these RSU nodes is to enhance the network's communication capabilities and improve its overall performance. It is also to examine whether the CBL algorithm can adapt to this new element and choose the most appropriate type.

2.3.1.2 Second use case (UC2)

The RSUs in the simulation is set to operate as "Cluster Head" (or "branch" state) by default and are unable to change to a "leaf" state. This configuration remains unchanged throughout the simulation. This means that these RSUs cannot assume a "leaf" state, which is typically used to extend the communication range of the network by relaying data from other nodes. Instead, they must serve as "Cluster Head" or central points of communication in the network.

2.3.2 Adaptation of control Message in CBL-I Architecture

The new Chain Branch Leaf Extended with Infrastructure (CBL-I) protocol requires adaptation of the periodic control message "hello". In the original CBL

architecture, all nodes are treated as identical and mobile which we refer to as category OBU. In the revised CBL-I architecture, a new category of node, referred to as the RSU, is introduced.
The messages transmitted by node Ni should include an enumeration of the addresses of neighboring nodes Nj that it is aware of, along with the nature of the connecting link. The messages must also encompass the following nine pieces of information:

- **Adress**, the address of the node Ni that sends the message ;
- **Type**, the current type of node Ni (branch or leaf) ;
- **Category**, the category of the node Ni (an OBU mobile node or a RSU fixed relay point);
- **Position**, the absolute position (Xi, Yi) of the node Ni ;
- **Speed**, in m/s of the average speed of the vehicle Vi over one second;
- **Steering angle**,the average steering angle of the neighboring node's vehicle over a second ;
- **ChainUP**, the address of the downstream node;
- **ChainDO**, the address of the upstream branch node ;
- **BranchChoice**, the address of the node chosen as the relay branch node number.

2.3.3 Implementation and Simulation Environment of CBL-I Protocol

The R2012b version of Matlab, was used to implement the CBL protocol. For our simulation to enhance CBL we will be reproducing the simulation parameters that are detailed by (RIVOIRARD, 2018). Therefore we used the KrauB model implemented in SUMO. the speed limit is set at 130km/h for the network. this speed corresponds to the legal speed limit of the freeways in France.
The parameters used for the traffic generation are the following: the acceleration capacity of the vehicles is $2m/s^2$ and $1m/s^2$ for the trucks, the deceleration is $3m/s^2$ for vehicles and $2m/s^2$ for the trucks, the imperfection of the driver is between (0 and 1s), the inter-vehicle time desired by the driver is 1s, the minimum space between two vehicles in case of congestion is 2.5meters for vehicles and 5 meters for trucks, and the maximum speed of the vehicle is 150km/s and 130km/h

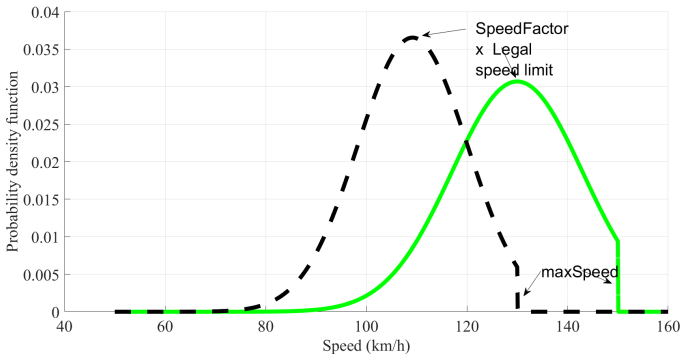

Figure 2.5: Representation of the probability density of the speed used by (RIVOIRARD, 2018) for CBL implementations for vehicles and trucks in the case of maximum authorized speed of 130km/h

Table 2.1: traffic simulation values and parameters

Car traffic (veh/h/direction)	**Truck traffic (veh/h/direction)**	**Density**	**RSU**
500	100	S1 - Low	UC1
			UC2
2000	400	S2 - Medium	UC1
			UC2
4000	800	S3 - high	UC1
			UC2

for trucks. To simulate a realistic driving behaviour it is necessary to use speed distributions otherwise all vehicles would have the same speed and there would be no overtaking of vehicles which is unrealistic. Therefore two other parameters have been introduced in order to use the distributions "speed factor" is set to 1 for vehicles and 0,84 for trucks and "speedDev" is set to 0.1, which will result in a speed distribution for which 95% of the vehicles drive at a speed ranging from 80% to 120% of the legal speed limit, as shown in figure 2.5.

The road environment used to illustrate the scenario proposals is a standard French and European three-lane one-way highway, 5 km long, where vehicles travel from west to east. Line-of-Sight (LOS) propagation model is used to simulate radio wave propagation in a short-range environment where there are no obstacles between transmitters and receivers. The usual configuration of a RSU is to be affiliated with a controller in the same way as a base station is with its controller. We assume that all nodes on the road are equipped and can communicate with other nodes on the road whether they are vehicles (OBU) or RSU using 802.11p

technology. For the following scenarios, Automated vehicles, on the other hand, are equipped with a range of sensors and communication systems that allow them to operate over a larger area. Vehicles communication range is 500 meters and RSUs are positioned at 350 meters from each other to take into account their communication range. The range of an RSU can be influenced by several factors, including the frequency band used, the transmission power, the environment, and the receiving antenna. In an urban or suburban environment, a range of 350 meters is typical for RSUs.
The area of the simulated road network is empty of vehicles at the initialization of the system and is loaded continuously, as the vehicles arrive in the simulation space. Table 2.1, presented by the author (RIVOIRARD, 2018) summarizes the traffic densities: low, medium, and high, by hour and by direction. With respect to the multitude of vehicles for each of the three densities, we use a ratio of 1/6 trucks and 5/6 cars. We estimate that the high-density values are 100% percent of the total vehicles on the road, medium density is 50% percent, and low density is 12,5%.

2.4 Impact of Free state and Branch state of RSUs on CBL Network Formation

From the initial simulation results in the two representatives Use Case (UC): (UC1) and (UC2), we can observe that RSUs have been successfully introduced into the initial CBL communication architecture and are considered zero-speed roadside vehicles. Each vehicle is equipped with an OBU (On-Board Unit), which is used to differentiate RSUs from stationary or broken-down vehicles on the roadside. Several metrics are used to evaluate the results including the number of chains in the network, the number of leaves per branch, the connection time between the leaf and its branch, and the duration of a node in the branch state. Following figures curves as mentioned in the legend: the mean value (in red), minimum value in (–), maximum in (-.-) and the distribution of a variable using quartiles (in blue). the last one allows to visualize the dispersion of the data.
Firstly, when the RSUs are free and close to each other, we notice that within the first few seconds, they become branches and form a stable chain. Vehicles arriving at different times connect to them. This shows that when the RSUs are in a free state, the distance between the RSUs has an impact on their state (leaf or branch). We have suppose that at 350 m the RSUs have a strong enough range to have high-quality communication with the other RSUs and therefore a stable enough chain covering the road of 5000m for the vehicles to attach to it. This information should be taken into account when deploying RSUs on the network.

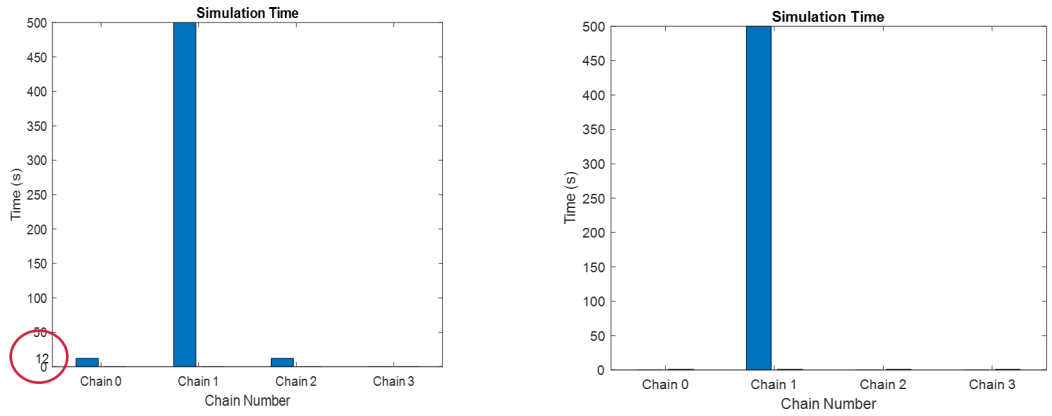

Figure 2.6: Scenario (S1)- Number of chains in the network for use case 1 (UC1) and use case 2 (UC2)

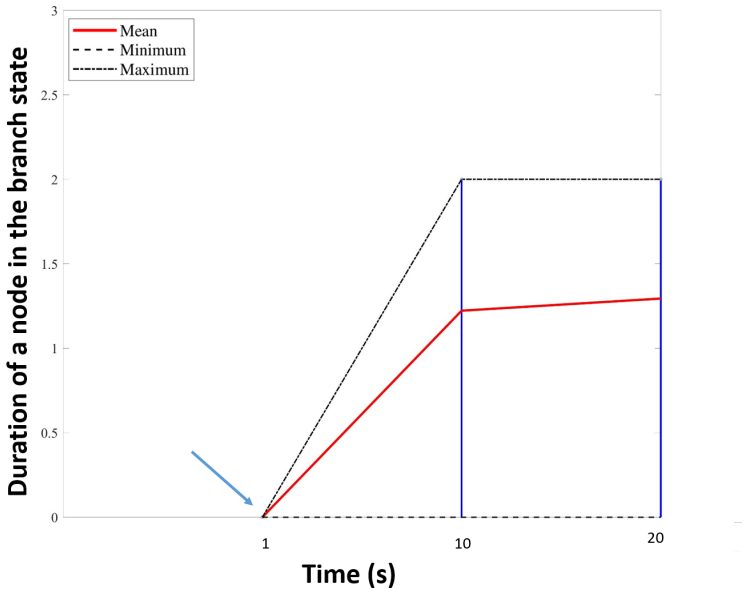

Figure 2.7: Scenario (S1)- UC2 figure showing The duration of a node in the branch which start at 1s

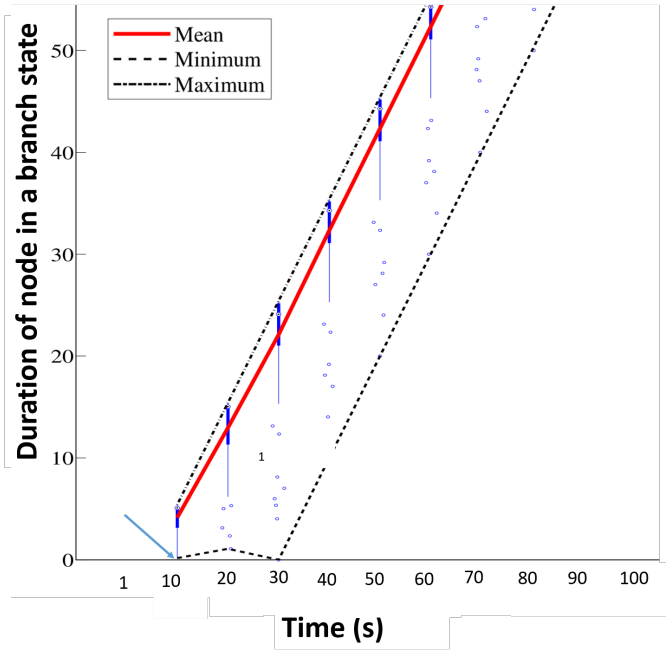

Figure 2.8: Scenario (S1)- UC1 figure showing The duration of a node in the branch which start at 10s

The simulation values obtained are taken when the network is stable (between 150 s and 500 s). For low density (80 vehicles on 3 lanes of 5 km), the second use case UC2 seems to be more efficient in terms of the number of chains in the network. We notice that the chain is built by the RSU branches at 1 s and becomes stable (only 1 main chain) faster after 3 s. The formation of the chain (figure 2.6) for the UC1 case requires more time in view of the instability of the types of nodes in the network, it will take 12 seconds on average to have a single chain. This is due to the large number of branch election steps compared to the second use case. Indeed, the leaf node must find a branch node to connect to. If it can't find one, it will elect a leaf node as a branch, so the node must become a branch, and then it will look for an upstream branch node to form a chain.
This requires some adaptation time compared to UC2, where there are already branches. Each of the branches will look for an upstream branch to form a chain. The number of branch nodes per chain and the number of one-hop neighbors gives the same results for the first and second use cases (average of 7 one-hop neighbors) since it is related to the density of the highway. That is, in a medium density, we get 16 branches per chain for a low density for the first use case, and 18 branches per chain for the second use case.

For the second use case and with low density, the attachment of the leaf nodes

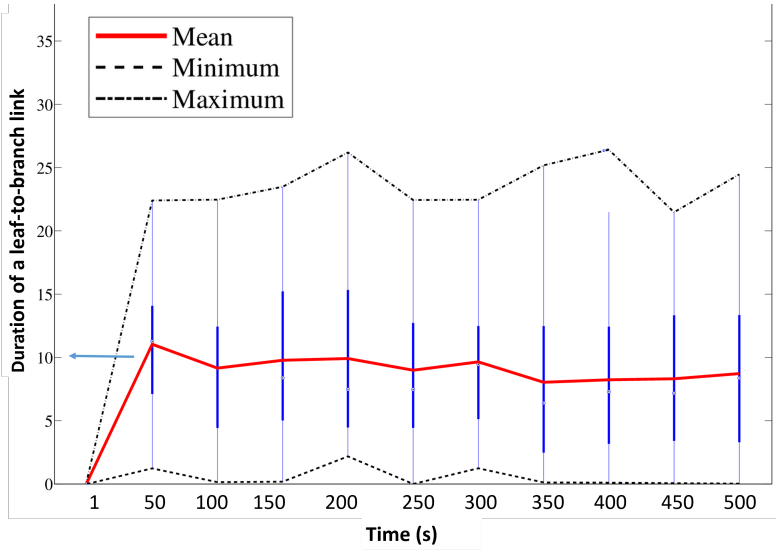

Figure 2.9: Scenario 1 - UC2- The leaf to branch link duration

to their branches (figure 2.7) starts at 1 s so immediately. Because the RSU branch chain is already formed on the road from the beginning to the end of the simulation. So vehicles only have to connect to it, unlike the UC1, which starts later at 10 s (figure 2.8), like CBL-V2V where it also starts at 10s.. This is because some of the vehicle nodes must become branches to form the chain. Same result are observed for medium and high density (S2 and S3).
We studied the stability of the connection/link by measuring the duration of the link between the leaf and the branch, we notice a difference between the first and the second use case since UC1 shows a longer link duration of about 25s, thus more transmissions. While in the UC2, the link duration is about 10 s (figure 2.9). This behaviour is due to the fact that with free RSUs, a leaf can be attached to a vehicle branch. This results in a longer connection. Unlike the case where the branches are RSU type (UC2), there will be a disconnection whenever the vehicle leaves the RSU coverage. Figure 2.9 show link duration between the leaf and the branch in low density (S1) and UC2.
In Use Case 1 (UC1) for Scenario 3, the connection time between a leaf and its branch is 20 seconds on average and 28s maximum as can be seen in Figure 2.10. whereas in the original CBL-V2V, each leaf node remains attached to the same branch for maximum 30 seconds and 21.3s on average.
The evaluations carried out by simulation in (Belmekki et al., 2020), for the first use case where the RSUs are free, show that for all the distribution modes previously explained, the RSUs automatically transform into branches, we deduce that the RSUs are the best candidates to build a stable chain.

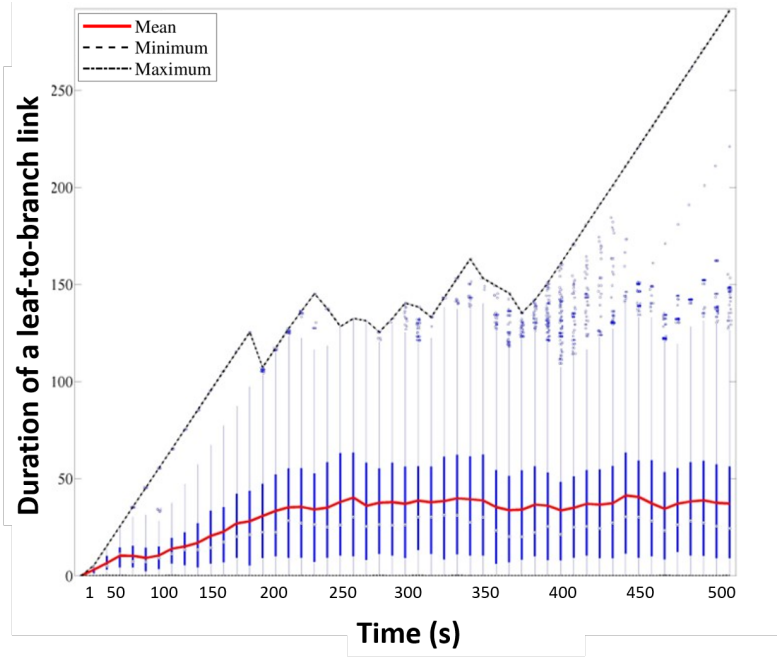

Figure 2.10: Scenario 3 - UC1-The leaf to branch link duration

2.5 Roadside unit communication nodes distribution models

By applying coordination modes to UC1 and UC2, we observed the behavior of nodes in a Full Roadside unit distribution that can be considered as an ideal environment (A) and then tracked their changes in adverse and degraded situations (B, C, D, and E). We define those modes in the following sections. The choice of positioning the RSUs at less than 350 meters apart is made to enable automatic transformation into branches and to form a chain between them. This distance is within the maximum range of 500 meters for the RSUs to detect each other but it also meets the criteria for selection defined by the CBL algorithm as described by (RIVOIRARD, 2018). Indeed, it is observed that when they are at a greater distance, the chain is formed inconsistently, which very often leads to transformations from branch to leaf and from leaf to branch as we can see in figure 2.11, which means an unstable chain because at this distance there are mobile vehicles that can meet the conditions of election of the branch and be a better candidate.

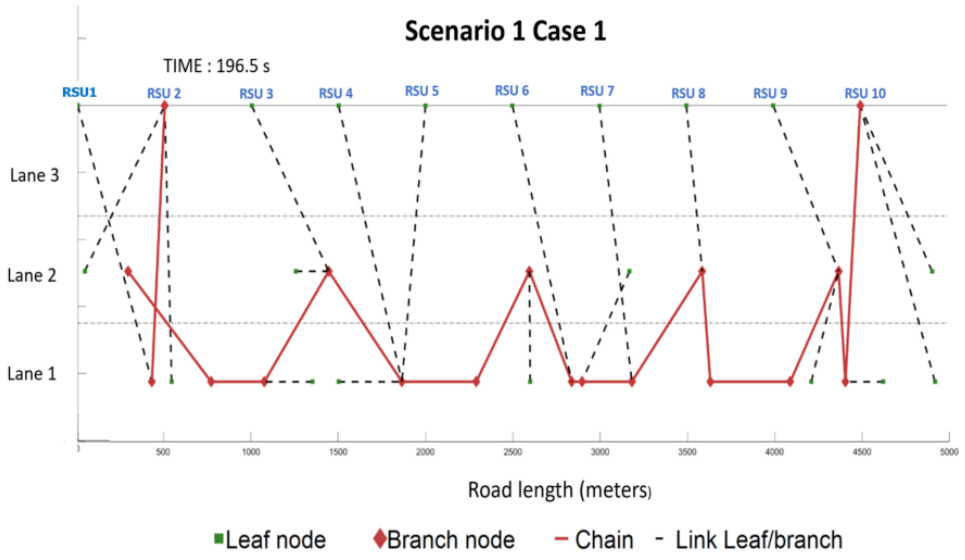

Figure 2.11: Chain formation observation in the CBL structure with RSU in a free state positioned at more then 350 meters

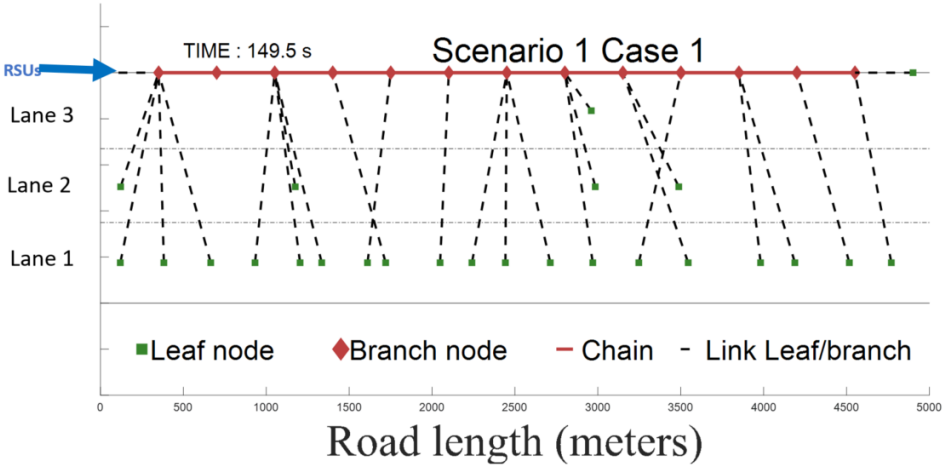

Figure 2.12: S1-UC1-Chain formation when RSUs are fully deployed along the road side (simulation A)

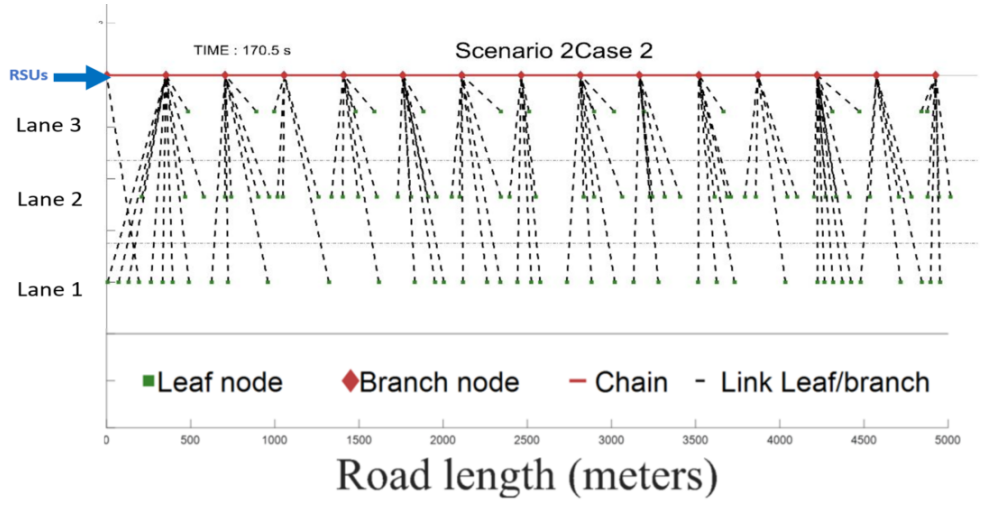

Figure 2.13: S2-UC2-Chain formation when RSUs are fully deployed along the road side (simulation A)

2.5.1 Simulation of a Full Roadside unit distribution (A)

We performed simulations on a road network with roadside perception units (RSUs) that were already deployed and present throughout the road. The first RSU was positioned at the beginning of the road section and the rest of the RSUs were spaced apart every 350 meters, as shown in figure 2.12. In the first UC1 (figure 2.14), RSUs tend to establish connections and form a branching network. This happens when the RSUs are within the range of each other, and one RSU elects another as its branch. This process continues until all RSUs are part of the network. In the second UC2, the RSUs automatically form a chain because they are in the branch state (figure 2.13). All vehicles that enter the network are attached to the RSU chain. This way, the vehicles can communicate with each other and the RSU network to improve perception and decision-making capabilities.

2.5.2 Simulation of vehicles leaving an infrastructure zone (B)

RSUs are deployed at the beginning of the route and along part of the route. For the first case (UC1) When vehicles leave an RSU area, the chain is built at the beginning of the route by RSUs once the vehicles leave the RSU coverage area, the last RSU elects the nearest node that meets the downstream branch conditions, in this way the chain is established on the route continuously. It is the same for UC2 A neighboring leaf node is selected to extend the chain to the exit of a RSU zone.

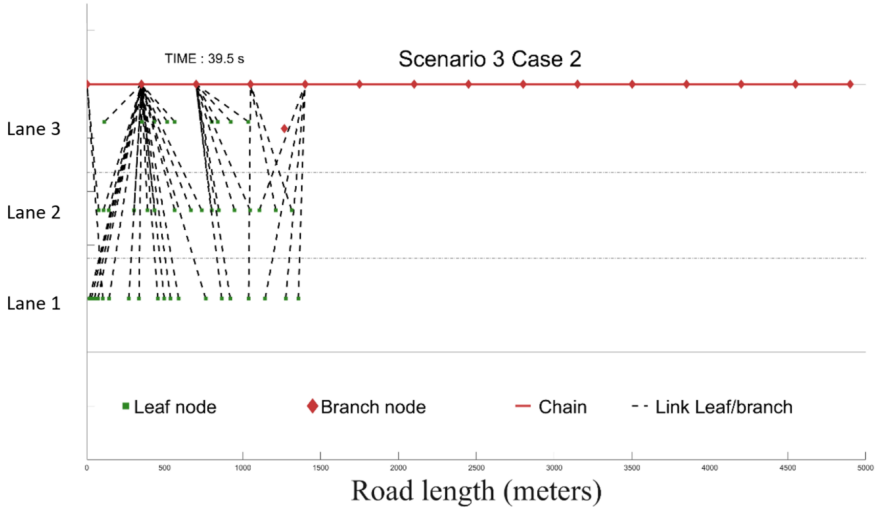

Figure 2.14: S3-UC2-Chain formation when RSUs are fully deployed along the road side (simulation A)

The illustration 2.15 represents the deployment of the RSUs, with the X axis representing the length of the road (5000 meters) and the Y axis representing the lanes (3 lanes). The RSUs are positioned on the upper roadside, with 4 RSUs at the beginning of the road.

2.5.3 Simulation of vehicles entering a RSU zone (C)

The RSUs are deployed along a specific portion of the road and are positioned at the end of the route (as shown in figure 2.16). In both use cases UC1 and UC2, the chain of vehicles is initiated at the start of the road by the entering vehicles. As the vehicles progress along the route and enter the RSU coverage area, they become connected to the chain of RSUs, which also form a chain along the same road. The merging of these two chains results in a single unified chain of both vehicles and RSUs along the route.

2.5.4 Technical issues causing the absence or malfunction of some RSUs in the simulation(D)

To simulate cases of total absence of RSUs or cases where physical and/or technical problems are encountered on some RSUs, we have simulated disconnections of RSUs that cause blind zones with no communication possibilities. Figure 2.17 is a screenshot of Chain formation for scenario 1 UC1 for simulation D, the X axis represents the length of the road which is 5000 m, and the Y axis represents the

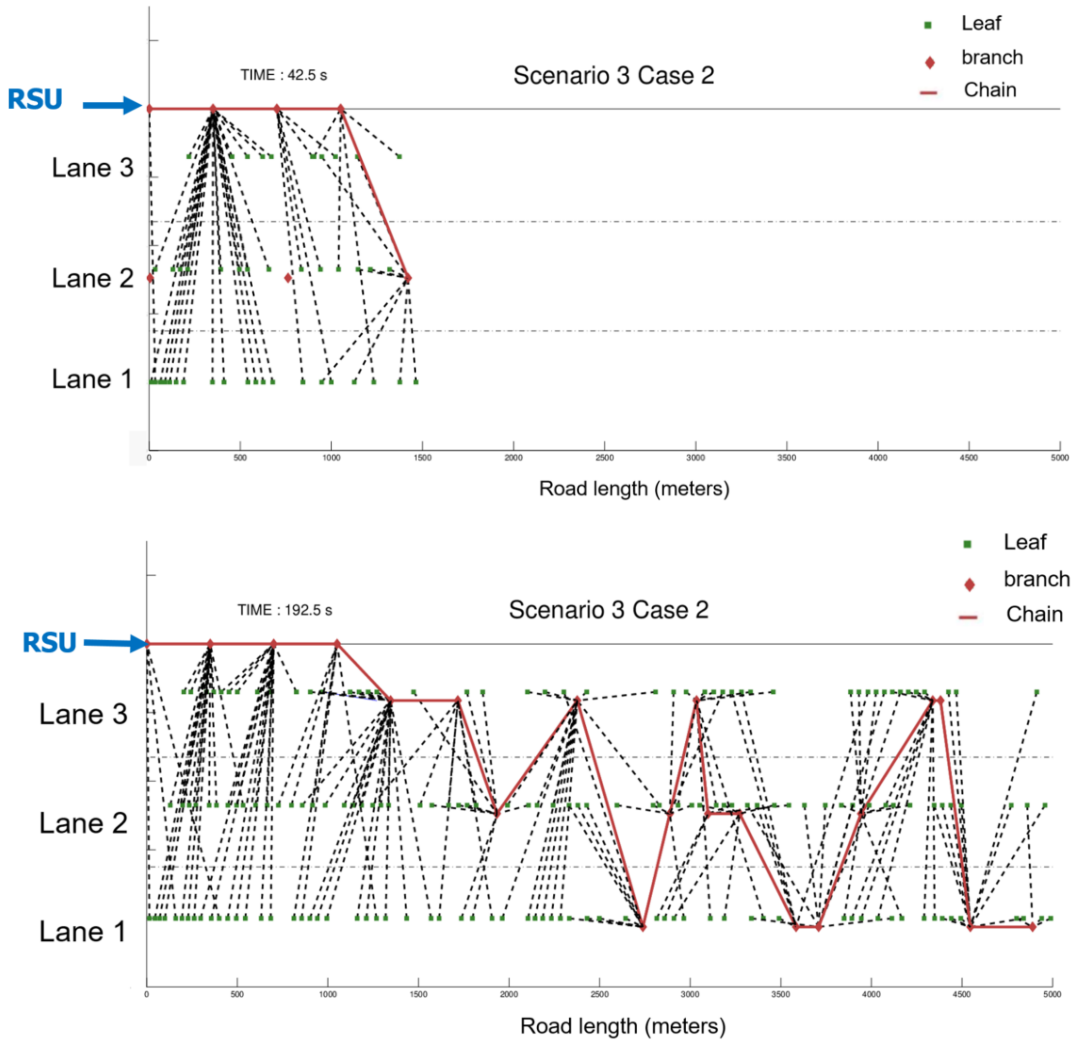

Figure 2.15: S3- UC2- Chain formation for simulation B when leaving a RSU area at different times (42,5 sec) and (192,5 sec)

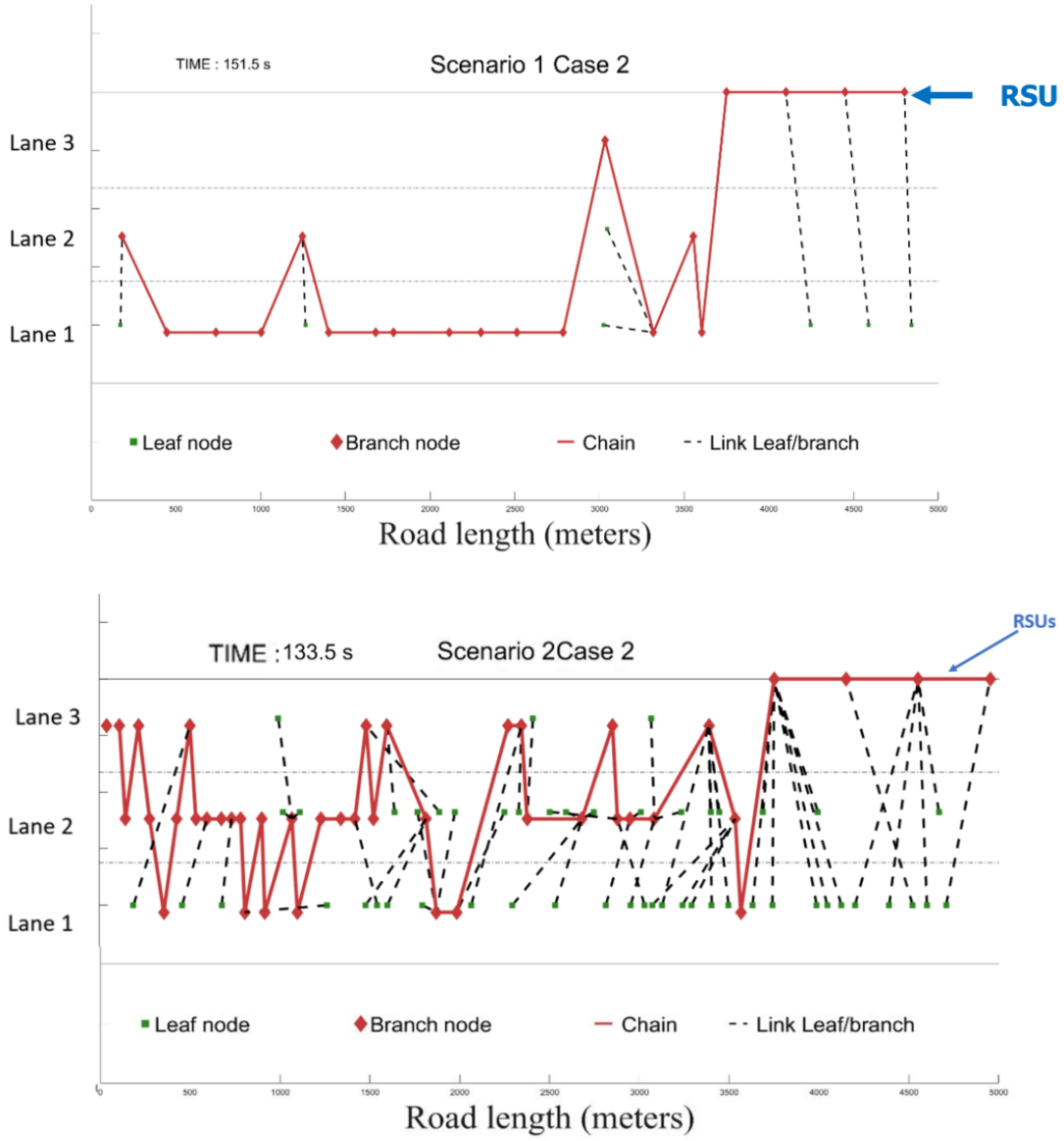

Figure 2.16: Scenario 1-2 - UC2 - Road structure for the Simulation of vehicles entering a RSU zone (C) at moment 105,5 sec and 151,5 sec

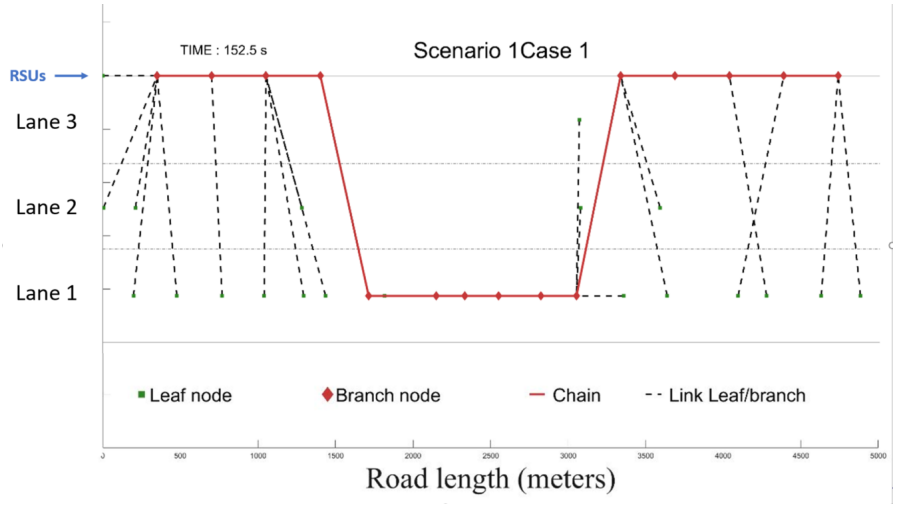

Figure 2.17: Scenario 1 - UC1 - Road structure for the simulation of absence or presence of technical problems on some RSUs

lanes (3 lanes).
The RSUs are positioned on the upper roadside: 5 RSUs at the beginning of the road and 5 at the end with an uncovered area in the middle. For (UC1), the vehicles connect to the branches of the RSU chain. As soon as they leave the RSU area and before entering a new RSU area, we observe for (UC1) and (UC2) that CBL-V2V takes over and the "vehicle" nodes turn into branches to maintain the chain.
Figure 2.18 shows Chain structure for scenario 3, UC1, it illustrates the dynamic changes in the formation of a vehicular chain as it moves through a connected transportation system. At the entrance, the Road Side Units (RSUs) act as branch points and form the initial chain with incoming vehicles. As the chain moves through an empty area, the vehicles continue to connect to each other, forming a chain without the presence of RSUs. Once the chain enters a new RSU zone, the vehicles switch back to connecting to the RSUs, as they are deemed more reliable as branch points compared to mobile branches. This dynamic process of chain formation highlights the importance of having both RSUs and connected vehicles in ensuring a high-quality of service in automated mobility.

2.5.5 Deployment of RSUs as relay points in blind spots (E)

In the scenario of a partially deployed RSU network, the deployment is limited to a portion of the road to simulate the lack of RSU deployment. Specifically, the RSUs are only present over a distance of 1 km, from 2500m to 3500m along

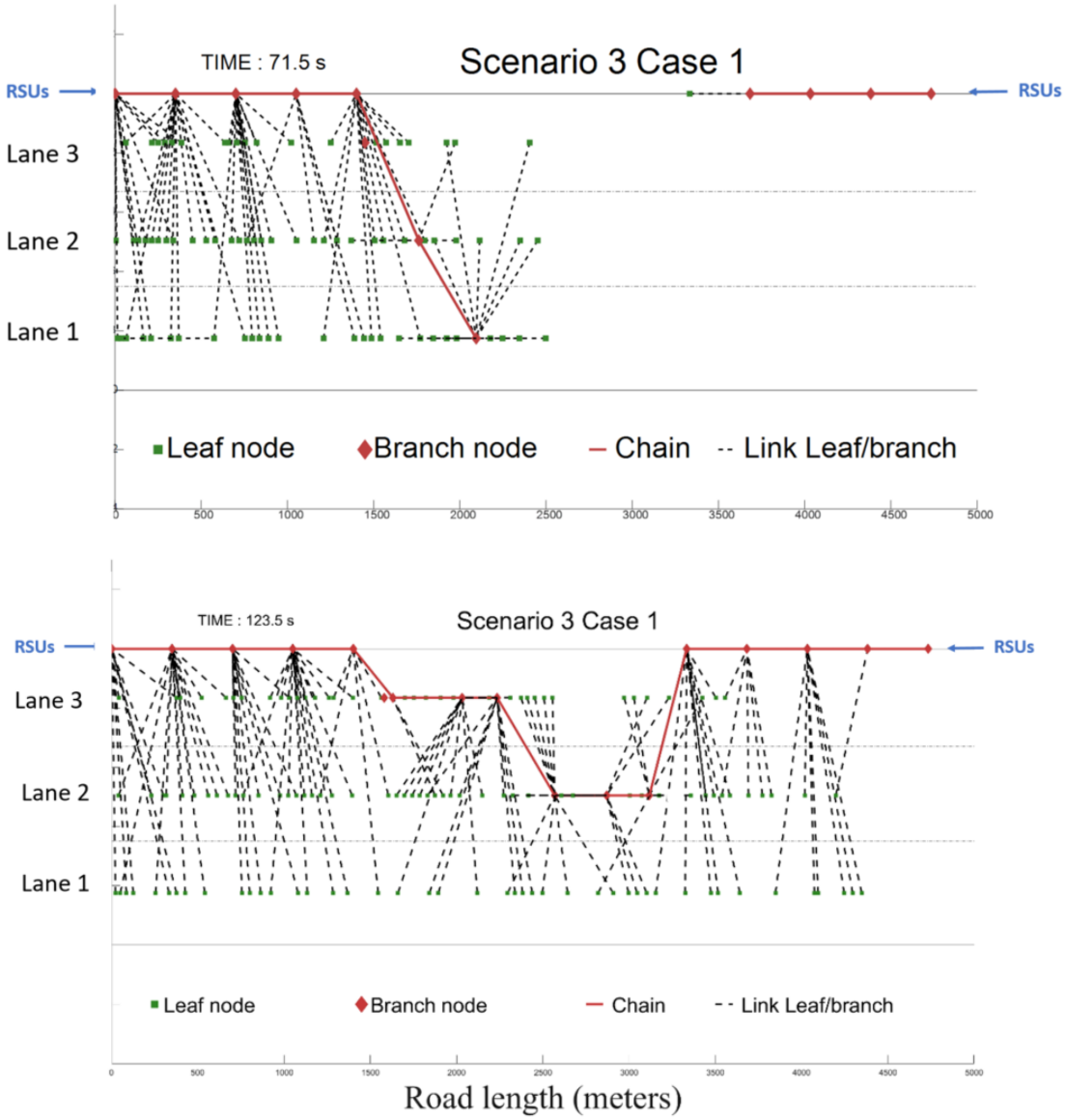

Figure 2.18: S3- UC1- Evolution of Chain formation for simulation D when Technical issues causing the absence or malfunction of some RSUs at different times (71,5,5 sec) and later at (123,5 sec)

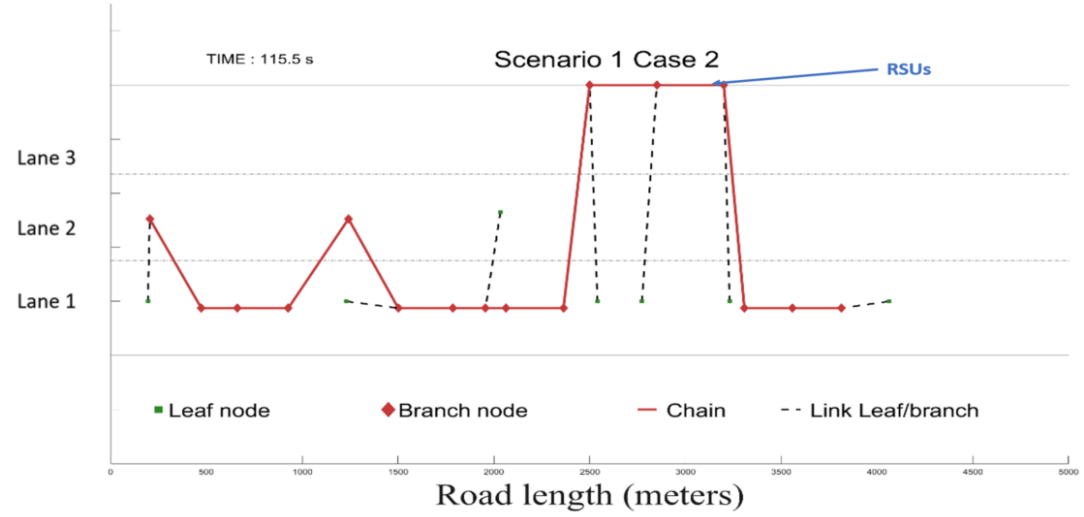

Figure 2.19: Scenario 1- UC2 - Road structure for the simulation of Deployment of RSUs as relay points in blind spots (SIMULATION E)

the 5 km road. As shown in figure 2.20 for Scenario 2 and scenario 3 for UC2, figure 2.19 for the scenario 1 and UC2. For both use cases (UC1) and (UC2), the RSUs located at the edge of the road section tend to branch off and form a chain, regardless of the presence or absence of other RSUs in other sections of the road. In UC1, when vehicles are outside the RSU coverage area, they form their own chain. Upon entering the RSU coverage area, the two chains (vehicles and RSUs) merge to form a continuous chain.
Similarly, in UC2, the RSU chain is formed and all vehicles are automatically attached to it, resulting in a continuous chain covering the RSU deployment zone.

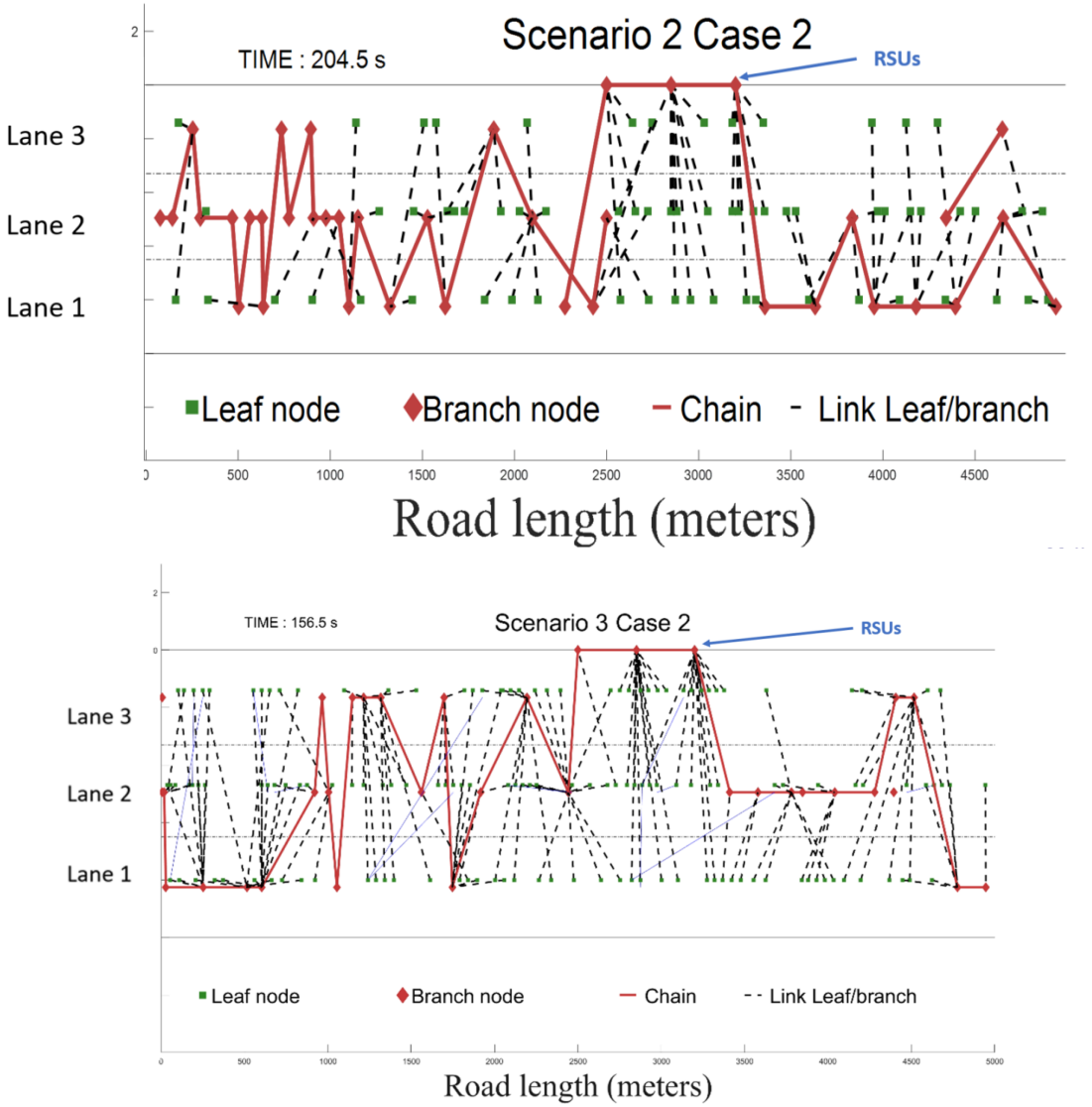

Figure 2.20: Road structure for the simulation of Deployment of RSUs as relay points in blind spots (SIMULATION E) for Scenario 2- UC2 and for scenario 3 UC2

2.6 Conclusion

The simulation results of UC1 and UC2 demonstrated the successful integration of RSUs into the CBL communication architecture. The close proximity of free RSUs leads to stable chains, enabling vehicles arriving later to attach to them. However, the distance between RSUs is a crucial factor that impacts the state of the RSUs in the chain, determining whether they act as leaf or branch nodes. Close RSUs tend to form stable chains, allowing vehicles to communicate with each other and access the Internet. But as the distance between RSUs increases, the stability of chains decreases, causing RSUs to switch between leaf and branch nodes, which affects the network's performance. Leaf nodes have limited connectivity and can only communicate with nearby RSUs or vehicles, while branch nodes have a broader coverage area and can forward messages from leaf nodes to other parts of the network. To ensure network stability, the distance between RSUs must be optimized based on the expected traffic density and network coverage requirements.
For low density, UC2 is more efficient in terms of the number of chains in the network, whereas the formation of the chain in UC1 takes more time due to the instability of node types. The stability of the connection between leaf and branch was measured by the duration of the link, with UC1 having a longer link duration due to leaf nodes being attached to vehicle branches. In contrast, UC2 has branches in the form of RSUs, resulting in a shorter link duration with disconnections when vehicles leave the RSU coverage. The evaluations showed that RSUs are the best candidates to build a stable chain.
Therefore, this chapter proposed an algorithm for adaptable communication in VANETs that leverages both V2V and V2I communication via RSUs. The integration of RSUs into the CBL algorithm was tested in UC1 and UC2, showing its behavior in both ideal and degraded environments. Based on these observations, an optimal coverage strategy was developed to improve the quality of service for critical functions such as risk assessment and accurate location.
In the upcoming chapter, we will delve deeper into the topic of isolated nodes and clusters, exploring a strategy that seeks to optimize coverage through a distributed and dedicated RSU topology. Furthermore, we will examine how to redirect isolated nodes and vehicle clusters to RSUs for enhanced connectivity.

Chapter 3

The CBL-Gateway (CBL-G) Protocol for a high quality of service automated mobility

Contents

3.1 Introduction

The main issue with embedded sensors in AV concerns their limited ability to react only to nearby events occurring in the sensor field of view. However, for safer operations, AVs must predict and anticipate distant events.
To achieve this goal, it is essential that C-ITS provide efficient communication architectures and strategies that guarantee a high QoS in terms of accuracy, certainty, accessibility, availability, and continuity. Moreover, the quality aspect also is related to the capability to send messages and data in a constrained time (low delay and latency).
Cooperation among interacting communication "nodes" is thus critical for establishing and maintaining links between vehicles (V2V) or between vehicles and infrastructure (V2I). However, communication links can be disrupted in certain situations, such as vehicles leaving the communication area or high vehicle speed limiting the stay in a specific area.
The goal is to create a dynamic communications clustering strategy with a distributed and dedicated RSU topology for optimal communications coverage in highway areas using both V2V and V2I configurations.
The CBL-I model is found to effectively integrate Road Side Units (RSUs) and handle V2I communications. However, the model also creates a significant number of disconnections from one RSU area to another, this impact the connection duration, this results in a reduced amount of data transmission leading to data loss. and more importantly, there is no mechanism available to prevent node isolation.
In this chapter, an improvement of the CBL strategy is proposed with the implementation of a gateway mechanism (CBL-G). The objective of CBL-G is to develop a dynamic communications clustering strategy with a distributed and dedicated RSU topology to guarantee optimal communications coverage and better continuity of data access.
In the next section, we aim to enhance CBL-I presented in chapter 2 by using RSU as the gateway for isolated node processing, which will lead to better communication coverage.

3.2 Enhancing Communication coverage: The CBL-G Extension

The proposed Chain Branch Leaf extended with Gateway (CBL-G) enables both V2V and V2I communication through the use of RSUs as gateway nodes. The CBL algorithm, as detailed in section 2.2.1, is limited to V2V communication.
The CBL-G algorithm builds upon the fundamental principles of the CBL algo-

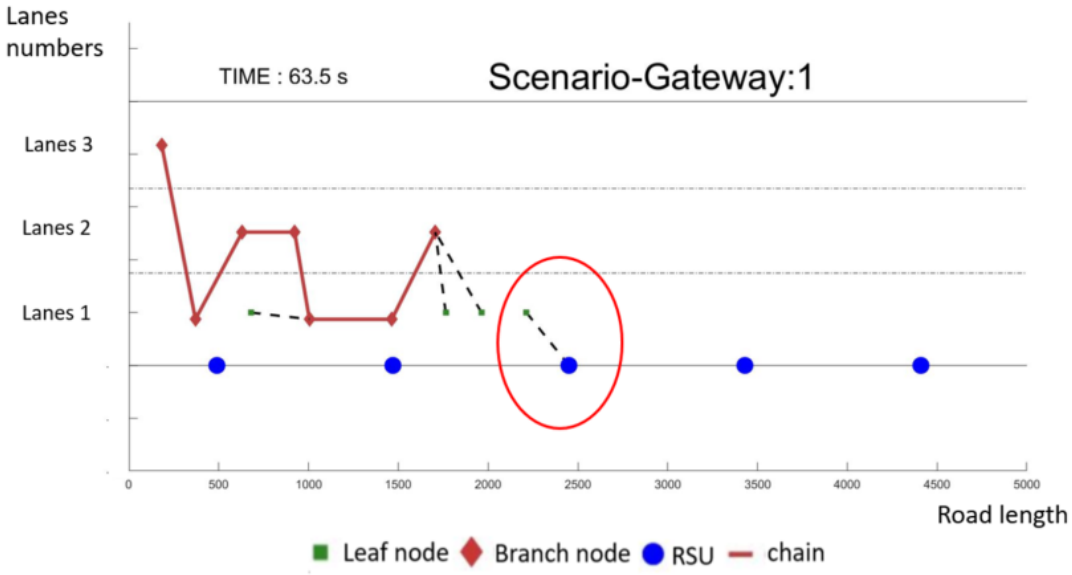

Figure 3.1: Example of an isolated node on lane 1, which connects to the nearest gateway RSU (their link is circled in red), at time t=63.5 seconds

rithm, which includes leaf, branch, and chain nodes, by incorporating roadside units as a new type of gateway node. These RSUs act as a relay point to provide communication for isolated nodes within the network. This extension aims to enhance the overall communication coverage and improve the QoS for critical functions such as risk assessment and accurate location determination.

3.2.1 Isolated node definition

A node is considered isolated if it has no neighbour at a hop if it is not connected to any branch and is not part of the chain. In this case, this node will have to connect to the gateway (RSU) that it detects in its neighborhood.
Illustration 3.1 clearly shows an isolated leaf node (green square) circled in red, this node is isolated from the rest of the other nodes that form a chain (red lines) connected (drawn in black) to the RSU closest to its position (blue point).

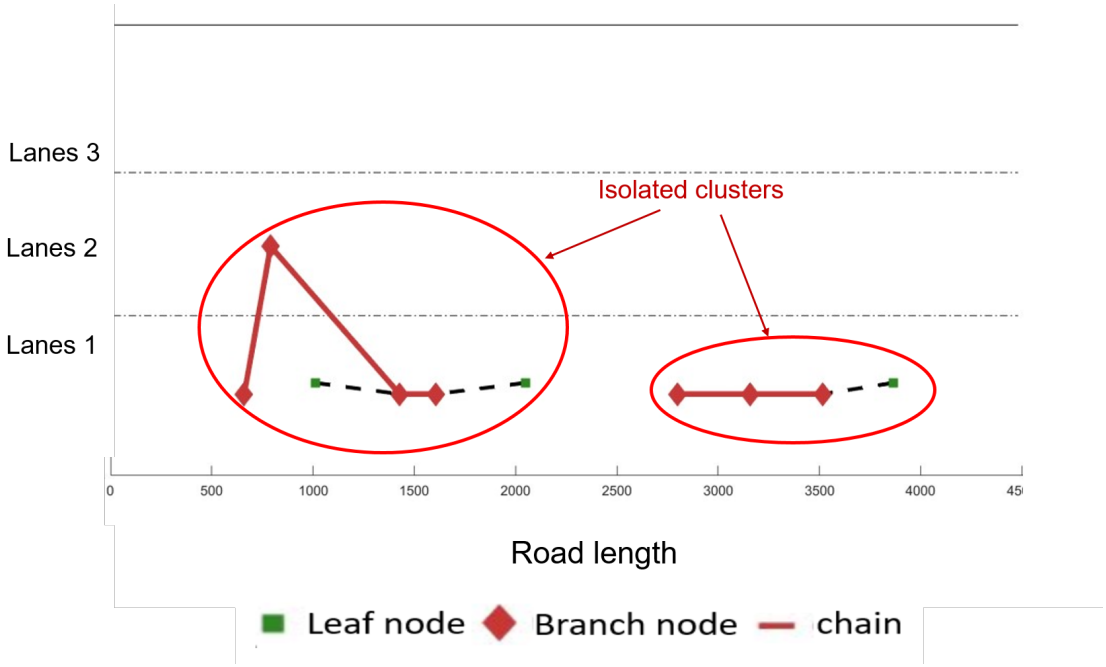

Figure 3.2: Illustration of two clusters out of isolation from each other

3.3 The chain branch leaf-Gateway protocol (CBL-G)

3.3.1 The CBL-G functional diagram

Upon entering the route, a leaf node seeks to connect to a branch node one hop away from its current position. The discovery of the neighbourhood is done by periodically (1s) sending the message HELLO. This discovery is continuous for all nodes even after being attached to a cluster.
If the node is isolated, i.e. it does not detect other nodes in the vicinity, it will select the RSU as the branch it sees near its position.
Once a branch node enters its perimeter, it will detect a potential branch in its neighbourhood. It then disconnects from its RSU to connect to the branch.
The RSU has acted as a relay point for the isolated vehicle. The vehicle was able to connect to the infrastructure via the RSU while the isolated node found a branch to connect to, thus avoiding the isolation of the node. Once the isolated leaf nodes are attached to the RSU, they continue to discover the neighbourhood by the periodic message "HELLO" as shown in the figure 3.1. Once this isolated leaf node detects another node in its vicinity, it will carry out the treatment applied

in CBL, i.e. it will calculate the connection time (CT) that it offers if it is greater than that offered by the RSU, it will elect it as a branch to connect to.
Afterward, the branch in turn will look for another branch with which to form a chain, if it doesn't find one, it will elect a leaf as the front branch, and the other nodes of the route will detect that there are branches and they will connect to them.
The diagram represented in figure 3.3 unwinds the mechanism of CBL-G from the reception of a Hello message until the end.

3.3.2 Defining a new type of node

Each node registers its variables, among them, its type which has been defined in the section 2.2.1 as being the current type of the node Ni̇n the new version of CBL-G, we introduce a new type of node. We thus obtain three types of nodes which we define below:

- Type=1, node Ni is a branch
- Type=0 the node Ni is a leaf
- Type=3 the node Ni is a gateway

3.3.3 Requirement of the node gateway

The requirements for the node gateway, also known as RSUs, in the CBL-G algorithm RSUs are designed to act as a relay point to provide communication for isolated nodes within the network. In order to achieve this, vehicles should be equipped with appropriate hardware and software to communicate with both V2V and V2I communication. Additionally, they should have the ability to detect and connect with nearby nodes and to process messages received from those nodes. It is likely that the RSUs must have a reliable and high-speed communication capability in order to provide a QoS for critical functions such as risk assessment and accurate location determination. The node gateway should be designed to ensure high availability, meaning it should be able to handle failures and provide continuous service. The node gateway should be easily configurable to meet changing business requirements and accommodate different use cases. In small networks with low traffic levels, a discovery frequency of once per second may be sufficient. However, in large networks with high traffic levels, a faster discovery frequency may be required to ensure that the network topology remains accurate and up-to-date. However, in high density networks there are very few cases of isolation so we keep the 1 second configuration for all densities studied.

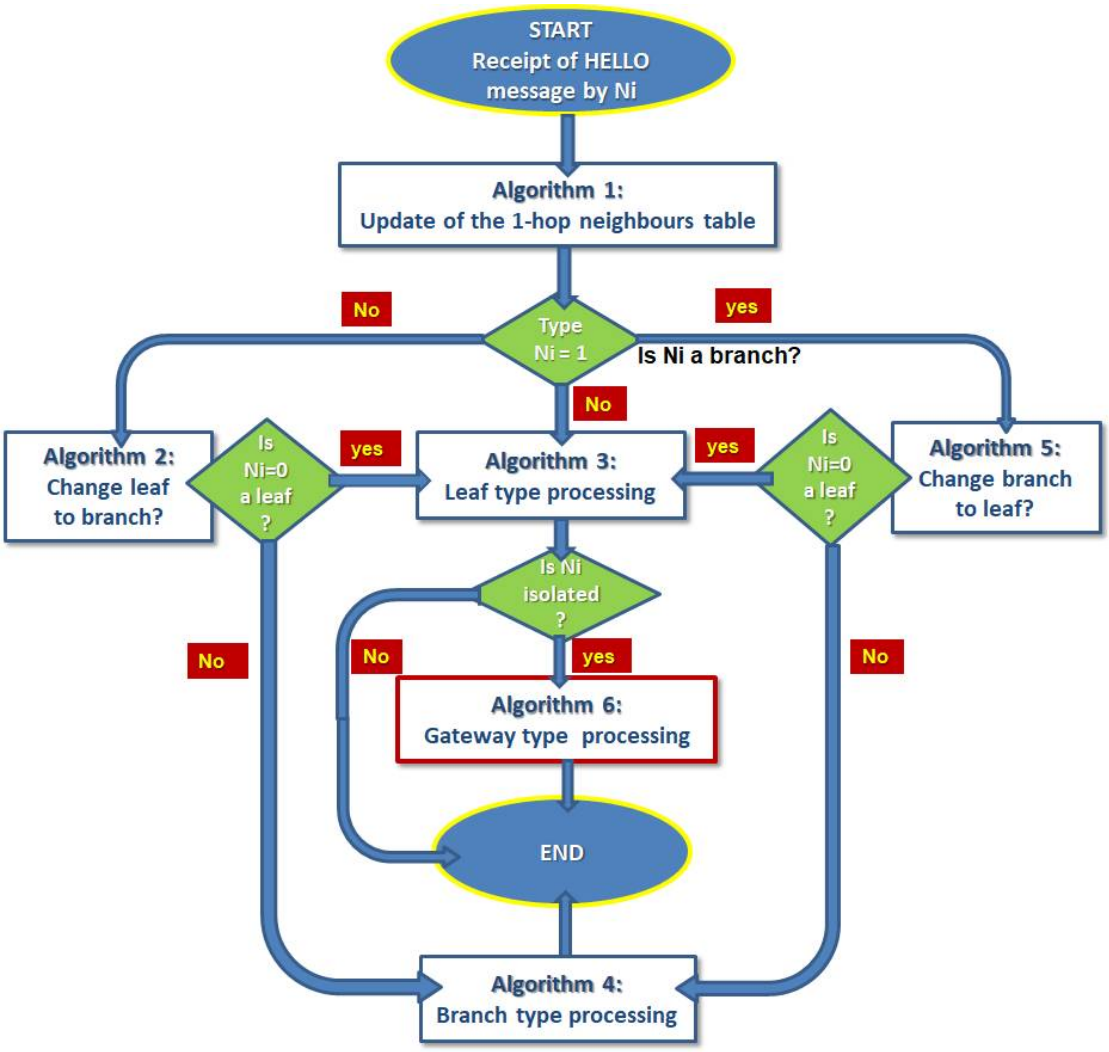

Figure 3.3: CBL-G algorithm processing upon reception of a Hello message

3.3.4 Adaptation of the vehicle structure and periodic control message for the CBL-G model

The content of the messages sent by node Ni contains the list of addresses of the nodes Nj neighbouring a hop of which it is aware as well as the type of their link. The messages must also contain the following ten attributes:

- **Address**, the address of the node Ni that sends the message;
- **Type**, the current type of node Ni (branch or leaf) ;
- **Category**, the category of the node Ni (an OBU mobile node or an RSU fixed relay point);
- **Position**, the absolute position (Xi, Yi) of the node Ni ;
- **Speed**, the value Vj, in m/s, of the average speed of the vehicle of the neighbouring node Nj over one second;
- **Steering angle**,the average steering angle of the neighbouring node's vehicle over a second ;
- **ChainUP**, the address of the upstream branch node;
- **ChainDO**, the address of the downstream branch node ;
- **BranchChoice**, the address of the node chosen as the relay branch node number.
- **BrancheChoiceType**, the type of node chosen as the relay connection node (this attribute is used to determine if the branch's OBU or RSU).

The extracted structure of a vehicle node from Matlab is represented in figure 6.4. The new specification compared to the old version is the field that concerns the type of the elected branch (mobile branch or RSU branch).

3.3.5 Algorithm 6: The processing of the gateway node

The CBL-G algorithm is based on the five algorithms previously defined in the work of (Rivoirard et al., 2018), plus a sixth algorithm that we introduce in this chapter, this new algorithm deals with the processing that a gateway node does. The algorithm is presented in Algorithm 1. Algorithm 6 concerns all processing done on a gateway RSU, first of all, the RSU node does not participate in the creation of the chain.

Algorithm 1 The gateway processing (which is algorithm 6 in CBL-I diagram)

```
1: procedure GATEWAY PROCESSING(Ni, Nj, Ny)
2:     Ni ← 0                                              ▷ Ni is a leaf
3:     Nj ← 1                                              ▷ Nj is a branch
4:     Ny ← 3                                              ▷ Ny is a RSU
5:     if Type.Ni ← 0 and Type.Nj ← 1 and Type.Ny ← 3 then
6:         @BranchChoice.Ni ← @Nj                          ▷ Branch election
7:         @BranchChoiceType.Ni ← 1
8:         [T1, T8, T11] ← [T, 0, T]
9:     end if
10:    if @BranchChoice.Ni and ((T > T1 + V and Ni ←!HELLO.Nj) Or
   (HELLO.Type.Nj ← 0)) then
11:        @BranchChoice.Ni ← 0                            ▷ Branch loss
12:        @BranchChoiceType.Ni ← 0
13:        [T1, T8, T11] ← [0, T, 0]
14:    end if
15:    if Ni ← HELLO.Ny then
16:        @BranchChoice.Ni ← @Ny
17:        @BranchChoiceType.Ni ← 3
18:        [T1, T8, T11] ← [T, 0, T] ▷ Waiting for an observation period from
   the neighbor
19:    else
20:        if (T > T8+C1 × HELLO INTERVAL) and Ni ← HELLO.Nj then
21:            @Nk ← Nj
22:            if CompareLeafNode(@Ny, @Nk) ← 1 then
23:                @BranchChoice.Ni = @Ny
24:                @BranchChoiceType.Ni = 3
25:                [T1, T8, T11] ← [T, 0, T]
26:            else
27:                @BranchChoice.Ni = @Nj                  ▷ Change of relay node
28:                @BranchChoiceType.Ni = 1
29:                [T1, T8, T11] ← [T, 0, T]
30:            end if
31:        end if
32:    end if
33: end procedure
```

This information is shared with its one-hop neighbors through the HELLO messages it sends. This is also how it receives information from its close neighbors.
The strategy proposed in CBL-G is the following: a leaf node attaches itself to the first gateway node, i.e. a gateway RSU that it detects upstream from its position. In the following cases:

- If a leaf node does not detect any branch or leaf node in its neighborhood, it elects an RSU node as the branch. This election of the gateway RSU as a branch node prevents the leaf node from being isolated.
- If a branch node does not detect any node in its perimeter, i.e. the validity time elapsed since the date of the last reception of a HELLO message from a node having elected it is exceeded, it returns to the leaf state (algorithm 5). Then if it does not find a branch to which it is attached it elects the nearest RSU as a branch.
- Once the isolated node has added the RSU as a branch, it continues to discover its neighborhood. As soon as it detects a branch node it will execute algorithm 3, that is to say, it will calculate the connection time that it offers. If it is greater than the one offered by the RSU it will elect it as a branch to connect to.

3.4 Analysis of the CBL-Gateway (CBL-G) results

To start it should be noted that the cases of isolated mobile nodes or clusters only occur when there is an extremely low density of vehicles, which is rare on a highway and usually only at off-peak times. A behaviour observed during the tests and the study of the road structure of the CBL algorithm is the formation of disconnected clusters when the density of vehicles is very low, which creates fragments of chains disconnected from each other, as shown in figure 3.2.
The handling of isolated nodes in the CBL-G system is studied by examining the behavior of mobile nodes in varying infrastructure densities.
The performance of the CBL-G system is evaluated using a set of metrics, including:

1. Number of nodes per RSU, This is the number of connected node pairs as defined in (Ben Jemaa, 2014) K(N_i; N_j; t), that are connected in one hop at a time t1, with N_i node category being RSU, and $N_i \neq N_j$. Node-number-per-RSU(N_i,N_j;t1) is a variable that indicates the connectivity between two nodes N_i and N_i at time t.

$$Node-number-per-RSU(Ni, Nj; t1) = \sum_{j=0}^{N} K(Ni, Nj; t1) \tag{3.1}$$

With, $N_i.Category = RSU$ & $N_i.category \neq N_j.category$

2. Number of nodes per branch, with N_j as a leaf node and N_i as the elected branch by N_j.

$$Node-number-per-branch(Ni, Nj; t1) = \sum_{j=0}^{N} K(Ni, Nj; t1) \quad (3.2)$$

With, $N_i.Type = Branch$ & $N_j.Type = leaf$

3. Duration of the link between a leaf node and its branch, as defined by (RIVOIRARD, 2018) and (Ben Jemaa, 2014) is CT-leaf-branch(N_i, N_j) with N_j as a leaf node and N_i as the elected branch by N_j.

$$CT-leaf-branch(N_i, N_j) = \frac{-(ab+cd) + \sqrt{(a^2+c^2) * P^2 - (ab-bc)^2}}{a^2+c^2} \quad (3.3)$$

Where:

$$\begin{aligned} a &= V_i \cos(\Omega_i) - V_j \cos(\Omega_j) \;\; ; \;\; b = X_i - X_j; \\ c &= V_i \sin(\Omega_i) - V_j \sin(\Omega_j) \;\; ; \;\; d = Y_i - Y_j; \end{aligned}$$

Where P is the range and it is a positive constant, N_i and N_j are two connected node pairs, V_i and Ω_i are the velocity and orientation of node i, X_i and Y_i are the coordinates of node i

4. Duration of the connection between an isolated node and its corresponding relay point RSU (in sec). This is the period during which two nodes N_i and N_j are connected. CT-node-relay(N_i; N_j) a variable that indicates the connectivity between two nodes: N_i category is a RSU and N_j category is different from N_i category.

$$CT-node-relay(N_i, N_j) = \frac{-(ab+cd) + \sqrt{(a^2+c^2) * P^2 - (ab-bc)^2}}{a^2+c^2} \quad (3.4)$$

Where:

$$\begin{aligned} a &= V_i \cos(\Omega_i) - V_j \cos(\Omega_j) \;\; ; \;\; b = X_i - X_j; \\ c &= V_i \sin(\Omega_i) - V_j \sin(\Omega_j) \;\; ; \;\; d = Y_i - Y_j; \end{aligned}$$

Where P is the range and it is a positive constant, N_i and N_j are two connected node pairs, V_i and Ω_i are the velocity and orientation of node i, X_i and Y_i are the coordinates of node i and $N_i.Category$ = RSU and $N_i.category \neq N_j.category$.

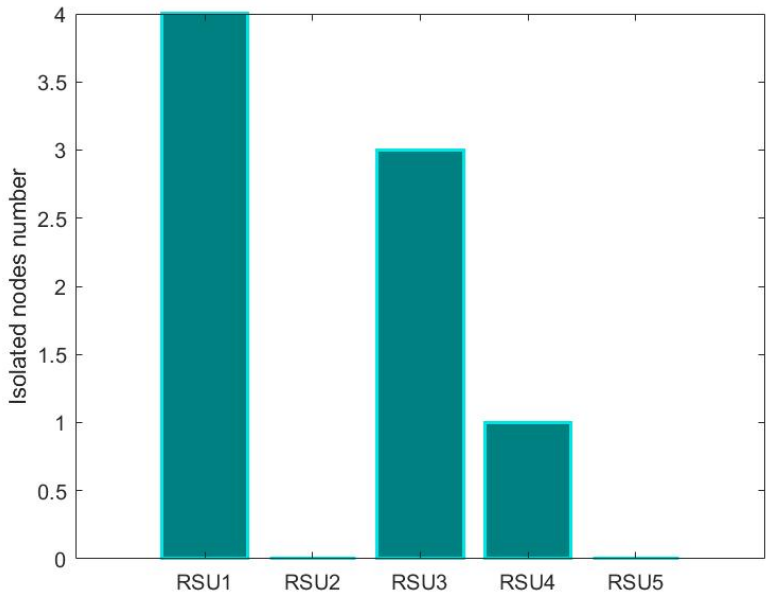

Figure 3.4: Number of isolated nodes per RSU

The number of isolated nodes in the first RSU is proportional to the density: in a high density, many vehicles enter simultaneously and connect to the first RSU. On the contrary, when the density is low, the isolated nodes attached to the first RSU are weaker but there are more isolated nodes attached to the rest of the RSUs.
Then, when the density of vehicles is low, a chain is formed only of branches or sometimes the branches are not in range of each other, so we obtain isolated nodes and clusters. About 4.13% of the nodes in the network are isolated. And this is because of the areas not covered by the chain, in which case the nodes will have an interest in connecting to the RSU.
In the case of high-density architecture, there are few cases of isolation; if we consider many vehicles on the same road, they will necessarily be close to each other. Thus, a chain is provided in nodes. In comparison with a low density, 0.43% of the nodes in the network are isolated when the density is high compared to 4.13% when the density is low. The cases of isolation that are observed in high density are mostly due to vehicles entering the road. The research presented in (RIVOIRARD, 2018) explains that for a high density a node remains attached for 30 seconds to its branch. In the work of (Belmekki et al., 2020), when the infrastructure is on the road and the RSUs are in the branch state continuously (UC2), we obtain a link duration between the leaf and the RSU whose state is "branch" of 10 seconds for a low density. The results for a medium density are

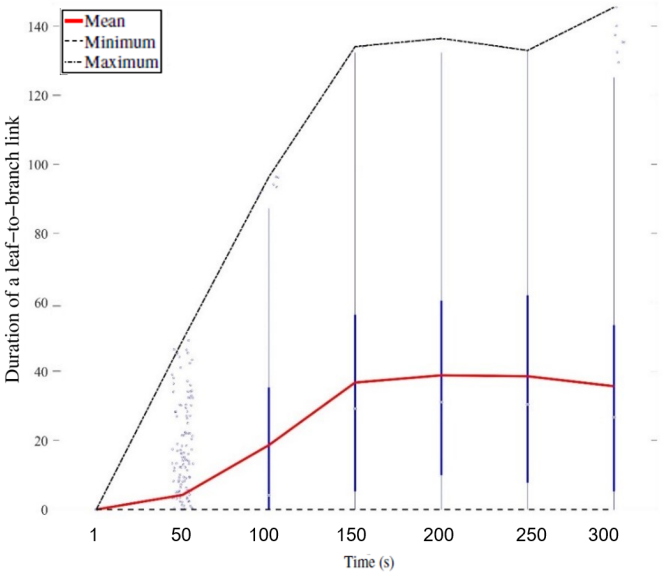

Figure 3.5: Duration of the leaf to branch link in a medium density of vehicles versus simulation time

shown in figure 3.5.
The time it takes for a node to attach to its gateway RSU depends on three factors:

- The speed of the vehicle.
- The range of an RSU.
- The absence of a branch

In the vicinity that would cause a disconnection from its RSU to attach to the branch.
Concerning the number of leaf nodes per branch, we obtain an average of 2.41 nodes for a low density. When we have a medium density we have 4.61 nodes per branch and for a high density 9 nodes per branch.
This does not differ globally from the initial results of CBL. We can therefore deduce that the metric of the number of leaf nodes per branch is not affected by the presence of RSU for this case.
CBL-G has allowed us to perform both V2V and V2I communications simultaneously in the same environment. Thanks to these two types of communication and their application to realistic road situations during simulations, we were able to observe the behavior of the nodes. This allows us to position ourselves as to the

relevance of using one type of communication to another or both types of communication depending on the environment and the situation.
I remind you that in our work, we consider equipped vehicles only. If we are on a road with a high density of vehicles but 50% of them are not equipped then we consider that we are on a road with a medium density, because 50% of the vehicles will not be used in our model.
It has been proven that in case of the low density of equipped vehicles, there will be more cases of isolated nodes and clusters (as shown in the figure 3.2) so if we are in an environment equipped with RSUs, it will be judicious to opt for a V2I communication rather than a V2V communication to bridge this isolation.
On the other hand, when you are in a medium to the high-density environment, there is no point in using V2I only.
Because there will be a lot of connection/disconnection to the RSU as the mobile nodes pass by. And the duration of connection of a mobile node with the RSU is limited and depends on the range of the RSU and on the speed of the vehicle (for example an isolated vehicle driving at 110km per hour wanting to connect to an RSU with a range of 500 meters: the duration of the link between the vehicle and its RSU will be 14.4 seconds, all this assuming that the node concerned does not detect any branch during its passage in the RSU zone).
In this case, the connection of a vehicle to another mobile vehicle offers a better link duration. So it is better to use V2V only. V2V communications are sufficient to maintain the chain between vehicles.
It is sometimes necessary to combine the two types of communication when we are in a low or medium density where there are enough equipped vehicles in the vicinity to build the chain, but with a rate of isolated nodes 4.13% that can be solved by combining V2V communications with V2I. The table 3.1 summarizes our findings.
The development and deployment of new mobility services involving autonomous vehicles imply addressing critical and important issues related to safety aspects.
In this context, it is essential to propose solutions, mechanisms, architectures, and functions that guarantee the robustness, reliability, accuracy, confidence, and efficiency of the systems (perception, decision, actions).
Information from other vehicles (Local Dynamic Perception Map) and from the infrastructure will be essential to build more extensive, improved, and long-range information. The use of remote data will allow the construction of an "extended dynamic perception map" useful for assessing critical hazard situations or remote data (e.g., overall risk level).
Remote information is essential to have enough time to react properly and to propose an efficient planning mechanism able to predict and anticipate events, configurations or risk situations. For this, we need efficient communication archi-

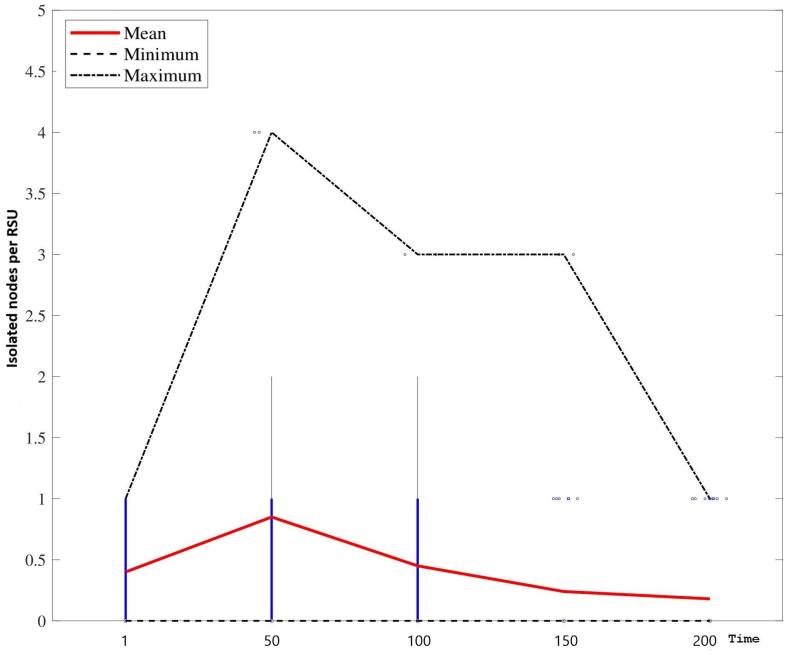

Figure 3.6: Rate of isolated nodes per RSU in a high density

tectures and strategies that guarantee a very high level of QoS.
In this section, an adapted communication architecture has been proposed to answer these questions. The architecture employs strategies and mechanisms to use the dynamic communication clustering of vehicles and infrastructure resources to ensure optimal communication coverage.
The proposed solution merges the functionality and benefits of V2V and V2I communications with the CBL-G system.
The main objective of CBL-G is to provide optimal communication coverage with efficient management of potentially isolated groups of vehicles. CBL-G addresses a new issue that CBL did not initially address: isolated nodes and the breaking of the backbone.
CBL-G prevents connection loss and improves QoS by redirecting isolated nodes and clusters to RSUs that act as gateways and guarantee the continuity of the communication chain (backbone built from the branch nodes). Indeed, it is able to solve the problem of isolated nodes rate in high density by decreasing the rate from 0.43% to 0%, and by decreasing the rate of isolated nodes in low density from 4.13% to 0.13% by combining V2V communications with V2I which increased the coverage of the road network from 96% to 100%.
The different scenarios and use cases applied to the CBL-G system confirmed the effectiveness of our method. Indeed, the resolution rate of isolated nodes is better in low densities because the average number of isolated nodes is higher.

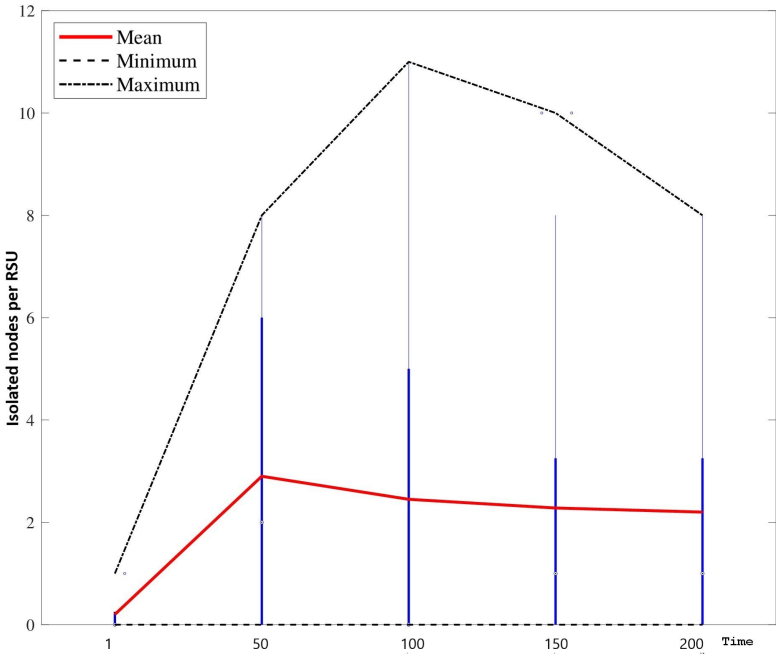

Figure 3.7: Rate of isolated nodes per RSU in a low density

From the obtained results, it is now possible to propose recommendations (table 3.1) in the deployment and the optimal communication topology according to the possible configurations and modes: V2V with only CBL, V2I with only UC2, or the use of a combination of vehicles and infrastructure equipment with CBL-G.

3.5 Conclusion

In this chapter, a suitable communication architecture has been proposed that involves strategies and mechanisms to utilize the dynamic communication clustering of vehicles and infrastructure resources to ensure optimal communication coverage. The proposed solution merges the functionality and benefits of V2V and V2I communications with the CBL-G system.
The main objective of CBL-G is to provide optimal communication coverage with efficient management of potentially isolated groups of vehicles.
CBL-G addresses a new aspect that was not initially managed in CBL: the issue of isolated nodes and backbone failure (a set of branch nodes without connection between them). CBL-G prevents connection loss and improves QoS by directing isolated nodes and clusters to RSUs that act as gateways and guarantee the continuity of the communication chain (backbone built from branch nodes).
Our model allows only branch and remote nodes to connect to the RSU when

needed, which greatly reduces the number of vehicle nodes requesting resources from the RSU at the same time, thus avoiding network congestion. Indeed, it is able to solve the problem of the rate of isolated nodes in high density by decreasing the rate from 1.5 % to 0%, and decreasing the rate of isolated nodes in low density from 14.23% to 0% by combining V2V communications with V2I which increased the road network coverage from 85% to 100%. Those results have been published in our paper (Belmekki, Gruyer, and Tatkeu, 2022).

Table 3.1: Recommendations on the best Communications Type (V2V, V2I, V2V+V2I) according to the equipped vehicles density in a freeway environment

	CBL (V2V)	UC2 (V2I)	CBL-G (V2V+V2I)
Low density	X	✓	✓
Medium density	✓	X	✓
High density	✓	X	✓

The different scenarios and use cases applied to the CBL-G system have confirmed the efficiency of our method. Indeed, the resolution rate of isolated nodes is better in low densities because the average number of isolated nodes is higher. The CBL-G is currently available to be evaluated in different vehicle density configurations with an implementation in the physical-realistic simulation platform SiVIC-MoboCoop (NS3, Pro-SiVIC, RTMaps) and can be exploited in future work. The next chapter explains Contribution 3 which consists in using this new version of CBL-G to estimate the collision risk at three levels: local, extended, and global.

Chapter 4

Multi-level Perception for autonomous vehicles

Contents

4.1 Introduction

The increasing advancements in Intelligent Transportation Systems (ITS) technology have opened new avenues to enhance traffic safety. V2V and V2I communication have been successful in mitigating crash severity and reducing collisions. However, the focus has primarily been on improving mobility and traffic operations, with little attention given to road safety.
This chapter introduces a multi-level collision risk estimation method based on CBL-G structure and communication, which aims to estimate local and extended collision risks. The CBL-G method will be adapted for CPM and reorganized to include better indicators for risk estimation. The chapter presents an analysis of different CPM generation policies and the balance between perception capabilities and communication performance.

4.2 State of art

Recent advancements in ITS technology have garnered significant attention as a potential means of enhancing traffic safety. Specifically, the utilization of V2V and V2I communication has been shown to mitigate crash severity and reduce the likelihood of collisions. (Fyfe, 2017) conducted a study in which they employed Vienna SIMulation Model (VISSIM) and the Surrogate Safety Assessment Model (SSAM) in conjunction with the Cumulative Travel Time (CTT) algorithm to assess safety in a V2V environment. The results of the study indicated a 40% reduction in the frequency of rear-end conflicts at a signalized intersection when utilizing Cooperative Automated Vehicles (CAV).
Similarly, authors (Olia et al., 2016) conducted an experiment utilizing CAV technology in PARAMICS and estimated that the safety index improved by up to 45% in such an environment. Furthermore, in (Paikari, Tahmasseby, and Far, 2014) the authors used PARAMICS, a simulation tool that combines V2V and V2I technologies, to demonstrate improved safety and mobility on highways in the context of connected vehicles (VC).
Vehicle platooning in conjunction with connected vehicle (VC) technology represents a critical component of future transportation systems, as it has the potential to simultaneously improve traffic operations and safety.
(Tian et al., 2016) proposed a stochastic model to evaluate the collision probability for a heterogeneous vehicle platoon. The model is able to account for the distribution of inter-vehicle distances, and the results have the potential to reduce chain collisions while also mitigating their severity. However, it only accounts for the distribution of inter-vehicle distances and does not consider other factors that may contribute to collisions, such as road geometry, vehicle speed, and driver be-

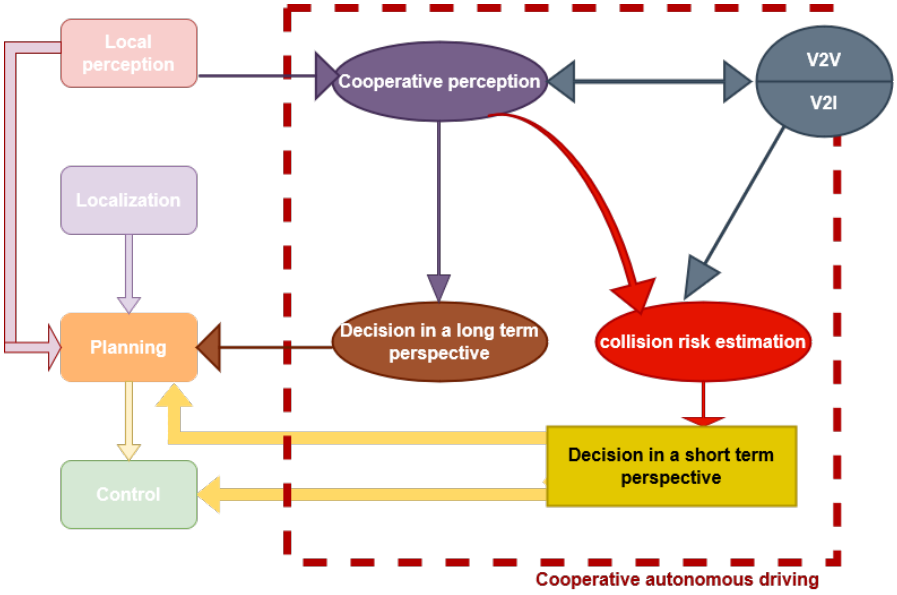

Figure 4.1: The global architecture of the autonomous driving system using cooperative perception

havior. Additionally, the results of the model may not accurately reflect real-world scenarios, as it is based on stochastic assumptions that may not perfectly match actual conditions. Despite these limitations, the results of the model have the potential to provide valuable insights into the potential reduction of chain collisions and their severity, and it may serve as a starting point for further research and refinement. The authors (Rahman et al., 2018) have demonstrated that connected vehicles can improve traffic safety in foggy conditions. The study applied two types of CV approaches:Connected Vehicles Without Platooning (CVWPL) and Connected Vehicles With Platooning (CVPL) and evaluated their impact on safety using three surrogate measures: standard deviation of speed, the standard deviation of distance traveled, and Rear-end Crash Risk Index (RCRI). The results indicated that both VC approaches significantly improve safety in foggy conditions.

Previous research has primarily focused on improving mobility and traffic operations in a CAV environment, with limited attention given to road safety.

In this chapter, we discuss the different levels of collision risk between vehicles traveling on the highway, with a focus on utilizing their local and extended local perceptions, conveyed through CPM messages introduced by ETSI (ETSI, 2019). These CPMs are also utilized in various projects such as the Transition Areas for Infrastructure-Assisted Driving (TransAID) project (Correa et al., 2019).

The analysis conducted demonstrates that certain CPM generation policies im-

prove perception capabilities, but also increase the risk of saturating the communication channel and making the network unstable. The dynamic policy currently considered by ETSI aims to achieve a balance between perception capabilities and communication performance.
Figure 4.1 illustrates the overall architecture of the autonomous driving system utilizing cooperative perception, with the fundamental role of supporting improved decision-making for autonomous driving. The left-hand boxes indicate the components for achieving autonomous driving, while the right-hand box, represented by a dashed line, highlights the components for autonomous driving using cooperative perception.
In this chapter, we introduce and explain in detail our Multi-level collision risk estimation based on CBL-G structure and communications, which we use to estimate collision risk (local and extended). In order to do so, we intend to adapt the CBL-G for CPM and reorganize and adapt the CBL-G method so that it takes the most elements to our indicators for better risk estimation.

Figure 4.2 represents three clusters in the CBL-G framework where the local

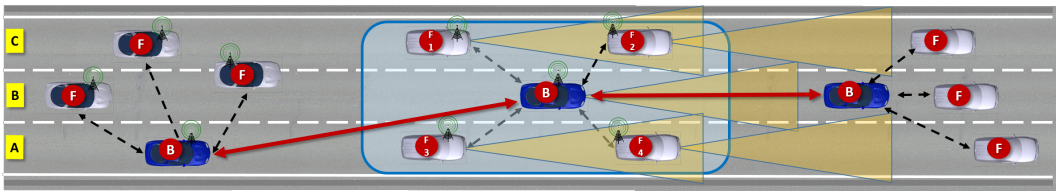

Figure 4.2: Vehicles (F1, F2, F3, F4, and B) local perception represented at the CBL-G structure

perception of each vehicle (F1, F2, F3, F4, and B) is shown.

4.3 Multi-level correct perception

4.3.1 The local perception

The local perception is limited to the capacity of the onboard sensor i.e. limited to its perceptive capacity and the surrounding obstacles (fields of vision). Figure 4.3 represents the local perception of vehicle F1 which is vehicle F2.

4.3.2 The extended local perception

The extended local perception is the perception of the cluster members shared with their cluster head which allows the cluster head to perceive what its leaves

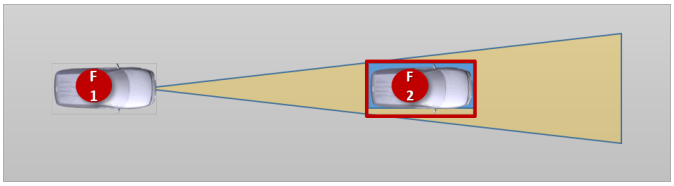

Figure 4.3: Vehicle "F1" local perception representation extracted from the figure 4.2

do.
As shown in Figure 4.2, vehicle B local perception does not allow it to detect any vehicle (figure 4.4); However, we will be able to detect the presence of the two vehicles F2 and F4 by using the information perceived by vehicles F1 and F3. In this example, we limit the perception to the front zone of the vehicles (i.e. RADAR) and apply a modeling of the uncertainties on vehicle localization obtained with a GPS as well as frontal obstacle detection obtained with the RADAR. Thanks to the CBL communication system, the branch will receive the local perceptions of its leaves (F1, F2, F3, F4). So the perception of B will be empty (no vehicle) however

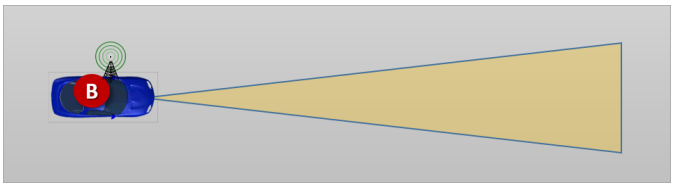

Figure 4.4: Vehicle "B" The local perception representation extracted from the figure 4.2

its extended local perception will contain the four nodes of its cluster (F1, F2, F3, F4).
Figure 4.5 represents the obtained extended local perception of B.

4.3.3 The extended branch perception

The extended branch perception is the perception of the downstream neighboring branch shared with its upstream branch and the perception of the upstream neighboring branch shared with its downstream branch, allowing the central branch to receive perceptions of objects (obstacles), that it cannot see using only embedded equipment from both sides (upstream and downstream). We can perceive further than we could previously with extended local perception, which is limited to the cluster.
Figure 4.6 illustrates the extended branch perception case: As shown in Figure 4.6,

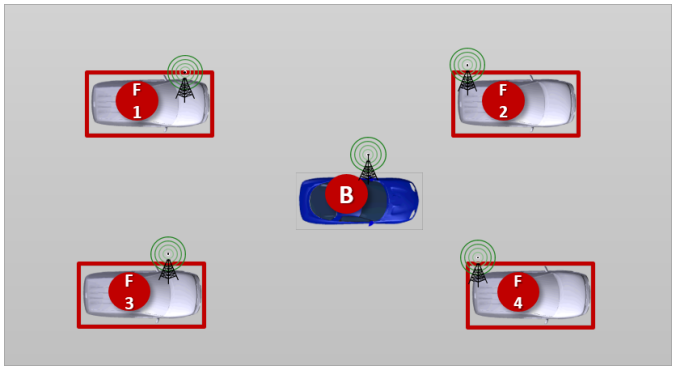

Figure 4.5: Vehicle "B" The extended local perception representation extracted from the figure 4.2

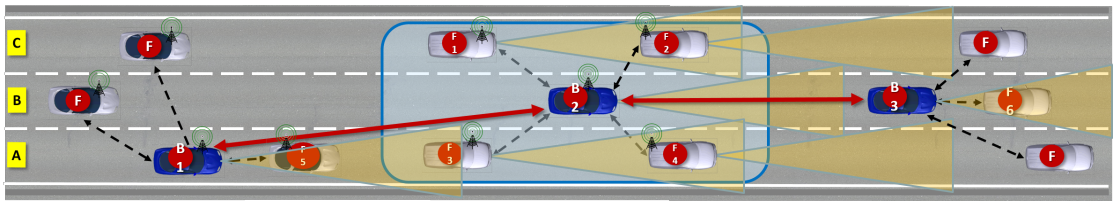

Figure 4.6: The representation of Branch B2 perception and its adjacent branches B1 and B3 perception in CBL environment

the extended branch perception of vehicle B does not allow it to detect any vehicle (figure 4.4, however, thanks to the CBL communication system, the branch will receive the local perceptions of its upstream and downstream branches (B3, B1). Indeed As the adjacent branches communicate to form a chain, the B2 branch will also be able to receive the GPS position of the B1 and B3 branches. The collection of all the information of the branch's perception will then make it possible to estimate a map of extended branch perception which will be able to be used to build a map of extended branch risks. B1 will share its perception which is represented in figure 4.7 with its Upstream branch B2. B3 will share its perception which is represented in figure 4.8 with its Downstream branch B2. Node B2 possesses a perception that solely comprises its own location information. Meanwhile, Node B1 generates a dynamic perception, incorporating its location and the detection of Nodes F5 and F3. Similarly, Node B3 generates a similar map, comprising its location and the detection of Node F6. From these perceptions, Branch B builds its own extended branch perception which is represented in figure 4.9.

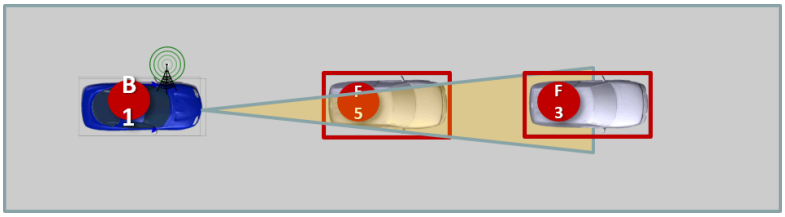

Figure 4.7: The representation of Branch B1 local perception in CBL environment which is nodes F5 and F3

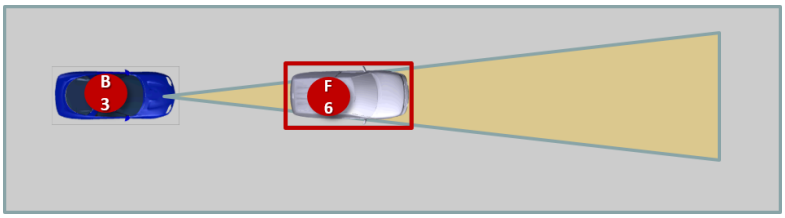

Figure 4.8: The representation of Branch B3 local perception in CBL environment which is node F6

4.3.4 The global perception

The perception of the ego vehicle can be expanded beyond its immediate vicinity by utilizing the perception of branch nodes that are positioned upstream and downstream of its location. This technique, referred to as global perception, allows for the sharing of perception information among branch nodes that are farther away from the ego vehicle. This enables the ego vehicle to gain a comprehensive understanding of its surroundings, including areas that are beyond the immediate upstream and downstream clusters. This technique enables the projection of global situational awareness while the vehicle is in motion

4.4 Uncertain perception

For the uncertain perception as shown in figure 4.10 , we use Kalman filter. This filter is a recursive algorithm that estimates unknown state variables from a series of noisy measurements. It can produce an optimal statistical estimate of the system's state as well as a variance-covariance matrix that provides the filter's estimated precision. The Kalman filter algorithm consists of two steps: prediction and update. The prediction step is given by:

$$x_{kp} = Ax_{k-1_p} + Bu_k \tag{4.1}$$

$$P_{kp} = A * P_{k-1_p} * A' + Q \tag{4.2}$$

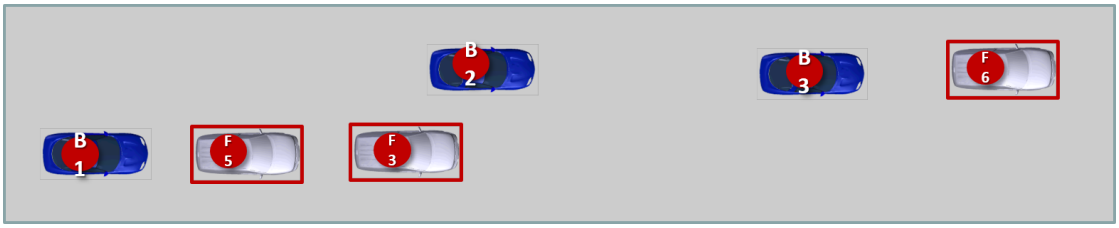

Figure 4.9: The representation of the extended Branch perception B2 in CBL environment built from CPDL of both branch B1 and B3

The update step is given by:

$$K_k = P_{kp}C'inv(CP_{kp}C' + R) \tag{4.3}$$

$$x_{kp} = x \tag{4.4}$$

Other estimators exist, such as alpha-beta lter, individual lters, and Luenberger observers, but none has achieved the celebrity status of the Kalman filter. Kalman filter principle diagram by (Aimonen, 25 November 2011) for prediction is represented in figure 4.11.

The state prediction equation is:

$$x_k = A_k x_{k-1} \tag{4.5}$$

The error covariance prediction equation is:

$$P_k = A_k P_{k-1} A_k^T + Q_k \tag{4.6}$$

The state estimate equation is:

$$x_k = x_k + K_k(z_k - H_k x_k) \tag{4.7}$$

In these equations, x_k is the state estimate, P_k is the error covariance matrix, A_k is the state transition matrix, Q_k is the process noise covariance matrix, K_k is the Kalman gain, H_k is the measurement matrix, R_k is the measurement noise covariance matrix and z_k is the measurement. We consider a simple linear system where the state of the system at time step k is represented by the variable x, the control input at time step k is represented by the variable u, and the measurement at time step k is represented by the variable z.

The state transition equation of the system is given by:

$$x_k = Ax_{k-1} + Bu_k + w_k \tag{4.8}$$

where A and B are the system matrices, u_k is the control input and w_k is the process noise which is assumed to be white noise with a covariance matrix Q. The measurement equation of the system is given by:

$$z_k = C * x_k + v_k \tag{4.9}$$

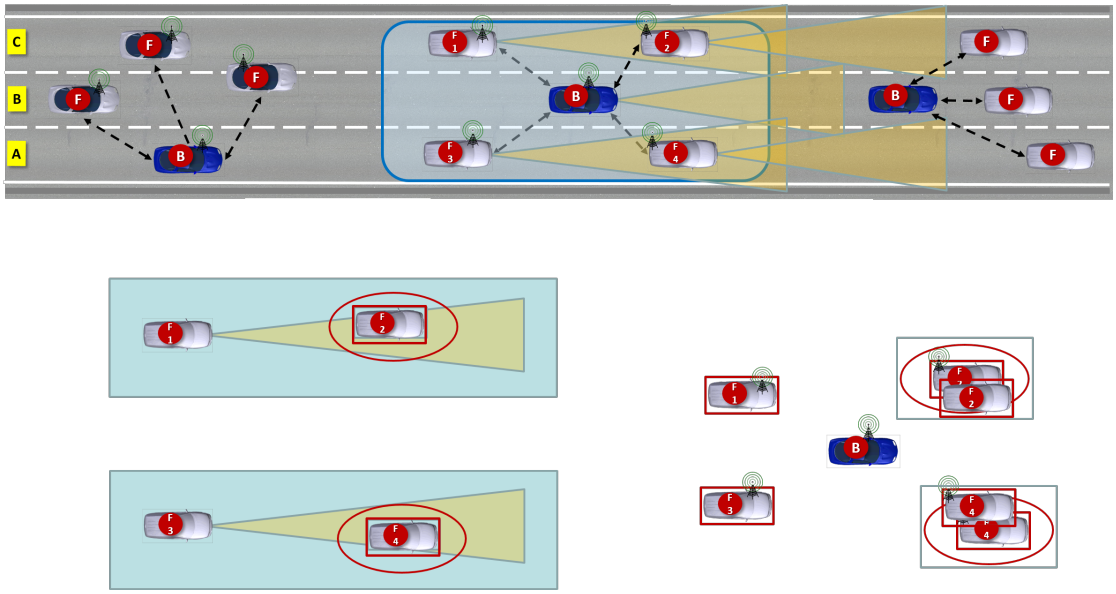

Figure 4.10: Schematic diagram of scenario B CBL extended local perception of branch B2 in the cluster 2 with Uncertain perception and perfect localization

where C is the measurement matrix, z_k is the measurement and v_k is the measurement noise which is assumed to be white noise with a covariance matrix R. We will use the following matrices: A = [1 1; 0 1]; B = [1; 0]; C = [1 0]; Q = [10 0; 0 10]; R = [10]; The used kalman filter is given in Algorithm 2 :

Algorithm 2 Kalman Filter

1: **function** KALMAN_FILTER($A, B, C, Q, R, x_{prev}, P_{prev}, u, z$)
2: $x_{pred} \leftarrow A * x_{prev} + B * u$ ▷ Predicted state estimate
3: $P_{pred} \leftarrow A * P_{prev} * A' + Q$ ▷ Predicted error covariance
4: $K \leftarrow P_{pred} * C' * inv(C * P_{pred} * C' + R)$ ▷ Kalman gain
5: $x_{est} \leftarrow x_{pred} + K * (z - C * x_{pred})$ ▷ Updated state estimate
6: $P_{est} \leftarrow P_{pred} - K * C * P_{pred}$ ▷ Updated error covariance
7: **return** x_{est}, P_{est}
8: **end function**

4.5 The Experimental plan

The Experimental Plan we used is described as follows:

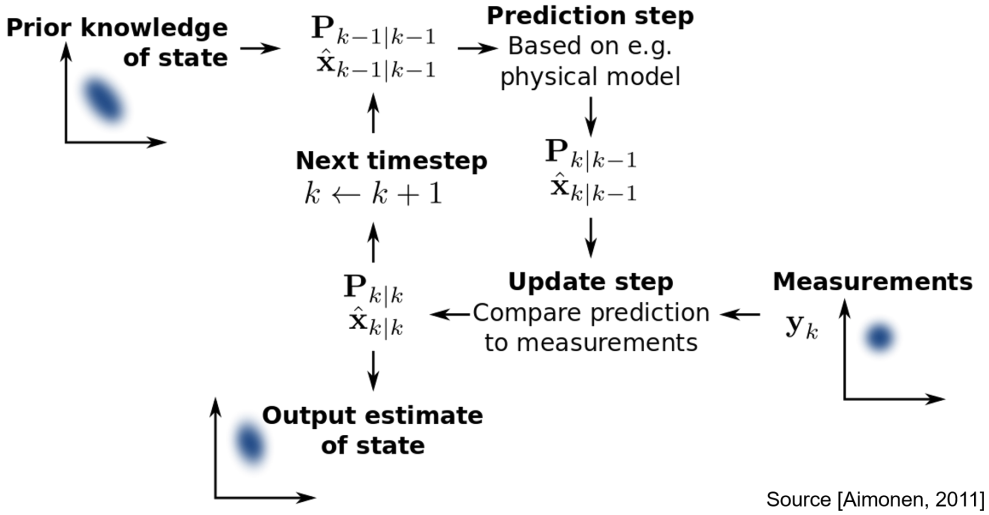

Figure 4.11: kalman filter principle diagram for prediction

1. Use the SUMO software to generate a real-world highway scenario with a section of the A27 highway.

2. Intentionally creates risky situations between vehicles traveling on the same route by changing the dynamics of the vehicles involved.

3. Use the Kalman filter algorithm to model uncertain perception and estimate the risk of collision in a degraded scenario.

4. Implement the Kalman filter algorithm using the prediction and update steps as described in the given equations.

5. Perform state prediction and error covariance prediction using the state transition and process noise equations.

6. Use the Kalman gain, measurement matrix, and measurement noise covariance matrix to estimate the state of the system and update the state estimate.

7. Evaluate the results of the Kalman filter algorithm to determine the risk of collision in the degraded scenario.

8. Compare the results to the results obtained in the perfect localization scenario to determine the impact of uncertain perception on collision risk.

4.6 Collective perception message (CPM)

In the context of Intelligent Transportation Systems (ITS) as defined by ETSI (ETSI, 2019; ETSI, 2020) and in section 1.3.3, and to achieve the multi-level perception defined above, we specify the CPM which is a message exchanged between ITS stations (such as vehicles or infrastructure) that contains information about the current environment.
The purpose of the CPM is to minimize the ambient uncertainty of ITS stations by providing them with contextual information from other stations. This information can include details about the presence and location of other vehicles, road conditions, and traffic congestion. The CPM can help ITS stations make more informed decisions about how to safely and efficiently navigate the road network.
The structure of the CPM as defined by ETSI can vary depending on the specific application or use case. However, in general, a CPM typically includes the following elements:

1. A header: This includes information such as the message type, the sender's identification, and the time the message was sent.

2. Contextual information: This includes details about the current environment, such as the presence and location of other vehicles, road conditions, and traffic congestion.

3. Security information: To ensure the authenticity and integrity of the message, CPMs may include security information such as digital signatures or encryption.

4. Payload: this include the actual information that is needed to be transmitted

The security information and the payload are considered optional elements, as they may not be needed for all use cases or applications. However, depending on the security requirements of a specific ITS system or application, the security information may become mandatory.
It's worth noting that ETSI defined that the contextual information and the safety information are both considered as mandatory parts of the payload, as they are necessary for ITS stations to make informed decisions about how to safely and efficiently navigate the road network.
It's worth noting that the CPM structure is designed to be flexible and extensible, so it can adapt to different use cases and be used in various ITS applications. It's also worth noting that ETSI also defined the structure of the payload which is divided into two parts:

1. Contextual Information: This includes information such as the location and heading of the sender, speed, and the presence of other vehicles, road conditions, and traffic congestion.

2. Safety Information : this includes information related to safety such as the presence of a dangerous object, warning, or an accident.

In the next section we define our CPM message structure used for our model.

4.7 CPM Generation Rules and Their Impact on V2X Communications

In the context of V2X communications, the CPM generation rules dictate the frequency and content of CPM transmissions. The ETSI standard establishes that a vehicle must check every T_GenCpm interval to determine if a new CPM should be generated and transmitted, with T_GenCpm ranging between 0.1s and 1s (Thandavarayan, Sepulcre, and Gozalvez, 2020). A new CPM must be generated if a new object is detected or if certain criteria, such as position or velocity changes, are met for previously detected objects. The frequency of CPM transmissions and the amount of information included in each message can impact the overall channel load and reliability of V2X communications.

4.8 Approach of CBL-G for Vehicle Detection and Collective Perception

In CBL, a periodic control message, referred to as the "HELLO message," is introduced in previous sections to discover neighboring vehicles. The HELLO message and the CPMs are important to separate as the first maintains the communication architecture and link between vehicles, while the second, the CPM shares each vehicle's perception information, allowing for the expansion of the nodes's local map. The vehicle is assumed to have a frontal view of 200 meters and a communication range of 500 meters. The ego vehicle generates CPMs in accordance with ETSI's current CPM generation rules, as described in section 4.7. From an algorithmic perspective, the Cooperative Awareness for Vehicle Safety (CBL-G) system detects vehicles by receiving control messages from neighboring vehicles. Upon receiving a new control message from a neighboring vehicle V_j, vehicle V_i will send a CPM containing information about the detected object V_j. If vehicle V_i does not detect any new vehicle after one second, it will send an empty CPM message, to signal that it is able to detect and share objects. The adaptation of

CBL-G for the collective perception is done by the adaptation of the structure of the vehicle, indeed we introduce a new element which is the detected object.

4.9 Integrating Vehicle Parameters in CBL-G: Representing Vehicle Structures and confidence

The sections below define the new vehicle's parameters. First we integrate in our model the "acceleration" (a), it is calculated as follows:

$$a = \frac{\Delta V}{\Delta t} = \frac{V_f - V_i}{t_f - t_i} \tag{4.10}$$

In CBL, all vehicles are identical nodes, we introduce in CBL-Gateway different types of vehicles with their dimensions (length X width) in meters most frequent on a road:

$$\text{urban car} = \begin{cases} \text{length} = 3{,}5 \text{ m} \\ \text{width} = 1{,}5 \text{ m} \end{cases} \tag{4.11}$$

$$\text{Van} = \begin{cases} \text{length} = 5 \\ \text{width} = 2{,}05 \end{cases} \tag{4.12}$$

$$\text{motocycle} = \begin{cases} \text{length} = 2{,}30 \\ \text{width} = 1{,}25 \end{cases} \tag{4.13}$$

Then we introduce the vehicle mass parameter corresponding to each vehicle type. The mass is useful for the calculation of the accident severity and the collision risk, which are explained in detail in the metric section 5.2.

$$\text{Vehicle masses} = \begin{cases} \text{urban car} = 1500\text{kg} \\ \text{Van} = 3500\text{kg} \\ \text{motorcycle} = 250 \text{ kg} \end{cases} \tag{4.14}$$

Regarding the dimensions of the RSU, they are (0m X 0m) because it is a unit that is on the side of the road and therefore not considered subject to collision.
Afterwards we integrate to our model the cape of the vehicle which gives at time (t) the information of the trajectory of the vehicle at time (t+1).

Finally, another element is the confidence using an optimistic approach. The variable "a" is a constant that determines the level of optimism, with higher values of "a" leading to higher levels of confidence. The variable "occurrence" is the number of occurrences of the event or set of events. The formula is an exponential decay function, where the confidence starts at 1 and decreases over time as the number of occurrences increases. Its representation in the CBL-G is illustrated in

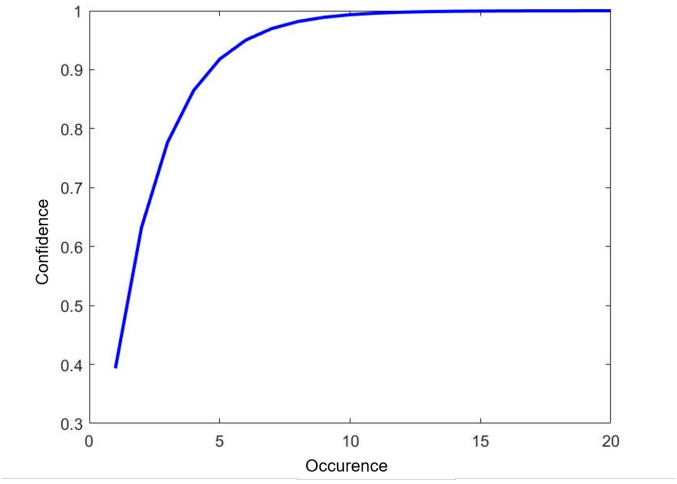

Figure 4.12: Curve representing the increase of the value of confidence versus occurence in CBL-G in optimistic mode

Figure 4.12 the confidence changes as the occurrence of the event increases. The plot will be a blue line with a width of 2 points. The x-axis will represent the occurrence and the y-axis will represent the confidence.
The value of "a" is set at 0.5 and can be adjusted to change the level of optimism. Higher values of "a" will lead to a faster decrease in confidence, while lower values will lead to a slower decrease.
It's worth noting that, this formula is a way to model the confidence based on the frequency of the event. The idea behind the formula 4.15 is that if an event occurred many times before, it's more likely to happen again, so the confidence will decrease. If the event never occurred before, the confidence will be at its maximum.

$$confidence = 1 - exp(-a * occurence) \tag{4.15}$$

4.10 Conclusion

This chapter presents a study on the utilization of CPMs in autonomous driving systems to improve road safety. We aim to present a comprehensive analysis of the various perception levels between vehicles travelling on the highway by utilizing local and extended local perceptions.
Specifically, we have defined and discussed the concepts of local, extended local, extended branch, and global perception. Furthermore, we have outlined the modifications and adaptations made to our CBL-G communication architecture to conform to the ETSI-standardised CPM message and the new properties incorpo-

rated into the vehicle to serve as collision risk measurement parameters.
In the subsequent chapter, we will delve deeper into the application of these perception levels in the estimation of risk levels. We will also provide a detailed analysis of the various risk metrics and explain our rationale for selecting a specific risk metric, along with relevant scenarios to illustrate its effectiveness.

Chapter 5

Multi-level Risk estimator with uncertainties and multidimensional configurations

Contents

5.1 Introduction

The goal of calculating collision risk in the context of ADAS is to enable the definition of various levels of alert, each of which corresponds to a specific reaction. For instance, the lowest level may correspond to audible alerts, while the highest level may involve the taking control of the vehicle to avoid an accident. This thesis focuses specifically on the estimation of risk, rather than the precise prediction of collision times.
To achieve this goal, a method is proposed that takes into account a set of instants sampled along the predicted interval. The collision probability is then calculated for each sample. This approach allows for the consideration of multiple potential collision events, as opposed to a singular predicted collision time. Additionally, the sampling period is sensor-independent, can be freely adjusted during trajectory prediction, and is finite enough to not interfere with real-time processing.
In this chapter, we present a method for multi-level collision risk estimation for autonomous vehicles (AVs) utilizing the multi-level perception system previously described in chapter 4. We will provide a detailed explanation of the method, including its operational principles and implementation. We will also present an analysis of the results obtained from simulations of various scenarios, and conclude with a discussion of the effectiveness and potential applications of the proposed method.

5.2 Collision risk indicators

We use various evaluation metrics to analyze and evaluate our method, which we explain in the following subsections. Those metrics are based on the research we conducted in chapter 1.

5.2.1 Collision probability based on TTC

As it was established in our state of the art, Time to Collision (TTC) refers to the time it takes a following vehicle to catch up to a preceding vehicle, which is following it on the right. In our context, it is the time it takes for each object's trajectory to be completed. Examination of the criteria for maintaining distance between vehicles helps to better understand the behavior of following behavior and traffic flow.
TTC is a projection of the time remaining at time (t) before a future collision between two vehicles, if they do not change their driving behavior (i.e., their speed, acceleration, or driving direction). It is compared to the driver's reaction time.

If the TTC is less than the driver's reaction time, the collision is inevitable. If the TTC is low, but not less than the driver's reaction time, subtracting the two values can give the time remaining for the driver, or an automated collision avoidance system, to take evasive action.

$$TTC_{i;j} = \frac{(X_j - X_i - L_i)}{V_i - V_j} \quad , \quad V_i > V_j \tag{5.1}$$

The TTC can be mathematically expressed by the Eq 5.1, with with Xi (respectively Xj) the positions and Vi (resp. Vj) the velocity of the following (resp. leading) vehicle, and Lj the length of the leader.
This indicator must be compared to the driver's reaction time and the reaction time of the vehicle's actuators.
The crash becomes unavoidable if the TTC becomes less than the sum of these reaction times. In this case, it is no longer a question of avoiding the crash but rather of limiting the damage of the possible collision.
Projects such as "ARCOS" and "PREVENT" have studied TTC and defined several limits to the cooperation between driver and automation.
The Glaser et al method (Vanholme et al., 2009; Glaser et al., 2010a) allows the generation of collision possibilities which is shown in red in Figure 5.1, the concept is explained as follow:

- For a TTC of 10 s, vehicle i is assumed to have no interaction.
- A TTC of 1.5 seconds is generally used to trigger a first level of alert.
- When the TTC falls below 1.3 seconds, the system may reinforce the warning.
- If the TTC becomes less than 1 s, the control by the automatism can be activated.

The Ammoun method (Ammoun, 2007)which is represented in blue in figure 5.1:

- For a TTC inferior to 2sec: in this case, they judge that the shock is unavoidable and the risk is maximum regardless of the duration of the shock.
- If the TTC is higher than 5 sec: the driver has at least 5 sec to anticipate the risk. This time is considered sufficient, that's why we mark the risk is minimum.
- The area between the two, i.e. between 2 and 5 seconds, is represented linearly.

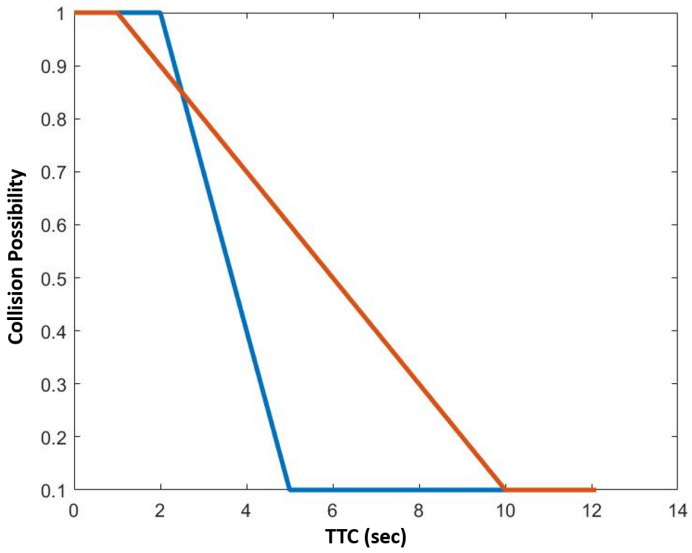

Source [Ammoun, 2007; Glaser et al., 2010a]

Figure 5.1: The Glaser's and Ammoun's Possibilities methods

5.2.2 Collision probability based on Time Inter-Vehicular (TH)

Time Headway (TH) refers to the time separating two successive vehicles in the same traffic lane. The traffic law defines a two-second safety TIV. Depending on the speed, the driver must deduce their safety distance from the vehicle in front of them. The TIV equation is detailed in (Eq 5.2).

$$TIV_{i;j} = \frac{(X_j - X_i - L_j)}{V_i} \tag{5.2}$$

Both TH and TTC are safety indices associated with rear-end collisions and are mathematically related. Therefore, it is possible that these two parameters are in fact significantly correlated and that a new safety index can be reached based on them.
To study this relationship, (WINSUM and HEINO, 1996) observed the behavior of drivers in the driving simulator in two different groups. In the first group, the speed of the leading vehicle was reduced from 60 to 40 km/h and in the second group, the speed decreased from 50 to 30 km/h.
TH and TTC were collected and plotted as the drivers began to brake. For the first group, the TTC at the beginning of braking was between 3 to 6 and the TH was 1.5 to 2.5 sec, and for the second group, the TTC was between 3 to 6 and the

TH was 1 to 1.5 sec. The TIV normalized function is computed in equation 5.3:

$$F_{TIV_{i,j}} = 2 - TIV, \quad If \;\; 1 \leq TTC_{i,j} \leq 2; \tag{5.3}$$
$$F_{TIV_{i,j}} = 1 \quad If \;\; 0 \leq TTC_{i,j} \leq 1; \quad else \;\; 0; \tag{5.3}$$

5.2.3 The equivalent energy speed (EES)

The Equivalent Energy Speed (EES) (km/h), gives the speed at which a vehicle would have to hit a static obstacle, such as a concrete wall, to dissipate the same kinetic energy as that dissipated by the collision of the two vehicles, considering a complete dissipation of the kinetic energy and the collision of two moving vehicles By developing the equation, we obtain the equation 5.4:

$$EES_{i;n} = (V_n - V_i) \times \frac{M_i}{M_i + M_n} \tag{5.4}$$

If the two vehicles have equivalent masses, it can be further simplified to the equation 5.5:

$$EES_{i;n} = (V_n - V_i) \times \frac{1}{2} \tag{5.5}$$

EES is linked to the Percentage of Fatalities and Serious Injuries, which are injuries to vehicle occupants through an analysis of the accident database, such as that commonly used in Europe by the LAB2, (Mangeas, LIVIC, 2003; Demmel, 2012).

5.2.4 Percentage of deaths and serious injuries (G)

G represents the severity of an accident where both vehicles involved have not changed their speed from the current time. The severity function G(EES) applied to EES and used in (Glaser et al., 2010b) and in (Demmel, Gruyer, and Rakotonirainy, 2013) is defined in eq 5.6.

$$g(Vn; Vi) = G(EES_i, n) = G((V_n - V_i) \times \frac{2.M_i}{M_i + M_n}) \tag{5.6}$$

On the other hand, the mathematical equation (eq 5.7) represents the severity of the accident that would occur if the vehicle (veh_n) performed a sudden emergency braking with deceleration (γ= 0.8g = 7.85 m/s-2), (Demmel, 2012).
Figure 5.2 represents the percentage of serious injuries by EES values.

$$g(V_n; V_i - \gamma TTC_{i;n}) = G(EES_{i-\gamma TTC_{i;n}}, n) \tag{5.7}$$

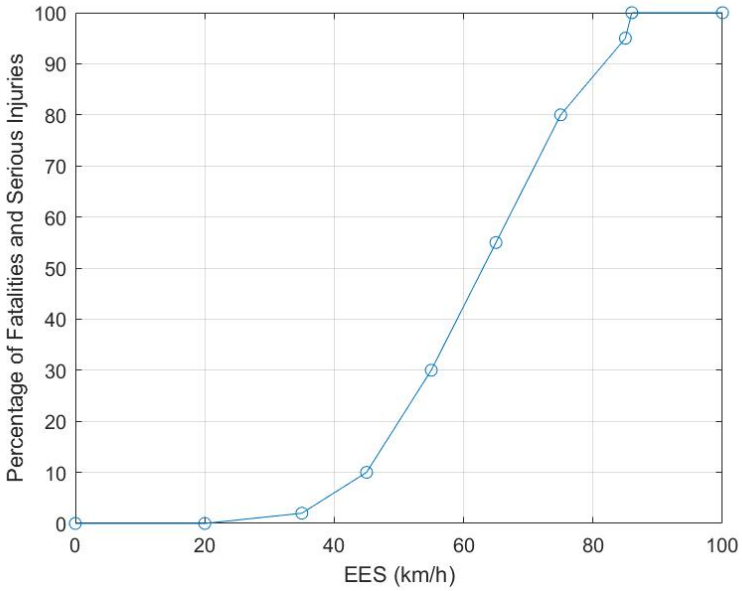

Figure 5.2: Percentage of fatalities and serious injuries considering EES (km/h)

5.2.5 Collision risk (R)

The risk $R_{i;n}$ for each vehicle is calculated according to the equation 5.8, where g is a function that calculates the severity of the potential accident using the SEA and G, which is the transfer function relating the SEA to the probability of injury or death, constructed from an analysis of car accident databases.
Note that (Demmel, 2012), only the probability of serious injury or death, the worst case scenario is considered, i.e. the maximum between the two scenarios (no driver action, emergency braking by the driver γ=0.8 = 7.85 m/s-2)).

$$R_{TTC(i;n)} = P_{TTC(i;n)} \times max[g(V_n, V_i),\ g(V_n; V_i - \gamma TTC_{i;n})] \tag{5.8}$$

Note that the TTC Equation is given in Eq 5.1 and the figure 5.2 represents the percentage of serious injuries by EES values.

$$R_{TIV(i;n)} = P_{TIV(i;n)} \times max[g(V_n, V_i),\ g(V_n; V_i - \gamma TIV_{i;n})] \tag{5.9}$$

5.3 Uncertainties configuration model

Despite the fact that all of these risk estimation metrics have demonstrated their worth and efficiency, none of them account for uncertainties and are multidimensional. Indeed as established in the section 1.3.5,an indicator should be able to integrate important aspects of different environments.

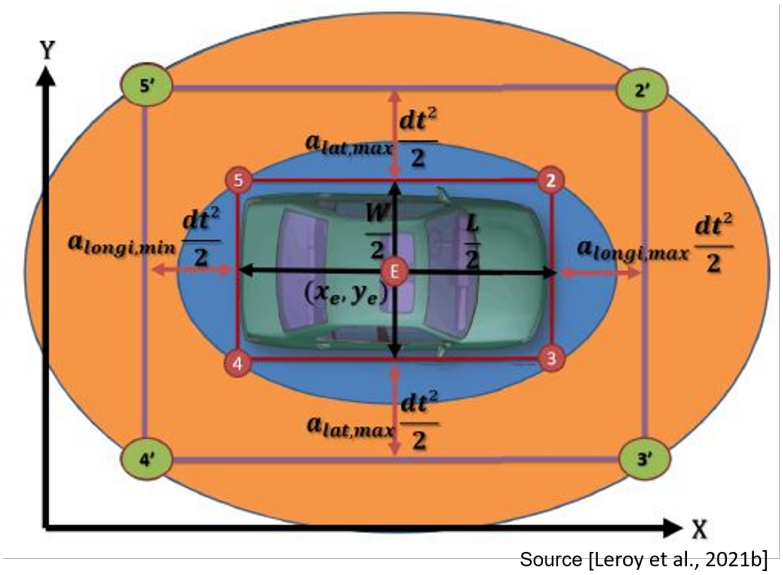

Figure 5.3: Schematic representation of the vehicle position uncertainties with ellipsoids representing the vehicular space occupancy (Leroy et al., 2021)

In a simple two-vehicle situation, we believe that a simple risk indicator based on time such as TTC can be used directly from the perspective of the passing vehicles. However, when we consider extended perception, there will be additional objects in the ego vehicle's perception field. This will allow us to construct a more complex representation of driving risk for the ego-vehicle as well as a different driving situation. Indeed, when two vehicles are following each other, the risk is accurate; however, when two vehicles are on different lanes but parallel this close without any planned lane change, we end up with an inefficient risk estimation because unfortunately, these metrics consider mainly for the majority distance and speed. in order to model the configurations existing between two vehicles, an ego-vehicle and an obstacle vehicle in the driving environment, it is important to have a physical representation of the two objects.
The vehicle is represented as a rectangle, oriented according to the vehicle heading, with five geometrical points: the center (x_e, y_e) of the rectangle and the four angles (x_i, y_i) of the rectangle. Their coordinates are given as follows:

$$x_i = x_e \pm \frac{L}{2}; \qquad y_i = y_e \pm \frac{W}{2} \tag{5.10}$$

with L and W respectively the length and the width of the vehicle. $\frac{+L}{2}$ is added for front points and $\frac{-L}{2}$ is used to rear points. $\frac{+W}{2}$ is used for upper points and $\frac{-W}{2}$ for lower points.

In addition, to model the positions uncertainties due to the accelerations of the moving objects, we assume that the borders of the vehicle shape (space occupancy) are a bit farther away. This means that an acceleration value (uncertainty on the vehicle dynamics) is applied on the current vehicle or obstacle positioning. Therefore, the extended vehicle space occupancy coordinates $(x\prime_i, y\prime_i)$ with uncertainties become:

$$x\prime_{i,front} = x_i + \frac{a_{longi,max}}{2}.dt^2 \tag{5.11}$$

$$x\prime_{i,rear} = x_i + \frac{a_{longi,min}}{2}.dt^2 \tag{5.12}$$

$$y\prime_i = y_i + \frac{a_{lat,max}}{2}.dt^2 \tag{5.13}$$

With $a_{longi,max}$ the maximal longitudinal acceleration, added to the front points, $a_{long_i,min}$ the minimal longitudinal acceleration in normal conditions (no emergency braking), or maximal deceleration, applied to rear points, $+a_{lat,max}$ the maximal lateral acceleration applied to upper points, $-a_{lat,max}$ applied to lower points. In (Mahajan, Katrakazas, and Antoniou, 2020), the lateral acceleration is fixed between -0.5 and $+0.5m.s^{-2}$.
Figure 5.3 represents the vehicle modeling with uncertainties. Those uncertainties are therefore used to represent the configurations of the vehicles in space to assess the relative risk between them.

5.4 Multi-dimensional configurations model between vehicles

In order to take into account a multiple-dimensional context with uncertainties, one of the more relevant distance indicators is the distance of Gruyer. This distance has already been used to assess the distance (similarity) between two vehicles represented by a probabilistic model of a set of points (two clusters of points). This distance is introduced in (Demmel, Gruyer, and Rakotonirainy, 2013), and applied to an ego-vehicle i, and an obstacle u is noted $D_{i,u}$. The chosen distance $D_{i,u}$ is defined as follows:

- First of all, this function $D_{i,u}$ gives a result scaled between 0 and 1 if the measurement has an intersection with the cluster u. The value 0 indicates that the measurement i is the same object as the cluster u with complete confidence.
- Secondly, the result is above 1 if the measurement i is out of the cluster u,
- Finally, this distance has the properties of distance functions.

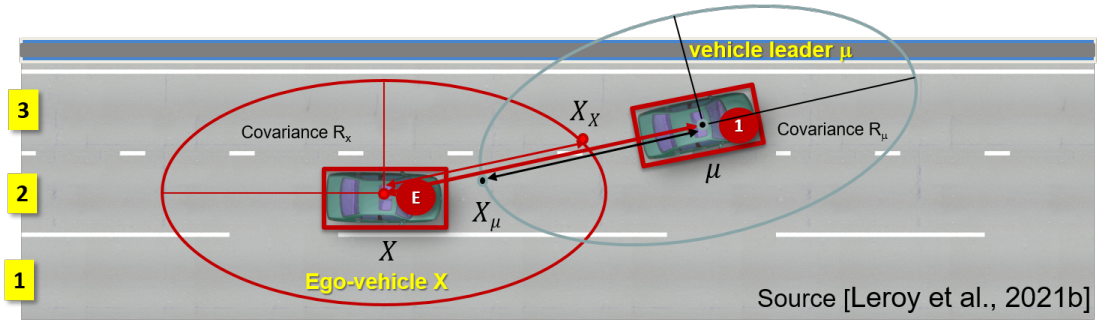

Figure 5.4: The distance of Gruyer representation between an ego-vehicle and an obstacle leader vehicle

The distance function uses both cluster and measurement covariance matrices. The chosen function computes an inner distance with a normalized part built from the sum of the outer distances of a cluster and a measurement. Only the outer distance uses the co-variance matrix information (Eq 5.14):

$$D_{i,u} = \frac{\sqrt{(X_i - u).(X_i - u)^t}}{\sqrt{(X_u - u).(X_u - u)^t} + \sqrt{(X_x - X_i).(X_x - X_i)^t}} \tag{5.14}$$

Figure 5.4 represents the ego-vehicle (measurement) X and the obstacle (cluster) u with the ellipsoids of uncertainties on their positions. In the normalizing part, the point X_u represents the border point of a cluster u (center u). This point is located on the straight line between the cluster u (center u) and the measurement i (center of X_i). The same border measurement is used with the measurement. The computation of X_u and X_x is made with the co-variance matrices R_x and P_u.
P_u and R_x are respectively the cluster co-variance matrix and the measurement co-variance matrix. The Gruyer distance can be considered as a special case of other recognized distances such as Batacharyya or Mahalanobis distance. Indeed they all take into account the variance and covariance matrix and the uncertainty between the vehicles. The Distance of Gruyer (DG) extended with the consideration of uncertainties on positions due to accelerations, is expected to fit better than the usual Euclidean distance between two geometrical points to represent the interactions between two vehicles in a close vicinity but also when they are driving on different lanes.

5.5 TTC and TH normalized functions for vehicle Collision risk estimation

The difficulty in dealing with risk estimation in a bi-dimensional space is that extrapolating the vehicle's respective trajectories does not always result in collision. As a result,

the proposed two approaching vehicles be represented by a projection on a single axis.
To represent the relative dynamics of the ego and obstacle vehicles, the scalar speed differential, i.e. the difference between the scalar projections of their speed vectors on the oriented axis connecting the two vehicles, was chosen. It is important to note that the axis is constantly changing depending on the relative positions of the vehicles.
To represent the relative dynamics of the ego and obstacle vehicles, the scalar speed differential, i.e. the difference between the scalar projections of their speed vectors on the oriented axis connecting the two vehicles, was chosen. the scalar speed differential is defined in Eq 5.15:

$$DV_{scal_{i,j}} = \overrightarrow{V_{ego}}.\frac{(u-X)}{||u-X||} - \overrightarrow{V_{obs}}.\frac{(u-X)}{||u-X||} \tag{5.15}$$

The extended Equivalent Energetic Speed and to apply the severity function related to the crash severity in Eq 5.16:

$$EES_{(DV_{scal_{i,j}})} = DV_{scal_{i,j}}.\frac{2m_i}{m_i + m_j} \tag{5.16}$$

The extended TTC is computed with the scalar speed differential and the intra-class length l_{ic} (Eq 5.17). The intra-class length l_{ic} is computed as the length of the segment on the directional axis of which extremities are the intersection points with the oriented rectangle boundaries of the vehicles and the centers of the vehicles. The aim of this computed length is a similar representation as the modeling used in the computation of the distance of Gruyer (with rectangles representing the vehicles instead of ellipsoids).

$$TTC_{scalar} = \frac{||u-x|| - l_{ic}}{DV_{scal,ij}} \tag{5.17}$$

The extended Time Headway is computed thanks to the scalar projection of the ego-vehicle speed vector $\overrightarrow{V_{ego}}$ on this axis (Eq 5.18).

$$TIV_{scalar} = \frac{||u-x|| - l_{ic}}{\overrightarrow{V.ego}.\frac{(u-x)}{||u-x||}} \tag{5.18}$$

Between the time the driver notices a hazard and the time he executes a maneuver to avoid it, it takes an average of 1 second for an attentive driver in good condition. This is the average value that we will use.
During the reaction time (about 1 second), the vehicle continues to move at the same speed since there is no reaction yet. However, this distance varies according to the speed: the faster I go, the greater the distance covered in 1 second.
We must therefore be able to estimate the distance covered in 1 second. This will allow us to deduce the regulatory safety interval to be left between the vehicle in front of me and mine (2 seconds minimum). Rounding to one decimal place gives us 1.8 seconds.

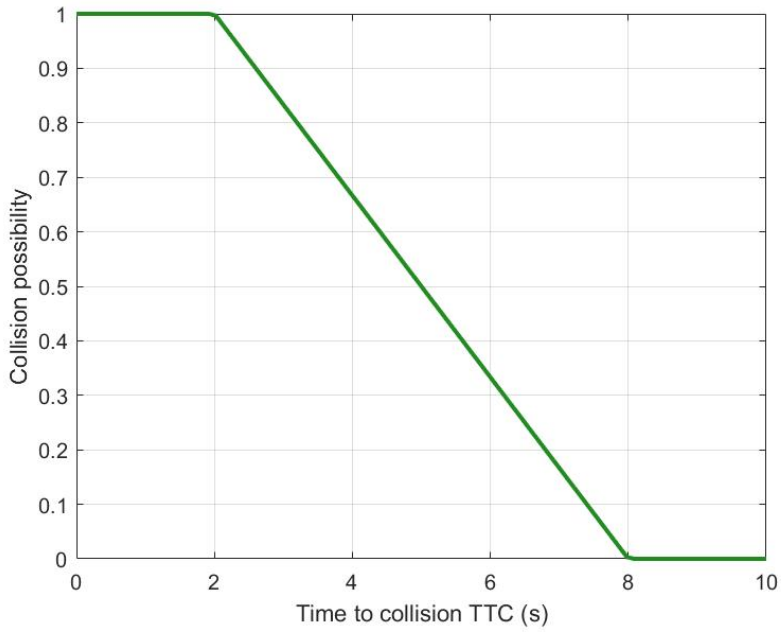

Figure 5.5: Our proposed normalized TTC function for the collision possibility

This is the maximum reaction time for the driver of this vehicle to put it in safety. According to (Vanholme et al., 2009), when the TTC is equivalent to 10s, the vehicle i is supposed not to have a collision, a TTC of 1 to 5s is commonly used to trigger the first level of alert, when the TTC goes down is 1 to 3s, the system can reinforce the alert if the TTC becomes lower than 1s, an automatic decisions collision avoidance system can be triggered. In our model, which is shown in Figure 5.5, we compute a collision probability $P_{i;n}$ for each vehicle.We propose to use the two extreme values to determine a collision probability of 0 (for a TTC of 8s) and 1 (for a TTC less than 2s). Between these values, the probability is linear with respect to the TTC. The Time to collision normalized function is computed in eq 5.19:

$$\begin{aligned} F_{TTC}(TTC_{i,j}) &= \frac{(8 - TTC_{i,j})}{6} \quad If\ 2 \leq TTC_{i,j} \leq 8; \\ F_{TTC}(TTC_{i,j}) &= 1 \quad If\ 0 \leq TTC_{i,j} \leq 2;\ \ else\ \ 0; \end{aligned} \tag{5.19}$$

If the TTC is less than 2 sec: we judge that the shock is inevitable and the risk is maximal whatever the duration of the shock. Indeed we estimate that the probability of collision is at the maximum during all the time that takes a driver to react to risk.
If the TTC is greater than 8 seconds: the driver has at least 8 seconds to anticipate the risk. This time is considered sufficient, so we mark the risk as a minimum. Similarly, the

Time headway normalized function is computed in Eq 5.20:

$$\begin{aligned} F_{TIV}(TIV_{i,j}) &= 2 - TH_{i,j} \quad If\ 1 \leq TIV_{i,j} \leq 2; \\ F_{TIV}(TIV_{i,j}) &= 1 \quad If\ 0 \leq TTC_{i,j} \leq 1;\ \ else\ \ 0; \end{aligned} \tag{5.20}$$

5.6 Risk indicator based on multi-dimensional and uncertainties modeling (RIMUM)

This Risk Estimator with Uncertainties and Multidimensional Model (RIMUM) is the collision probability defined as an extension of the distance of Gruyer with a normalized collision probability function (Leroy et al., 2021).

$$RIMUM_{i,j} = F(D_{i,j}) \times G(EES(DV_{scal,i,j})) \tag{5.21}$$

The normalized function associated to the distance of Gruyer in Eq 5.22:

$$F(D_{i,j}) = \frac{1}{D_{i,j}} \qquad if\ \ D_{i,j} \geq 1; \qquad else\ \ 1; \tag{5.22}$$

In any dimensional configuration with consideration of the position uncertainties and the relative dynamics of the vehicles. To provide insight into the possibility to use this estimator by the autonomous driving systems risk assessment Using the scalar speed differential, the severity function computes the probability of fatality based on the EES (Leroy et al., 2021).
It is the sum of two components: collision probability and severity function. It is scaled from 0 to 1, with 0 representing no risk and 1 representing the greatest risk of a fatal accident.

5.7 Simulation configurations

For nodes mobility evaluation, modelling and structural analysis, we used the communication strategy developed and implemented in Matlab software. Moreover, We use the microscopic traffic simulation software called SUMO to generate vehicle tracks for highway scenarios. The mobility scenario is built from a real road network corresponding to a section of the A27 highway. It's a three-lane highway road with a west-to-east direction. Perception is performed by a simple modelling and simulation of onboard sensors. The characteristic of these sensors are a small field of view and a short range limited to 200 meters of visibility. This perception allows to detect only frontal obstacle in the ego-lane with a straight road geometry.
GPS data is obtained with a simple modelling (either perfect positioning or noised positioning with a Gaussian uncertainty). GPS data (vehicle position providing by mobility data coming from SUMO) is available through communication means between cluster

members. The communication range is up to 500 meters with free space propagation channel.
To investigate the risk of collision, we must create risky situations between vehicles travelling on the same route without threat. To study this collision risk in the perfect localisation scenario, we extracted the vehicles to be studied from our given Sumo file and intentionally cause a collision in real time by changing the dynamics of the vehicles involved (velocity). To generate collisions by remapping the state vector by using a linear model. Details about uncertain perceptions are given in the section 4.4.

5.8 Collision risk levels

CAVs can improve their sensing capabilities if vehicles exchange information about what they are sensing in the CPM using V2X communications.
We propose to use the distributed, connected, and dynamic communication strategy of CBL-G which takes into account the information of the vehicles that are close (the leaves) by cluster to allow the calculation of local risk first (within the cluster), then the extended risk estimation (outside of the cluster) and finally global risk. By using both sensor's perception and inter-vehicle communications (sharing of the local perception by each node) we can achieve risk estimation at different levels. The diagram in figure

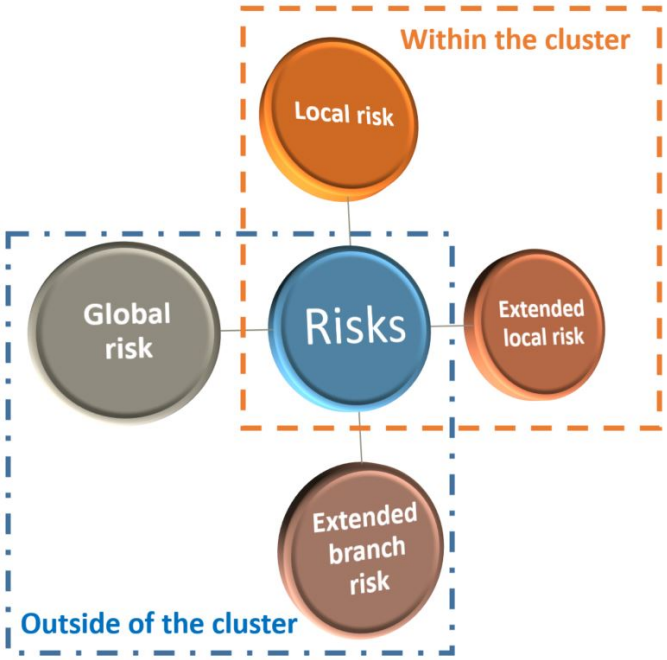

Figure 5.6: Illustration of our collision risk multi-levels propositions

5.6, depicts the four levels of collision risk: the two local collision risks: local risk, and

Table 5.1: simulation configuration for local risk scenarios

Risk estimation	Scenarios	Situations
Local Risk	Scenario 1: Perfect localization, certain perception	E1:Collision from the back
		E2: close driving in parallel lane
	Scenario 2: Perfect Localization, uncertain perception	E1: Collision from the back
		E2: close driving in parallel lane

extended local risk, which are calculated based on local perception, i.e. by the vehicle's onboard sensors. Which are limited in their perceptive capacity, and the surrounding obstacles (vision fields). The two extended and global collision risks, are calculated from the information collected during the communication exchanges, i.e. from the objects detected by the on-board sensors of the vehicles with which there is communication thanks to the CBL-G algorithm, which allows to widen the field of vision of the vehicle and not to be limited to the local perception of the vehicle.

5.8.1 Local collision risk

The local risk is the risk calculated by each vehicle based on its local perception defined in section 4.3.1. In this section, we will estimate the risk of collision between two vehicles locally in two different scenarios. For each scenario, the normalized risk functions of the extended TTC in Eq 5.19, the extended TH in Eq 5.20, and the extended distance of Gruyer (DG) in Eq 5.22 are computed, as well as the risk associated to TTC in Eq 5.8 and TH in Eq 5.9 and the risk indicator based on multidimensional and uncertainties modeling (RIMUM) in Eq 5.21. The simulation parameters are summarized in table 5.1.

5.8.1.1 Scenario 1: good conditions

Good condition scenario, the vehicles have a perfect location (without uncertainty). The perception of the vehicles is perfect in their field of perception which is limited to the capacity of the front radar (200m). The communication is perfect in the cluster (instantaneous, without delay, and without loss). For the local risk estimation (5.7), scenarios are presented as follows:

1. The ego-vehicle collides with a slower obstacle vehicle from the back on central lane (E1).
2. The ego vehicle drives in lane 2 in the parallel lane of the lead vehicle (obstacle vehicle) which is driving in lane 3 (E2).

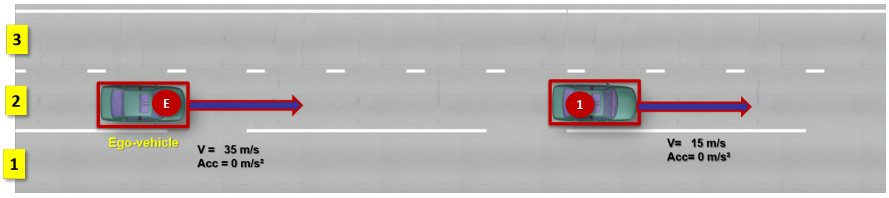

Figure 5.7: schematic illustration of the scenario 1 E1

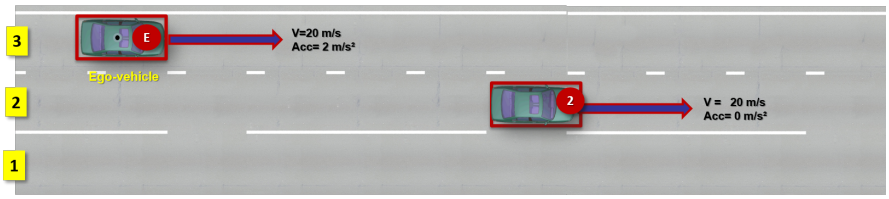

Figure 5.8: schematic illustration of the scenario 1 E2

For the E1: the vehicle E is the ego vehicle positioned at 205 meters, lanes 2 with 35m.s-1 speed. Vehicle 1 is the obstacle leader positioned at 370 meters, lane 2 with 15m.s-1 speed.

For the E2: the vehicle E is the ego vehicle positioned at 431 meters, lanes 2 with 20m.s-1 speed. Vehicle 2 is the obstacle leader positioned at 491 meters, lane 1 with 20m.s-1 speed.

5.8.1.2 Scenario 2 Degraded condition

For this scenario, we will study the perception uncertainty and perfect localization scenario, The vehicles have a perfect localization (without uncertainty: GPS RTK++), The perception of the vehicles is imperfect in their perception field as we can see it in figure 4.10. The perception field is limited to 200m. The communication is perfect in the cluster (instantaneous, without delay, and without loss).
For the Scenario 2 - E1 as shown in Figure 5.9: vehicle E is the ego vehicle positioned at 205 meters, lanes 2 with 35m.s-1 speed. Vehicle 1 is the obstacle leader positioned at 370 meters, lane 2 with 15m.s-1 speed. For Scenario 2 - E2 as shown in Figure 5.10: Ego vehicle (E) is positioned at first 431 meters, lanes 2 with 20m.s-1 speed. The leader

Figure 5.9: Scenario 2 E1

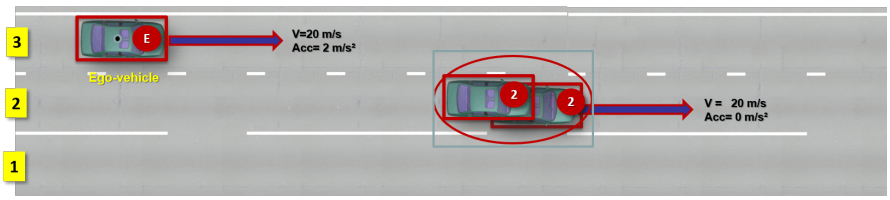

Figure 5.10: Scenario 2 E2

vehicle (2) is positioned at 491 meters, lane 1 with 20m.s-1 speed.
We will use kalman filter (Iglesias, Law, and Stuart, 2013), which is well known for its applications of data assimilation to state and parameter estimation, to simulate our uncertain perception, precisely to predict the vehicle's behavior (its next position) at the next moment regarding the system and sensor's noise, Because it is calculated from the data returned by the sensor, GPS noise is not taken into account in this structure. When there is perception uncertainty, the figure 5.11, depicts an example of the real positioning (green square) of a vehicle and the new positioning values (red diamond) obtained by applying the Kalman filter to our application, indeed we add noise to the signal then we estimate the position using the Kalman filter.

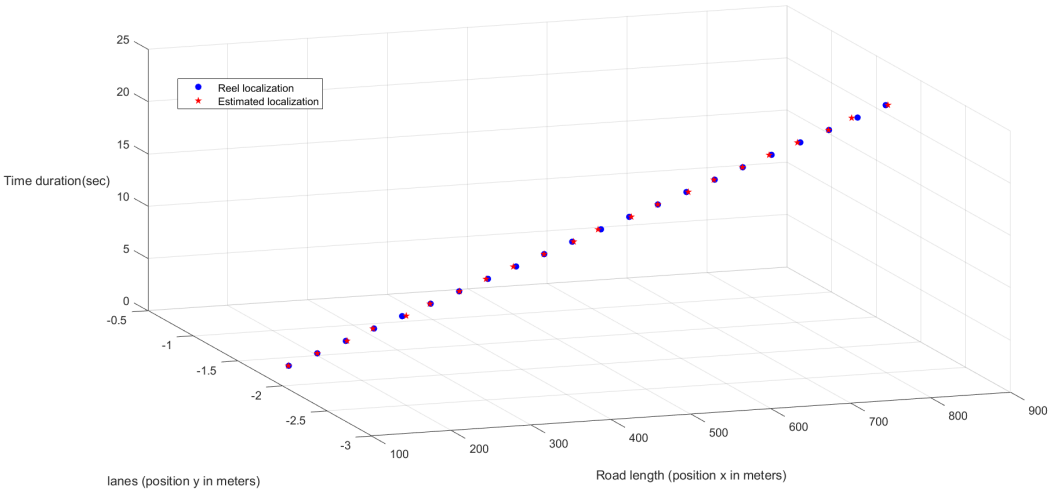

Figure 5.11: Representation of the real vehicle position superimposed on the estimated location obtained by applying a white Gaussian noise in Kalman filter method.

5.8.1.3 Analysis and discussion

The normalized risk functions of the extended TTC, extended TH, and extended distance of Gruyer (DG) are computed for each scenario, as well as the risk associated with TTC and TH and the risk indicator based on multidimensional and uncertainty modeling (RIMUM).
In scenario 1-E1, The probability functions of both the extended TTC and the extended TH show a maximal collision probability of 1 in this scenario even though the ego-vehicle and the obstacle do not actually collide in scenarios 1-E2, since they are not on the same lanes. On the contrary, the probability function of DG presents a maximal value lower than 1 (0.7 for scenarios 1-E2). The collision happens at 9 s, the risk increase to 1 for the three estimators (extended TTC, extended TH, and RIMUM). The risk curves of extended TTC, extended TH and RIMUM are very similar to the collision probability curves related to TTC, TH and DG. That is explained because in this scenario, the risk related to EES is maximal with a scalar speed differential constantly equal to 20 m.s-1.
The results on the scenario 1 -E1, show that both the collision probability related to

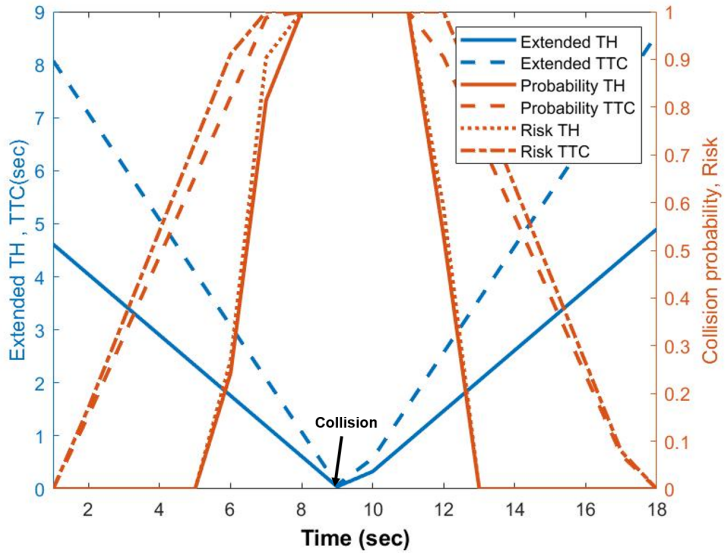

Figure 5.12: Scenario 1- E1 extended TH et TTC,Risk based on TH, Risk based on TTC

the distance of Gruyer and the RIMUM reach 1 at the exact moment of the collision.
Regarding the fatality risk, RIMUM values are low in scenario 1-E2. This is not only because when the scalar speed differential is lower than 7 ms-1, the severity function is null. It is also due to the function that was used to normalize the distance of Gruyer. TTC-based risk and TH based prompt a risk that reaches 0.15 which means 15% of fatality probability. This is a high value considering the studied scenario where vehicles are not evolving on the same driving lane. RIMUM still shows a high value 0.07 but is

lower than TTC and TH-based risk estimators. In this situation, RIMUM is then more realistic than TTC and TH-based estimators However TTC and TH-based estimators are more efficient regarding anticipation.
In scenario 1-E1, the TTC risk and TH risk increase earlier and faster than the RIMUM and therefore can be more efficient for anticipation, while the RIMUM risk increase is closer to the collision time. That can be explained because both TTC and TH-based risks are maximal several seconds before the actual collision, while the RIMUM is maximal only when the two vehicles actually collide.
Although the ego-vehicle and the obstacle do not actually collide in scenario 2 - E2, the probability functions of both the extended TTC and the extended TH show a maximum collision probability of 1. The probability function of DG, on the other hand, has a maximum value less than 1 (0.72 for scenario E2) which is more realistic. Furthermore, in scenario 1- E2, the collision probability function estimated by extended TH reached 1 approximately 2 seconds before the actual occurrence of overtaking, which is not realistic. TTC-based collision probability reaches 1 approximately 1.8 seconds before overtaking. The probability functions of both the extended TTC and the extended TH show a maximal collision probability of 1 in this scenario 2- E2 even though the ego-vehicle and the obstacle do not actually collide in scenarios 1-E2, since they are not on the same lanes. The DG probability function has a maximum value of less than 1 (0.77 for scenarios 1-E2). This value is higher than for the first scenario because of the perception uncertainty: indeed, the position of vehicle 2 is closer to vehicle E than it was in scenario 1-E1.
The extended TTC, extended TH, and RIMUM risk curves are very similar to the collision probability curves for TTC, TH, and DG. This is explained by the fact that in this scenario, the risk of EES is maximal, with a scalar speed differential that is always equal to 20 m.s-1. In terms of fatality risk, RIMUM values in scenario 2-E2 are low. This is not only because the severity function is null when the scalar speed differential is less than 7 ms-1. It's also because of the function that was used to normalize Gruyer's distance. TTC-based risk and TH-based risk prompt a risk of 0.17, indicating a 17% chance of fatality. Given the studied scenario, where vehicles are not evolving on the same driving lane, this is a high value. RIMUM has a high value of 0.072, but it is lower than TTC and TH-based risk estimators. RIMUM is thus more realistic than TTC and TH-based estimators in this situation.
In scenario 2-E1, with the leading slower vehicle on the same lane as the ego-vehicle, the TTC and TH risks rise earlier and faster than the RIMUM, making them more efficient for anticipation, whereas the RIMUM risk rises closer to the collision time. This is explained by the fact that both TTC and TH-based risks are at their peak several seconds before the actual collision, whereas the RIMUM is at its peak only when the two vehicles collide. In the following section, we will define our extended risk levels in our structure and organization of AV in CBL and how to exploit them in order to have different levels covering the maximum number of possible routes.

Table 5.2: Simulation scenarios and configuration

Risk estimation	Situation	Scenarios	Density
Extended local risk	Scenario A: Localization perfect perfect perception	S1	Low density
		S2	Medium density
		S3	High density
	Scenario B: Localization perfect, uncertain perception	S1	Low density
		S2	Medium density
		S3	High density
Extended branch risk	Scenario A: Localization perfect perfect perception	S2	Medium density
	Scenario B: Localization perfect, uncertain perception	S2	Medium density
Global risk	Scenario A: Localization perfect perfect perception	S2	Medium density
	Scenario B: Localization perfect, uncertain perception	S2	Medium density

5.8.2 Extended local collision risk

The extended local risk is the risk calculated by the branch using the cooperative CBL application and the built local extended perception through communications.
which implies that we will have for each Branch (B) a number of risks (R):
$\{R\{i,B\},...R\{n,B\}\}$ with i $\in$ [1, n], n the number of leaves in the cluster, i$\neq$ B .
The number of leaves per branch in CBL-G is around 1,94 for a low density scenario (S1), 4,75 in a medium density (S2) and 7,03 in a high density (S3). However due to perception limitation the local risk per branch is 0,5 in a low density (S1) and 3,48 for a medium density (S2) and 5,89 for a high density (S3). Which translate by an inconsideration of important data and i.e. a loss of risk estimation: 75% for (S1), 26,74% for (S2) and 16,22% for (S3). To correct this , we propose to use the local extended perception that we defined in section 4.3.2.

We illustrate our scenario in figure 5.13, for this extended local risk estimation we will

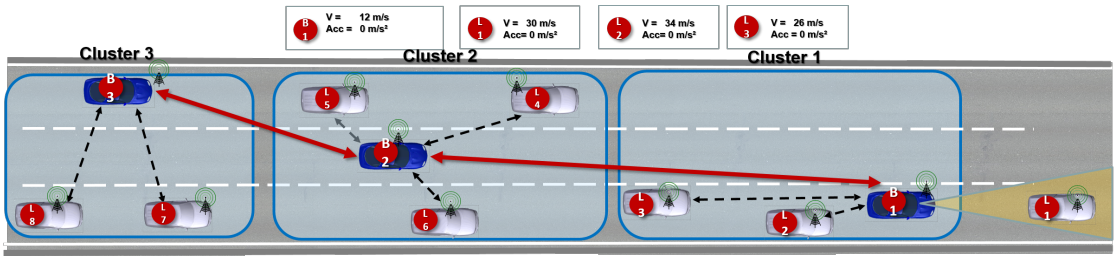

Figure 5.13: The CBL extended local risk scenario in a medium density high way environment

be performing simulation in a high way environment using CBL structure and the local extended perception, the ego vehicle is the branch B1 of the cluster 1 illustrated by the blue leading vehicle. Its average velocity is 12m.s-1.
The obstacles are the 2 following leaves (L2 and L3) illustrated by the gray vehicles. Their perspectives velocity are 34m.s-1 and 26m.s-1. The local perception map of the ego-vehicle is obtained using RADAR or Light Detection and Ranging (LiDAR). The localization uses a GPS.
Because branch B1 can only perceive the leading leaf L1 and cannot see the two leaves L2 & L3, there are potentially two risks that are ignored R2:{B1,L2} and R3:{B1,L3}. By using our extended local perception method we can detect two new extended local risks: R2{B1,L2} and R3 {B1,L3}. The risk between the branch B1 and the leaf L2, R2 {B1,L2} is represented in figure 5.8.2. Vehicle B1 and L2 collide at 5sec in this scenario, The extended TH exhibits an exponential value 2 seconds prior to the actual collision, reaching its maximum collision probability value one second prior to the collision. Extended TTC shows an exponential collision probability from 1 sec to 3 sec, and a maximum value of 2 sec before the actual collision.
If we consider a critical hazard threshold at risk value 0.7, then the driver will be alerted

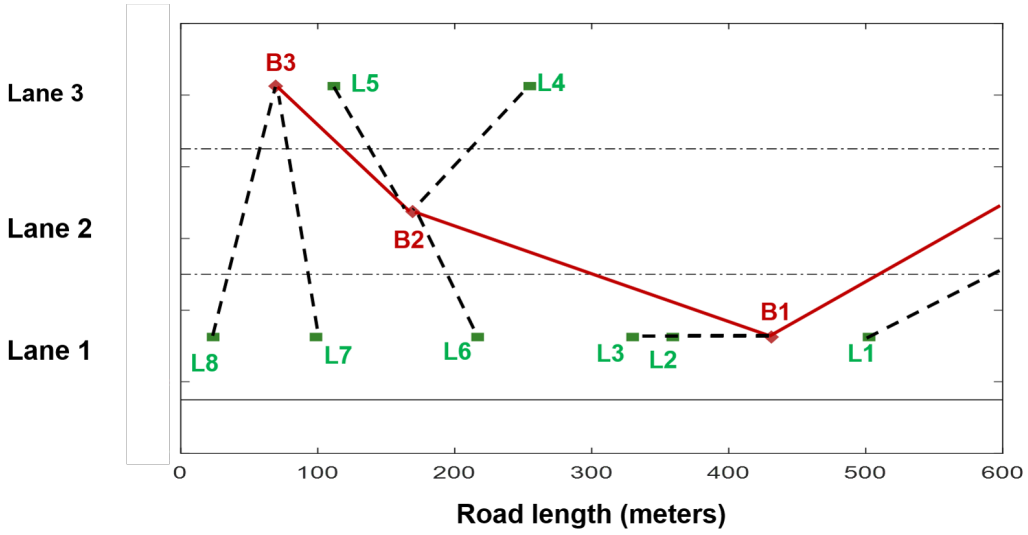

Figure 5.14: screenshot of the scenario of extended local risk scenario in a medium-density high way environment of CBL

2 seconds before the collision with the extended TH considering the minimum reaction time is 2 seconds, considering that the minimum reaction time is 2 seconds, so this warning time is very short and allows only emergency braking. On the other hand with the extended TTC the driver will be alerted 5 seconds before the collision which is still a short reaction time but still longer than the extended TH. Those values are efficient for anticipation however they saturate the risk to its maximum several seconds before the actual collision thus they are not realistic. For R3 at the beginning of the simulation, the risk is null it starts increasing as the vehicles get close to each other, on the contrary for R1 at the beginning of the simulation is 0.18 and decreases since the vehicles drift apart.
The global risk (GR) of the cluster is the maximum risk the branch has with its leaves and the maximum of the branch risk with its upstream and downstream branches.
GR=Max{RL,RB} with RL=Max{R{B,i}...,R{B,n}} being the maximum branch to leaf's risk with n the leaves number in the cluster.
RB=Max$\{R\{B, B_{upstream}\}, R\{B, B_{downstream}\}\}$being the maximum branch to branch risk. We achieved two goals as a result of the extended local risk: the first was to raise the perception of the branch to the same level as the number of leaves in the cluster; we noticed that the number of leaves in the cluster is 1.94 in a low-density scenario (S1), 4.75 in a medium density (S2), and 7.03 in a high density (S3). However, there was a loss of risk due to the limiting perception when using the local perception: the local risk per branch is 0.5 in a low density (S1), 3.48 in a medium density (S2), and 5.89 in a high density (S3) .

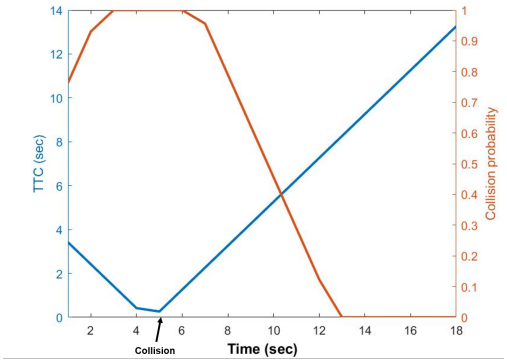

Figure 5.15: Extended local Risk of R2 {B1,L2} and collision probabilities for the CBL scenario (A) based on TTC

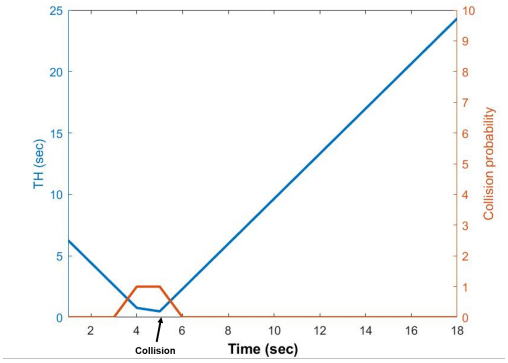

Figure 5.16: Extended local Risk of R2 {B1,L2} and collision probabilities for the CBL scenario (A) based on TH

We estimate the average of the extended local risk equivalent to the number of leaves per cluster using the extended local perception, which is 1.94 for a low-density scenario (S1), 4.75 for a medium-density (S2), and 7.03 for a high-density (S3) i.e. 100% of the average number leaves per cluster are considered for a collision risk estimation with their branch .
The second goal is to be able to calculate all of the potential risks earlier within our cluster without being constrained by the embedded equipment's perception. Although B1 had a unique local risk R1{B1,L1} , we were able to estimate two new extended local risks R2{B1,L2} and R3{B1,L3} using this method. R2 is the higher risk of all of them. We could estimate the danger of the second risk 5 seconds before the collision. The results of scenario B are very close to those of scenario A (the difference is to the nearest cent).

5.8.3 Extended branch Collision risk

The extended branch risk is the risk calculated by the branch in the CBL-G structure from the information transmitted by the adjacent branches (Upstream & Downstream) of the ego vehicle. i.e their local perception. This implies that we will have for each Branch (B) a number of risks (R): $\{R\{B, B_{Upstream}\}$, R$\{B, B_{downstream}\}$, R$\{B, i\}$,....R$\{B, n\}\}$ with i $\in$ [1, n], n being the number of perceived vehicles by the adjacent branches.
The branch B2 is the branch of cluster 2, its local perception of B2 is empty, while its extended local perception contains the leaves belonging to its cluster (L1,L2,L3,L4).
The two adjacent branches of B2 are B1 (the branch of cluster 1) and B3 (the branch of cluster 3), indeed vehicle B1 perceives the vehicle L6, while B3 perceives two vehicles: L5 and L3.
All of these vehicles (B1,B3,L3,L5,L6) are outside of B2's perception range. So for

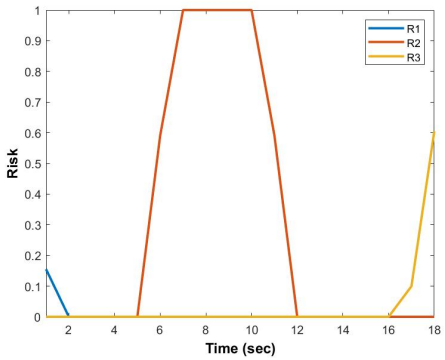

Figure 5.17: The extended local Risk probabilities (R1,R2,R3) of B1 in the CBL scenario A

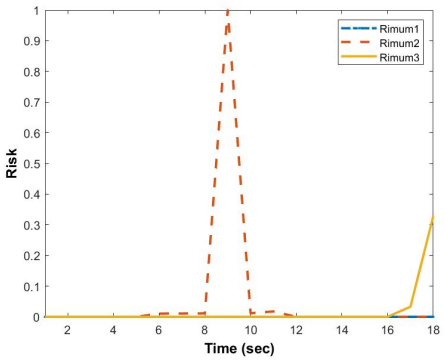

Figure 5.18: The extended local risk Rimum probabilities (R1,R2,R3) of B1 in the CBL scenario A

the vehicle B2 extended risk branch estimation, it will be considering multiple risks: R{B2,B1},R{B2,B3}, R{B2,L3}, R{B2,L5} and R{B2,L6}.

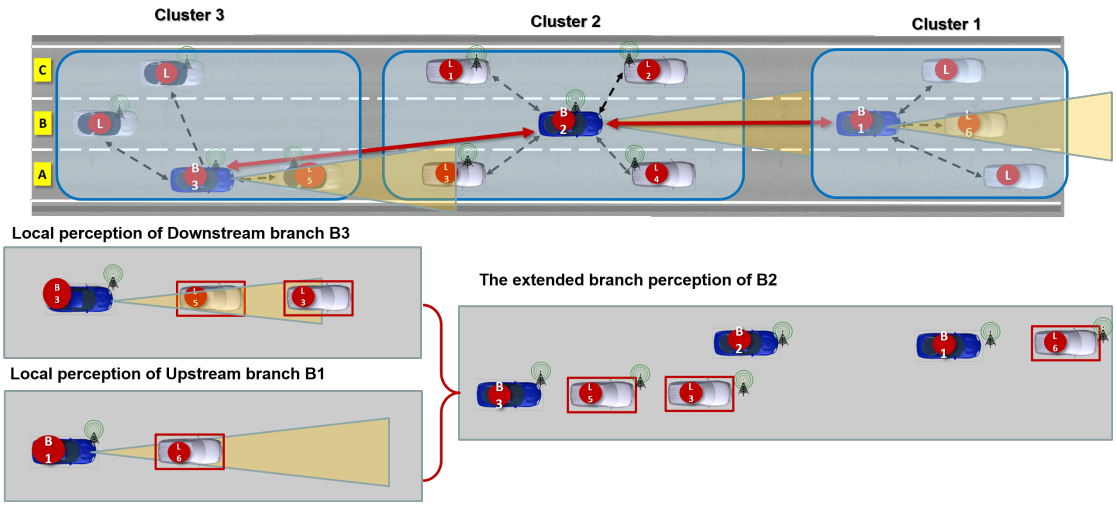

Figure 5.19: Schematic diagram of scenario A: extended branch perception of branch B2 in cluster 2 with correct perception and perfect localization

The extended branch risk scenario is represented in figure 5.19. Unlike the other risk, vehicle L3 is a member of the second cluster B2, so the risk between vehicle B2 and L3, R{B2,L3}, is estimated in the extended local risk of B2. The branches' inter-distance between B1, B2, and B3 is 500 meters. Vehicle B2 is in lane B at 15m.s speed. Vehicle

L5 is in lane A with 32m.s speed. Extended branch risk of B2 and L5 is R5{B2,L5}. R5 results show that the risk is low since the speed difference is 5m.s; However, it showed an increase at second 19 when vehicle L5 overtakes vehicle B2. Regarding the risk, RIMUM has a very low value (0.17) which can be explained by the differential speed which is equal to 5m.s but also regarding the severity function is null; for the extended TTC and TH values which are low (0.49 and 0.42) but still high considering this driving situation since the vehicles are in different lanes, for this case RIMUM has the lowest value thus is the most realistic.
We observe that the perception of the downstream branch is part of the ego branch's local extended perception, which creates a redundancy. Indeed the detected vehicles in the extended branch perception are most of the time already present in the local extended perception which creates a duplication of risk assessment since this risk is already calculated at the level of the extended risk of the ego branch.
On the other hand, we noticed that extended branch risk based on the Upstream branch perception, brings a new perception and thus allows us to estimate a more distant risk which makes it more relevant. Following these results, we will only use the perception of the upstream branch in our future works. Nonetheless, this discovery is not a flaw, but rather a strength of the method. This redundancy can be used to improve the certainty, reliability, and robustness of the risk indicators that use it. As a result, more risk estimation will be required.

5.8.4 Global collision risk

This is the risk calculated by the branch nodes only, based on the information collected from the communications outside of the clusters i.e. indirect communications between branches that are at more than one hop away. Figure 5.20 represent the section of the road studied in the context of global estimation The scenario of global risk estimation is described as follows: the ego vehicle is the branch B3 illustrated in figure 5.20. The neighboring branches are B2 and B4. The vehicle B3 perception contains vehicle B4, the perception of the vehicle of the downstream branch B2 contains vehicles B3 and B4, and the perception of the upstream branch B4 does not contain any vehicles. In this case, these neighboring branches (one hop) do not give the ego vehicle (B3) the possibility to add new vehicles to its perception outside its two neighboring branches (up & down).
However the global risk is based on the extended local perception of the branches beyond one hop, so to calculate the global risk of the branch (B3), we use the extended local perception of the B1 and B5 branches, i.e. the leaves: L1, L2, and L3. Global risk between the branch (B3) and the leaf (L1) is the risk R1{B3,L1}, the global risk between the branch (B3) and the leaf (L2) is the risk R2{B3,L2} and the global risk between the branch (B3) and the leaf (L3) is the risk R3{B3,L3}. The overall global risk of branch (B3) is GR= Max{R1,R2,R3}.
In this scenario, we do not create any risk situations; instead, we estimate the overall risk. B3 travels in the second lane at an average 35m/s speed, while L2 travels in the third lane at about 26m/s speed. The collision probability evolution is shown in figure

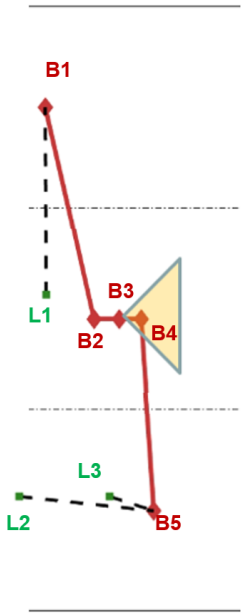

Figure 5.20: Road section studied in the context of the global risk estimation

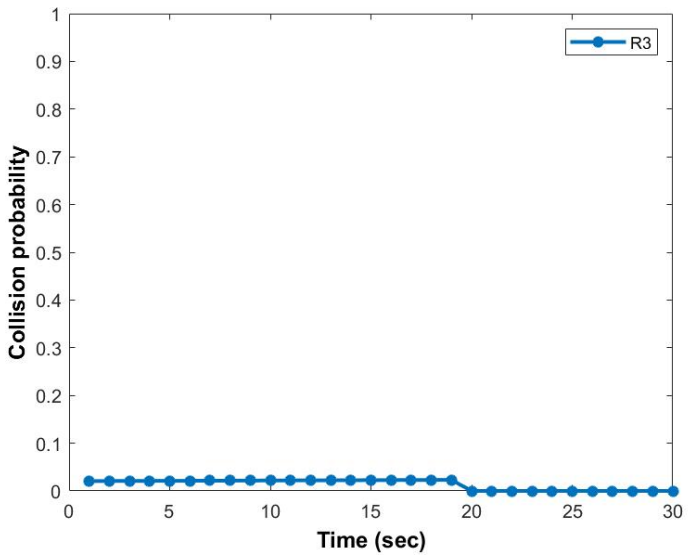

Figure 5.21: Representation of collision risk R3{B3,L3}

5.23.

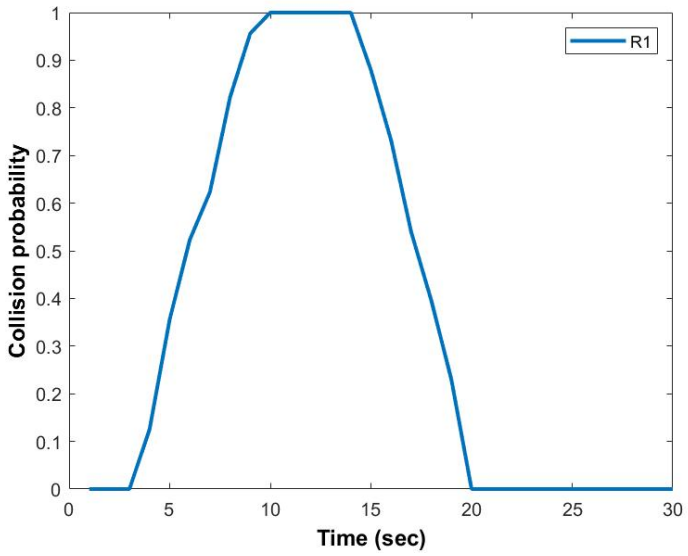

Figure 5.22: Representation of collision risk R1{B3,L1}

The vehicle (L3) is traveling in the third lane at a speed of 29 meters per second. This means that the L3 vehicle and the ego vehicle are nearby and parallel. In a longitudinal position, the two vehicles are less than 4 meters apart at moment (6s). this type of scenario can be considered similar to the scenario1-E2 studied for the estimation of the local risk.
Vehicle L1 is driving in the same lane and behind vehicle B3 at a speed close to the B3 branch speed (35m/s). At the start of the simulation the distance between B3 and L1 is 100m, so the R1 risk should be very low. To simulate a risky situation we adapt the speed of the rear vehicle, i.e. we assume that the driver accelerates until reaching the speed of 45m/s; the collision happens at 14 second.
By using the global risk we have estimated a collision risk 7 seconds before the actual collision. Indeed the local risk of B3 allows us to estimate only one close risk (with B4), however, the global risk allows us to estimate many new distant risks (R1, R2, R3) represented in figure 5.21, 5.22 and 5.23 by their definitions, these risks are physically distant for the most part and the level of risk remains low however in term of anticipation it proves to be effective. Indeed if we charge the RSU or another element to launch an alert system with a threshold of 0.6 for example, we will be able to detect the vehicle 14 seconds ahead and anticipate the risk of collision by 7 seconds.

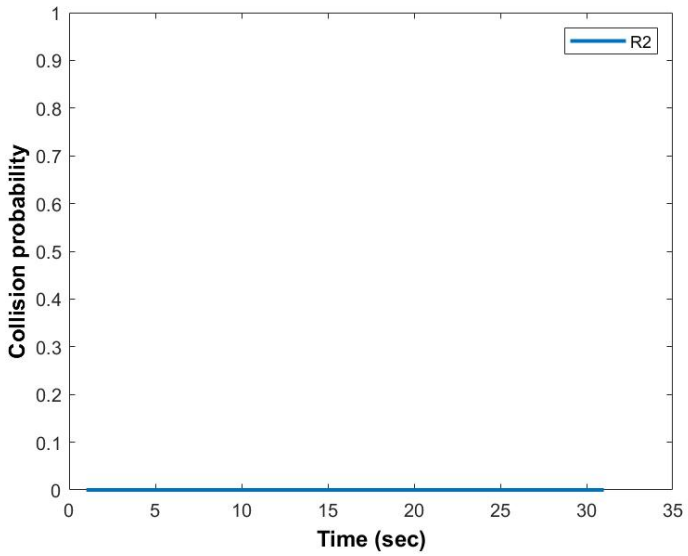

Figure 5.23: Representation of collision risk R2{B3,L2}

5.9 Conclusion

In this chapter, we developed a multi-level method for estimating risk in highway situations involving various dimensions by utilizing an adapted risk estimator. By applying this approach and calculating extended and global risks, we are able to anticipate critical distance scenarios, providing ample time for safe reactions. We demonstrated how detecting risks from a distance can result in significant time savings for drivers. In our simulations, we evaluated our method against various risk indicators such as extended TH, TTC, and DG,RISK, RIMUM. We considered two examples of collision risk situations (front collision, rear collision) in two scenarios: one in optimal conditions and another in degraded conditions that include perception uncertainty. For the latter scenario, we applied the Kalman prediction method. Our results indicate that the collision probability values between the two scenarios differ by only around 2% error rate.
In our analysis, we found that the collision probability functions estimated by extended TTC and TH are better for anticipating collision scenarios, as they provide early warnings. However, the extended distance measurements used by Gruyer and RIMUM better reflect the reality of the situation. Additionally, the TTC and TH-based risks do not consider any potential evasive actions by the vehicles, while RIMUM is reactive to potential collision avoidance maneuvers. Our results also indicate that the collision probability related to DG and RIMUM are better suited for motion planning in characterizing the reality and dynamics of vehicles in overtaking and crossing situations on multi-lane configurations more accurately than the extended TTC and extended TH. Furthermore,

collision probability related to DG incorporates uncertainties and sensitivity to unforeseen events due to its reversible nature, which can help with motion planning.
In conclusion, the extended perception capabilities of VANETs provide us with the ability to detect the presence of a vehicle with potentially dangerous behavior. However, the method of risk estimation is critical because it directly impacts the effectiveness of the collision avoidance system. If the risk estimation is based on real-time data, the alert is only given at the moment of collision even though it was detected long time before, leaving the driver no time to react and avoid the impact. Therefore, the method of risk estimation is equally, if not more important, than the detection of the vehicle in advance. An accurate and reliable method of risk estimation is crucial to ensure the safety and security of vehicles on the road.

Chapter 6

Conclusion and perspectives

Contents

6.1 General conclusion

The widespread deployment of automated vehicles on public roads has the potential to drastically alter today's transportation modes. Despite the fact that this pursuit began decades ago, there are still open challenges in reliably ensuring that such vehicles operate safely in open contexts. While functional safety is a well-established concept, measuring a vehicle's behavioral safety is still a work in progress. It is critical to investigate the various communication algorithms involved in the design of active embedded systems.
In this thesis work entitled "Multi-level risk and collective perception for high quality of service automated mobility in a highly dynamic V2X connected environment", we have addressed several questions. The first one is automated vehicle communication related. The goal is to improve communication between the entities that comprise the road ecosystem: cooperative vehicles, RSU, road users, infrastructure managers. This enables a more robust and efficient deployment of automated mobility services. By gaining access to remote information from mobile objects or fixed infrastructures and utilizing it, it is possible to broaden the perception range and, as a result, improve its quality.
Firstly, the central objective is to have a vehicular communication system that allows V2V and V2I communication in a simultaneous and interoperable manner. Next is a robust algorithm that is able to maintain a high connectivity quality even in degraded conditions according to the actual road conditions.
Many scientific studies have demonstrated the value of the clustering scheme as a model for node organization and route typologies in high traffic density environments. After conducting a comparative study of the existing models in our present state of the art, we have oriented ourselves towards an extended model of the Chain Branch Leaf (CBL) algorithm. Which has proven to be an efficient clustering hierarchy builder between communication nodes that uses direct communication through one hop without the need to go through an intermediate node. The deployment of automated vehicles on public roads has the potential to significantly change current transportation modes. Despite the fact that research in this area has been ongoing for decades, there are still challenges in ensuring the safe operation of these vehicles in open contexts. Functional safety is a well-established concept, but measuring a vehicle's behavioral safety is still a work in progress. It is essential to investigate the various communication algorithms involved in the design of active embedded systems.
In this thesis, we address several questions related to automated vehicle communication. The primary goal is to improve communication between the entities that make up the road ecosystem, such as CV, RSUs, road users, and infrastructure managers, in order to enable a more robust and efficient deployment of automated mobility services. By gaining access to remote information from mobile objects or fixed infrastructures, it is possible to broaden the perception range and improve its quality.
The central objective is to have a vehicular communication system that allows for both V2V and V2I communication in a simultaneous and interoperable manner. Additionally, we aim to develop a robust algorithm that can maintain a high connectivity quality even in degraded conditions.

Many scientific studies have demonstrated the value of the clustering scheme as a model for node organization and route typologies in high traffic density environments. After conducting a comparative study of existing models, we have chosen to use an extended version of the CBL algorithm. This algorithm has been shown to be an efficient decentralized clustering hierarchy builder that uses direct communication through one hop without the need for an intermediate node. Our extended model CBL-I has proven its efficiency in terms of adaptation to the infrastructure, indeed the communication structure (the chain) is maintained in both use cases. we explored the RSUs in the two known states in the initial CBL UC1: free (leaf or branch) and UC2: Branch.
We were able to observe the nodes behavior in an ideal infrastructure deployment environment first and then their evolution in degraded situations such as vehicles leaving an infrastructure area, vehicles entering an infrastructure area, lack RSUs deployment o the road or technical problems on some of them and RSUs as a relay point in blind area.
For the first use case in which the RSUs are free, demonstrate that for all of the previously explained distribution modes, the RSUs automatically transform into branches, thus we conclude that the RSUs are the best candidates for building a stable chain. The CBL-I has proven its hybrid capabilities by adapting to all situations in order to maintain a strong chain. We were able to expose our observations in our paper (Belmekki et al., 2020).
However for the connection/stability link's, we noticed that UC1 has a longer link duration of about 25 s, resulting in more transmissions. In the second use case, the link duration is approximately 10 seconds. This behavior is caused by the fact that a leaf can be attached to a vehicle branch using free RSUs. As a result, the connection is extended. In contrast to the UC2, there will be a disconnect whenever the vehicle leaves RSU coverage. which is unlikely for a strong connection. In line with these findings, we focused the next stage of our thesis's research on the gateway.
To ensure optimal communication coverage, we proposed a suitable communication architecture CBL-G which includes strategies and mechanisms for employing dynamic communication clustering of vehicles and infrastructure resources. The main objective of CBL-G is to provide optimal communication coverage while managing potentially isolated clusters of vehicles. Indeed, we have investigated the role of gateway that we assign to the RSU in CBL-G. We published our results in our paper (Belmekki, Gruyer, and Tatkeu, 2022).
In our model, Only branch and remote nodes can connect to the RSU when necessary, reducing the number of vehicle nodes requesting resources from the RSU at the same time and avoiding network congestion. Indeed, by combining V2V communications with V2I, it is able to solve the problem of the rate of isolated nodes in high density by decreasing the rate from 1.5% to 0 %, and decreasing the rate of isolated nodes in low density from 14.23 % to 0 %.
Based on our findings, we proposed deployment and communication topology recommendations for the following configurations and modes: V2V with only CBL, V2I with only UC2, or a combination of vehicles and infrastructure equipment with CBL.
After establishing our system's optimal coverage, we investigate another aspect of our

thesis research by using our model to deploy multi-level embedded collision risk estimation systems for automated vehicles. These systems rely on extended perception and vehicular communication to make decisions and perform maneuvers based on an estimation of perceived risk. The design of automated vehicles involves repeating the steps of perception, interpretation and understanding, risk estimation, decision-making and planning of trajectories and maneuvers, and finally execution of the action. It is crucial to estimate the risk of the current situation according to the attributes of the scene's key components obtained from the vehicle's perception. To react or estimate that a situation is dangerous, an automated vehicle must anticipate risks, both near and far, and therefore, we propose the concept of multi-level perception and multi-level risks. In most cases, the risk is calculated using locally available information, such as TTC or TIV, to which a collision probability is applied. However, new operators have emerged, attempting to be more comprehensive and representative of the road situation's complexities such as RIMUM metrics. These metrics, however, remain local and are primarily used to react to an event rather than predict it.

Remote information sent from infrastructure or other road users is required to allow the anticipation of risk situations. As a result, methods for dynamically grouping single-hop communication nodes have been proposed. Within the framework of this thesis, we proposed to use our architecture and adapted communication strategies that take into account the information of the vehicles surrounding the ego-vehicle to allow, on the one hand, extended perception, and on the other hand, extended risk estimation. Our proposed communication system, CBL and CBL-G, are both appropriate and effective for distributed processing tasks such as extended dynamic perception and estimation of local, extended, branch-extended, and global risk metrics.

We began by defining the levels of extended perception that are unique to our communication system. Extended perception is the perception of cluster members shared with their cluster head, which allows the cluster head to perceive what its leaves are doing. Extended perception is a crucial aspect of cluster-based communication systems, where a cluster head coordinates and manages a group of nodes, known as leaves. By sharing their perception with the cluster head, leaves can provide a more comprehensive view of the environment, including the presence and movement of other vehicles, road conditions, and traffic congestion. This shared perception allows the cluster head to make more informed decisions and take appropriate actions to ensure safe and efficient navigation of the road network. Therefore, extended perception can help the cluster head to see through the whole cluster, represented by the branch, and enable effective communication and coordination among the nodes in the cluster. Next, we determined the branch's extended perception, which allows the central branch to receive perceptions from its upstream and downstream, which it would not be able to see if only the equipment on both sides was used. Finally, we discussed global perception, which is the sharing of the perception of branch nodes that are farther away than the upstream and downstream branches of the ego-vehicle, providing a global perception of the road.

We incorporated ETSI's CPM into our algorithm, which allowed us to transmit on-board unit information. We then implemented all of these extended perceptions in our CBL-G

algorithm, resulting in the ability to recover vehicle perceptions via our communication system. Finally, with all of this information gathered, we can estimate the collision risk levels according to the perception level.
With the goal of building a more complex representation of driving risk for both the ego-vehicle and different driving situations, we reviewed the most pertinent risk indicators in the current scientific literature. Most of them demonstrated their efficiency in a simple two-vehicle situation. However, when we consider extended perception, there will be more objects in the ego-vehicle's perception field.
From a theoretical standpoint, we must consider as many parameters as possible, which is why we have included more vehicle attributes such as mass, dimensions (length and width), acceleration, capes, and energy equivalent speed. The challenge in dealing with risk estimation in a bi-dimensional space is that extrapolating the respective trajectories of the vehicles does not always result in collision. As a result, we propose that the two approaching vehicles be represented by a single axis projection.
We deployed the risk indicator based on multi-dimensional and uncertainties modeling (RIMUM) on our model, which performs in any dimensional configurations with consideration of the position uncertainties and the relative dynamics of the vehicles. We used it to estimate the multi-level risks in two scenarios: good conditions (perfect localization and perception) and degraded conditions (the perception uncertainty and perfect localization scenario) for both of them, we simulated two types of collision.
RIMUM can plan movement more accurately by characterizing the reality and dynamics of vehicles in passing and overtaking situations on multiple lane configurations. The results reveal that RIMUM better describes the reality of the situation as it is reactive to a potential collision avoidance maneuver. It defines the fatal accident risk by incorporating the severity due to relative dynamics and thus better describes the expected damage during a hazardous event. The fatality risk calculated in RIMUM is also adequate for non-collision situations. The risk metric RIMUM gives a risk indication at the exact moment of the risk because it is based on real-time data from sensors in the vehicles, such as speed and direction, to calculate the risk of a collision in real-time. On the other hand, temporal based risk such as TTC or TH are more anticipatory in nature as it predicts the risk of a collision based on the time it would take for two vehicles to collide if their current trajectory does not change. It calculates the time that is left for the driver to react and avoid a collision. Since it is based on predicted information, it gives a better anticipation of the risk compared to RIMUM which is based on real-time data. In conclusion, while RIMUM provides a real-time risk indication, TTC-based risk can provide better risk anticipation, making it more effective in helping drivers avoid potential collisions.
In conclusion, we believe that our research work has resulted in a good optimization of the automated vehicle system. We have proven the interoperability and adaptability of CBL to the infrastructure in CBL-I and then improved this communication system by optimizing the coverage with our second model, CBL-G. We then used this system for multi-level perception and used these extended perceptions to estimate collision risk at several levels. For risk estimation, we have established that RIMUM is more realistic.

We recommend the collision probability function estimated by the extended TH and the TTC-based collision probability for local risk and extended local risk in a one-dimensional collision configuration, as they result in good anticipation management. However, the risk of death calculated from RIMUM is still adequate for two-dimensional or collision-free situations, while the risks based on TTC and TH are excessive given the configurations. For the extended branch risk and the global risk, RIMUM and the DG probability function seem to be more adequate as they allow a realistic estimate for a distant event by definition. In conclusion, the values obtained by RIMUM are more accurate in general.

6.2 Perspectives on future Work

In future work, we plan to extend our study of vehicle risk to include specific configurations such as road intersections, highway insertions, highway exits, and roundabouts. In addition, we want to assign additional functions to RSUs in the CBL-G method, such as global risk management. Another situation we want to study is the impossibility to recover the location between the nodes via the chain which can be explained by the passage in a tunnel (figure 6.1) for example; in this case, the RSUs are in charge of relaying the information and sending it to the concerned vehicles so that they can estimate their risk on the one hand local extended and then global which will be relayed by several RSUs located further on the road. We believe that the insights offered in this perspective have important implications for future research and practice in collision risk estimation. In order to share these insights with a broader audience, we plan to submit this work for publication in a leading journal such as Springer. In order to be more comprehensive

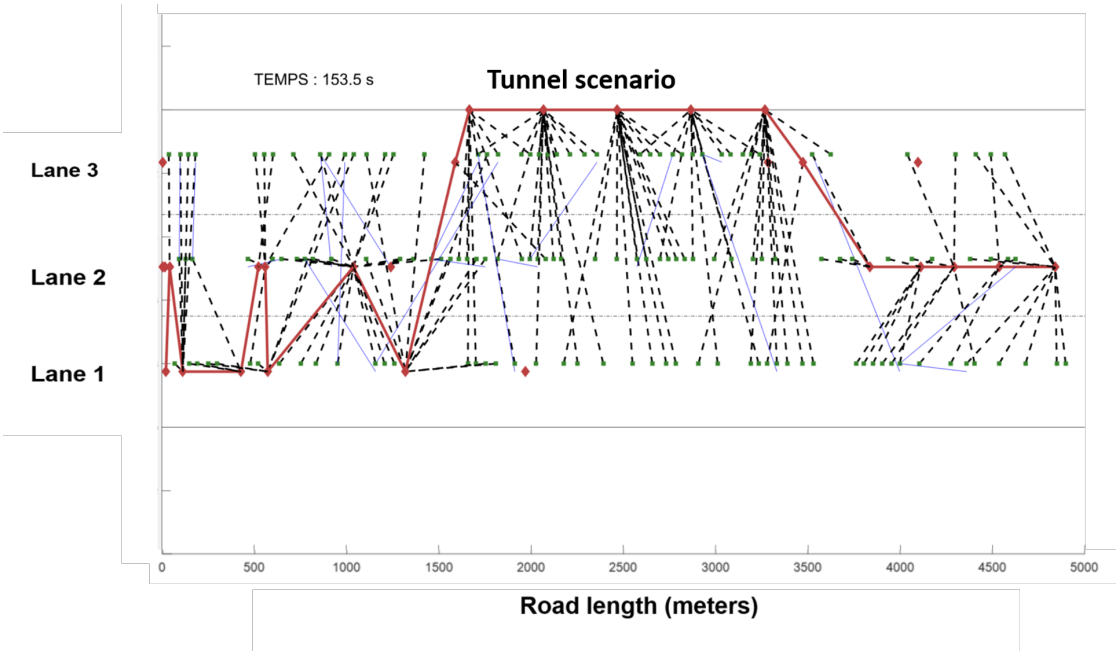

Figure 6.1: Tunnel scenario for global risk managed through RSU in CBL-G

and efficient, we also plan to take into account the complexity of the road scene. As we have highlighted, the road scene includes many "actors" that must be considered when estimating the risk of a situation, including obstacles, the road, the ego-vehicle, the environment, and the driver. To achieve this, we will propose fusion operators that take into account the uncertainties and constraints of each actor. that the proposed solutions and advancements in collective perception for CAVs come with limitations and challenges.

One major challenge is the real-time processing and handling of large amounts of data generated by multiple vehicles. This data must be processed quickly and accurately to ensure the safe operation of CAVs. Additionally, the communication channels used for the exchange of collective perception information must be secure to prevent malicious attacks and interference.
Another challenge is ensuring the interoperability of collective perception systems across different regions and countries, as well as between different types of vehicles. Finally, there is still a need for further research and development to improve the reliability and accuracy of collective perception systems, and to address any unexpected issues that may arise during their deployment and use.
Lastly, we recognize that the proposed solutions and advancements in collective perception for CAVs come with limitations and challenges, including real-time data processing, secure communication, interoperability, reliability, and unexpected issues. Therefore, it is essential to continuously monitor and assess the development and deployment of cooperative systems and traffic responses, and to address any limitations and challenges as they arise.
Future research on risk estimators should broaden and clearly highlight all interactions between key components. For example TLC is a very pertinent lateral risk estimator, however by incorporating the speed of the vehicle, the TLC lateral risk estimator can also be improved by considering longitudinal risk factors as well. Longitudinal factors, such as the vehicle's acceleration, deceleration, and following distance, can also play a role in the likelihood of a collision and should be taken into account. By considering both lateral and longitudinal risk factors, the TLC risk estimator can provide a more comprehensive and accurate assessment of the risk of a collision.
Indeed, categorizing risks based on the scene's five key components (ego-vehicle, road, environment, obstacles, and driver) can obscure the interactions between the various identified risks (Gruyer, 2023). Figure 6.2 illustrates it. Although this is a disadvantage of the classification method, it can also be viewed as a strength because the redundancy of parameters across different key components can improve the reliability and robustness of risk indicators.
It is therefore advised to employ multi-source data fusion methods in order to effectively utilize complementary and redundant information. However, this classification method does not emphasize the interactions between key components, leading to potential calculation errors and system failures if a risk indicator is estimated using only one of them.
To ensure that risk indicators include all key components, system designers can use the representation that (Leroy et al., 2020) proposed.

Figure 6.2: (Gruyer, 2023) Proposition Risk indicators and key components for future work

Graphic Appendices: Additional Illustrations

The software tool known as netconvert enables the creation of a road network file that is compatible with SUMO, while the accompanying tool netedit facilitates the visualization of the network constructed. In addition, it is possible to automatically import a network by exporting it from Open Street Map. The file employed for this purpose comprises a set of vehicle parameters that are as follows (Time of vehicle's entrance, vehicle ID, longiditunal position, lateral position, longiditunal speed, lateral speed, Type, category). an extraction of the used file is represented in figure 6.3

Time	ID	Position X	Position Y	Longitudinal speed	Lateral velocity	Type	Category
1	100000	5.100000000(	-1.650000000(	36.1000000000000	0	1	1
1	100001	5.100000000(	-4.950000000(	33.8700000000000	0	1	1
1	200000	15.10000000(	-8.250000000(	30	0	0	1
2	100000	41.15000000(	-1.650000000(	36.0500000000000	0	1	1
2	100001	38.48000000(	-4.950000000(	33.3800000000000	0	1	1
2	100002	5.100000000(	-1.650000000(	35.4300000000000	0	1	1
2	200000	44.81000000(	-8.250000000(	29.7100000000000	0	0	1
3	100000	76.51000000(	-1.650000000(	35.3600000000000	0	1	1
3	100001	71.81000000(	-4.950000000(	33.3300000000000	0	1	1
3	100002	40.29000000(	-1.650000000(	35.1900000000000	0	1	1
3	100003	5.100000000(	-4.950000000(	35.4800000000000	0	1	1
3	200000	74.43000000(	-8.250000000(	29.6300000000000	0	0	1
4	100000	112.1500000(	-1.650000000(	35.6300000000000	0	1	1
4	100001	105.1200000(	-4.950000000(	33.3100000000000	0	1	1
4	100002	74.64000000(	-1.650000000(	34.3500000000000	0	1	1
4	100003	40.32000000(	-4.950000000(	35.2200000000000	0	1	1
4	100004	5.100000000(	-1.650000000(	30	0	1	1
4	200000	104.4000000(	-8.250000000(	29.9700000000000	0	0	1
5	100000	147.5600000(	-1.650000000(	35.4200000000000	0	1	1
5	100001	138.6800000(	-4.950000000(	33.5700000000000	0	1	1
5	100002	109.7600000(	-1.650000000(	35.1200000000000	0	1	1
5	100003	74.04000000(	-4.950000000(	33.7200000000000	0	1	1
5	100004	34.59000000(	-1.650000000(	29.4900000000000	0	1	1
5	100005	5.100000000(	-4.950000000(	36.0300000000000	0	1	1
5	200000	133.9300000(	-8.250000000(	29.5300000000000	0	0	1
5	200001	15.10000000(	-8.250000000(	26.8700000000000	0	0	1
6	100000	183.2600000(	-1.650000000(	35.7000000000000	0	1	1
6	100001	172.5200000(	-4.950000000(	33.8400000000000	0	1	1
6	100002	144.2000000(	-1.650000000(	34.4500000000000	0	1	1
6	100003	109.2700000(	-4.950000000(	35.2300000000000	0	1	1

Figure 6.3: The SUMO data file used for the simulation on the Matlab

The structure of the vehicle has been updated to integrate the new data structure required for a vehicle in CBL-I. As a result, the parameters of the novel vehicle model

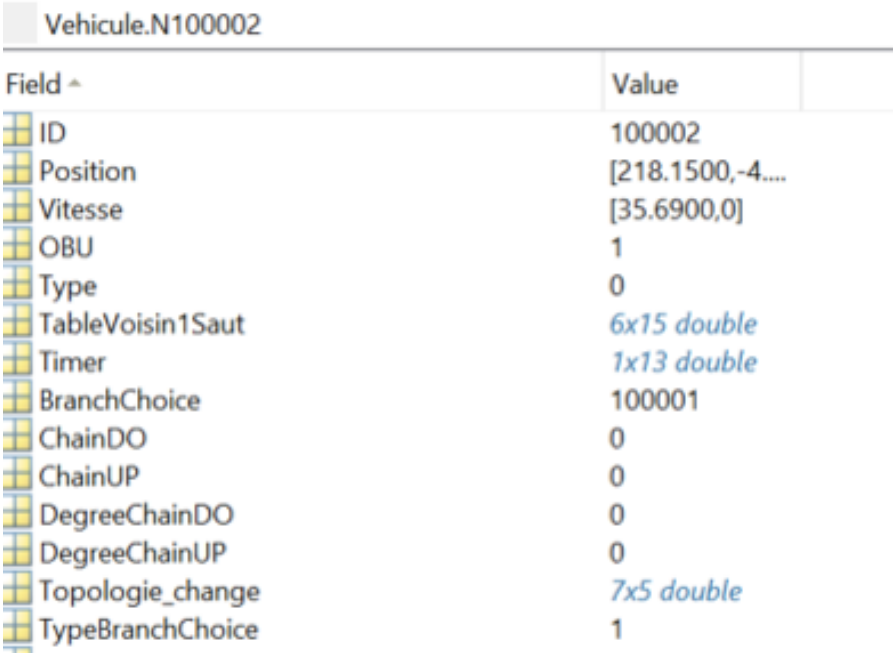

Figure 6.4: Example of extracted structure of a vehicle node (including type of branch: OBU or RSU) in the CBL-I algorithm from matlab

are presented in Figure 6.4. Then, in accordance with the updated CBL-G model, the structure of the vehicle has been more enhanced to accommodate the new data structure of a vehicle in CBL-G. The figure 6.5 presented below outlines the parameters of this novel vehicle model taking into account more parameters such as acceleration, dimensions, mass, heading..ect. Our Collective Perception message structure proposition for our application is shown in Figure 6.6.

Field	Value
ID	1000001
Position	[4.9905e+03,-8.2500]
Vitesse	[35.1800,0]
OBU	1
Type	0
TableVoisin1Saut	*6x14 double*
Timer	*1x12 double*
BranchChoice	100005
ChainDO	0
ChainUP	0
DegreeChainDO	0
DegreeChainUP	0
Topologie_change	*141x5 double*
TypeBranchChoice	1
Mass	3500
Cap	0
Dimensions	[5,2.0500]
Acceleration	0.5000

Figure 6.5: Example of the new vehicle data structure in CBL-G with new attributes: acceleration, dimensions, mass, heading

Vehicle Vi					Vehicle Vj												Date
Identifier	Position		Speed		Identifier	occurrence	Position		Speed		Node's Type	Acceleration	heading	Dimensions		Mass	Confidence	Time of measurement
ID	X	Y	V1	V2	ID	Occ	X	Y	V1	V2	Type	A	Heading	Length	Width	M	C	Date

Figure 6.6: The format of a CPM broadcasted by vehicle V_i containing the detected object which is vehicle V_j

Author Contributions

- Belmekki, D. Gruyer and C. Tatkeu, (2020). “Toward the Integration of V2V Based Clusters in a Global Infrastructure Network for Vehicles”. In: Communication Technologies for Vehicles. Ed. by Francine Krief et al. Cham: Springer International Publishing, pp. 113–122. isbn: 978-3-030-66030-7.
- S. Belmekki, D. Gruyer and C. Tatkeu, "Chain Branch Leaf-Gateway, a Strategy for Dynamic Clustering and Optimal Coverage of Communication for Automated Mobility," 2022 IEEE 2nd International Conference on Digital Twins and Parallel Intelligence (DTPI), 2022, pp. 1-5,
doi: 10.1109/ DTPI55838.2022.9998893.

Bibliography

Jeffs, James (Sep 17, 2021). *Barriers Fall Unleashing Autonomous Cars in 2021.* URL: https://www.idtechex.com/en/research-article/barriers-fall-unleashing-autonomous-cars-in-2021/24763.

WINSUM, WIM VAN and ADRIAAN HEINO (1996). "Choice of time-headway in car-following and the role of time-to-collision information in braking". In: *Ergonomics* 39.4. PMID: 8854979, pp. 579–592. DOI: 10.1080/00140139608964482. eprint: https://doi.org/10.1080/00140139608964482. URL: https://doi.org/10.1080/00140139608964482.

Basu, P., N. Khan, and T. D. C. Little (2001). "A mobility based metric for clustering in mobile ad hoc networks". In: *Proceedings 21st International Conference on Distributed Computing Systems Workshops*, pp. 413–418.

Minderhoud, Michiel and Piet Bovy (2001). "Extended time-to-collision measures for road traffic safety assessment". In: *Accident; analysis and prevention* 33, pp. 89–97. DOI: 10.1016/S0001-4575(00)00019-1.

Bin, M., N. Uno, and Y. Iida (2003). "A study of lane-changing behavior model at weaving section considering conflicts". In: *Journal of the Eastern Asia Society for Transportation Studies* 5. cited By 11, pp. 2039–2052.

Borgonovo, F. et al. (2003). "MAC for ad-hoc inter-vehicle network: services and performance". In: *2003 IEEE 58th Vehicular Technology Conference. VTC 2003-Fall (IEEE Cat. No.03CH37484)*. Vol. 5, 2789–2793 Vol.5. DOI: 10.1109/VETECF.2003.1286106.

Mangeas, M. (LIVIC, 2003). "Rapport d'activités". In.

Mammar, Saïd et al. (2004). "Time-to-line crossing and vehicle dynamics for lane departure avoidance". In: *Proceedings. The 7th International IEEE Conference on Intelligent Transportation Systems (IEEE Cat. No.04TH8749)*, pp. 618–623.

Gerla, Mario et al. (2006). "Vehicular grid communications: the role of the internet infrastructure". In: *WICON '06*.

Ammoun, Samer (2007). "Contribution des communications intervéhiculaires pour la conception de systèmes avancés d'aide à la conduite". Thèse de doctorat dirigée par

Nashashibi, Fawzi Informatique, temps réel, robotique et automatique Paris, ENMP 2007. PhD thesis, 1 vol. (201 p.) URL: http://www.theses.fr/2007ENMP1517.

AZIONI, CENTRO RICERCHE FIAT SOCIETA' CONSORTILE PER (2007). *Cooperative systems for road safety "Smart Vehicles on Smart Roads.*

Lochert, C. et al. (2007). "The feasibility of information dissemination in vehicular ad-hoc networks". In: *2007 Fourth Annual Conference on Wireless on Demand Network Systems and Services*, pp. 92–99.

Frotscher Alexander Scheider, Thomas (2008). "COOPERS Project: Development of an ITS Architecture for Co-Operative Systems on Motorways". In.

DTR/ITS (2009). "intelligent transport systems (ITS); vehicular communications; basic set of applications; definitions". In.

Ferretti, Stefano and Marco Roccetti (2009). "Smart Access Points on the road for online gaming in vehicular networks". In: *Entertainment Computing* 1, pp. 17–26. DOI: 10.1016/j.entcom.2009.07.001.

Vanholme, Benoit et al. (2009). "Manoeuvre-based trajectory planning for highly autonomous vehicles on real road with traffic". In: *2009 European Control Conference (ECC)*, pp. 3281–3286. DOI: 10.23919/ECC.2009.7074911.

Borsetti, D. and J. Gozalvez (2010a). "Infrastructure-assisted geo-routing for cooperative vehicular networks". In: *2010 IEEE Vehicular Networking Conference*, pp. 255–262. DOI: 10.1109/VNC.2010.5698271.

— (2010b). "Infrastructure-assisted geo-routing for cooperative vehicular networks". In: *2010 IEEE Vehicular Networking Conference*, pp. 255–262. DOI: 10.1109/VNC.2010.5698271.

Boyinbode, Olutayo et al. (2010). "A Survey on Clustering Algorithms for Wireless Sensor Networks". In: vol. 1, pp. 358–364. DOI: 10.1109/NBiS.2010.59.

Glaser, Sebastien et al. (2010a). "Maneuver-based trajectory planning for highly autonomous vehicles on real road with traffic and driver interaction". In: *IEEE Transactions on Intelligent Transportation Systems* 11.3, pp. 589–606. DOI: 10.1109/TITS.2010.2046037. URL: https://eprints.qut.edu.au/120878/.

Glaser, Sébastien et al. (2010b). "Maneuver-Based Trajectory Planning for Highly Autonomous Vehicles on Real Road With Traffic and Driver Interaction". In: *IEEE Transactions on Intelligent Transportation Systems* 11.3, pp. 589–606. DOI: 10.1109/TITS.2010.2046037.

Korkmaz, Gökhan, Eylem Ekici, and Füsun Özgüner (2010). "Supporting real-time traffic in multihop vehicle-to-infrastructure networks". In: *Transportation Research Part C: Emerging Technologies* 18.3. 11th IFAC Symposium: The Role of Control, pp. 376–

392. DOI: https://doi.org/10.1016/j.trc.2009.05.001. URL: https://www.sciencedirect.com/science/article/pii/S0968090X09000564.

Labayrade, Raphaël et al. (2010). "Sensor data fusion for road obstacle detection: A validation framework. In : Sensor Fusion and its Applications". In: *Sensor data fusion for road obstacle detection: A validation framework. In : Sensor Fusion and its Applications*. SCIYO, pp 375–394. URL: https://hal.archives-ouvertes.fr/hal-01072463.

Souza, E., I. Nikolaidis, and P. Gburzynski (2010). "A New Aggregate Local Mobility (ALM) Clustering Algorithm for VANETs". In: *2010 IEEE International Conference on Communications*, pp. 1–5.

Viriyasitavat, W., Fan Bai, and O.K. Tonguz (2010). "UV-CAST: An Urban Vehicular Broadcast Protocol". In: *2nd IEEE Vehicular Networking Conference (VNC 2010)*. Jersey City, NJ: Institute of Electrical and Electronics Engineers, pp. 25–32. ISBN: 978-1-4244-9525-2. DOI: 10.1109/VNC.2010.5698266.

Yang, Hong, Kaan Ozbay, and Bekir Bartin (2010). "Application of Simulation-Based Traffic Conflict Analysis for Highway APPLICATION OF SIMULATION-BASED TRAFFIC CONFLICT ANALYSIS FOR HIGHWAY SAFETY EVALUATION". In.

Annese, Stefano et al. (2011). "Seamless Connectivity and Routing in Vehicular Networks with Infrastructure". In: *IEEE Journal on Selected Areas in Communications* 29.3, pp. 501–514. DOI: 10.1109/JSAC.2011.110302.

Davis, Gary A. et al. (2011). "Outline for a causal model of traffic conflicts and crashes". In: *Accident Analysis Prevention* 43.6, pp. 1907–1919. DOI: https://doi.org/10.1016/j.aap.2011.05.001. URL: https://www.sciencedirect.com/science/article/pii/S0001457511001205.

Maslekar, N. et al. (2011). "Modified C-DRIVE: Clustering based on direction in vehicular environment". In: *2011 IEEE Intelligent Vehicles Symposium (IV)*, pp. 845–850.

Ramakrishnan, B et al. (2011). "CBVANET: A Cluster Based Vehicular Adhoc Network Model for Simple Highway Communication". In: *Int. J. Advanced Networking and Applications* 755, pp. 2–4.

Zhang, Zhenxia, Azzedine Boukerche, and Richard Pazzi (2011). "A Novel Multi-Hop Clustering Scheme for Vehicular Ad-Hoc Networks". In: *Proceedings of the 9th ACM International Symposium on Mobility Management and Wireless Access*. MobiWac '11. Miami, Florida, USA: Association for Computing Machinery, 19–26. DOI: 10.1145/2069131.2069135. URL: https://doi.org/10.1145/2069131.2069135.

Demmel, Sébastien (2012). "Construction of extended maps of road difficulties based on the fusion of local maps". PhD thesis, 1 vol. (279 f.) URL: http://www.theses.fr/2012VERS0051.

Guizani, Badreddine (2012). "Clustering algorithms and routing protocaols in wireless mobile networks". Theses. Université de Technologie de Belfort-Montbeliard ; Université de la Manouba (Tunisie). URL: https://tel.archives-ouvertes.fr/tel-00703257.

Liang, Hao and Weihua Zhuang (2012). "Cooperative Data Dissemination via Roadside WLANs". In: *IEEE Communications Magazine - IEEE Commun. Mag.* 50. DOI: 10.1109/MCOM.2012.6178836.

Liu, Xuxun (2012). "A Survey on Clustering Routing Protocols in Wireless Sensor Networks". In: *Sensors* 12.8, pp. 11113–11153. DOI: 10.3390/s120811113. URL: https://www.mdpi.com/1424-8220/12/8/11113.

Mershad, Khaleel, Hassan Artail, and Mario Gerla (2012). "ROAMER: Roadside Units as Message Routers in VANETs". In: *Ad Hoc Netw.* 10.3, 479–496. DOI: 10.1016/j.adhoc.2011.09.001. URL: https://doi.org/10.1016/j.adhoc.2011.09.001.

St-Aubin, Paul (2012). "Traffic safety analysis for urban highway ramps and lane- change bans using accident data and video-based surrogate safety measures". In: *McGill University*.

Zhang, Wuxiong et al. (2012). "Multi-Hop Connectivity Probability in Infrastructure-Based Vehicular Networks". In: *IEEE Journal on Selected Areas in Communications* 30.4, pp. 740–747. DOI: 10.1109/JSAC.2012.120508.

Ansari, Keyvan et al. (2013). "Vehicle-to-Vehicle Real-Time Relative Positioning Using 5.9 GHz DSRC Media". In: *2013 IEEE 78th Vehicular Technology Conference (VTC Fall)*, pp. 1–7. DOI: 10.1109/VTCFall.2013.6692454.

Bruno, Raffaele and Maddalena Nurchis (2013). "Robust and efficient data collection schemes for vehicular multimedia sensor Networks". In: *2013 IEEE 14th International Symposium on "A World of Wireless, Mobile and Multimedia Networks" (WoWMoM)*, pp. 1–10. DOI: 10.1109/WoWMoM.2013.6583399.

Demmel, Sébastien, Dominique Gruyer, and Andry Rakotonirainy (2013). "Comparing cooperative and non-cooperative crash risk-assessment". In: *2013 IEEE Intelligent Vehicles Symposium (IV)*, pp. 1007–1013. DOI: 10.1109/IVS.2013.6629598.

Iglesias, Marco A, Kody JH Law, and Andrew M Stuart (2013). "Ensemble Kalman methods for inverse problems". In: *Inverse Problems* 29.4, p. 045001.

Liao, Cong et al. (2013). "A trust model for vehicular network-based incident reports". In: *2013 IEEE 5th International Symposium on Wireless Vehicular Communications (WiVeC)*, pp. 1–5. DOI: 10.1109/wivec.2013.6698224.

Liu, Yazhi et al. (2013). "File Downloading Oriented Roadside Units Deployment for Vehicular Networks". In: *J. Syst. Archit.* 59.10, 938–946. DOI: 10.1016/j.sysarc.2013.04.007. URL: https://doi.org/10.1016/j.sysarc.2013.04.007.

Bali, Rasmeet S, Neeraj Kumar, and Joel J. P. C. Rodrigues (2014). "Clustering in vehicular ad hoc networks: Taxonomy, challenges and solutions". en. In: *Vehicular Communications* 1.3, pp. 134–152. DOI: 10.1016/j.vehcom.2014.05.004. URL: http://www.sciencedirect.com/science/article/pii/S2214209614000217 (visited on 06/02/2020).

Ben Jemaa, Inès (2014). "Multicast communications for cooperative vehicular systems". Theses. Ecole Nationale Supérieure des Mines de Paris. URL: https://pastel.archives-ouvertes.fr/tel-01144454.

Dua, Amit, Neeraj Kumar, and Seema Bawa (2014). "A systematic review on routing protocols for Vehicular Ad Hoc Networks". In: *Vehicular Communications* 1.1, pp. 33 –52. DOI: https://doi.org/10.1016/j.vehcom.2014.01.001. URL: http://www.sciencedirect.com/science/article/pii/S2214209614000059.

Kakkasageri, M. S. and S. S. Manvi (2014). "Information management in vehicular ad hoc networks: A review". In: *Journal of Network and Computer Applications* 39, pp. 334 –350. DOI: https://doi.org/10.1016/j.jnca.2013.05.015. URL: http://www.sciencedirect.com/science/article/pii/S1084804513001434.

Louazani, Ahmed, Sidi Mohammed Senouci, and Mohammed Abderrahmane Bendaoud (2014). "Clustering-based algorithm for connectivity maintenance in Vehicular Ad-Hoc Networks". In: *2014 14th International Conference on Innovations for Community Services (I4CS)*, pp. 34–38. DOI: 10.1109/I4CS.2014.6860550.

Ou, Chia-Ho (2014). "A roadside unit-based localization scheme for vehicular ad hoc networks". In: *International Journal of Communication Systems* 27.1, pp. 135–150. DOI: https://doi.org/10.1002/dac.2352. eprint: https://onlinelibrary.wiley.com/doi/pdf/10.1002/dac.2352. URL: https://onlinelibrary.wiley.com/doi/abs/10.1002/dac.2352.

Paikari, Elahe, Shahram Tahmasseby, and Behrouz Far (2014). "A simulation-based benefit analysis of deploying connected vehicles using dedicated short range communication". In: *2014 IEEE Intelligent Vehicles Symposium Proceedings*, pp. 980–985. DOI: 10.1109/IVS.2014.6856462.

Zhu, Jinqi et al. (2014). "Parking Backbone: Toward Efficient Overlay Routing in VANETs". In: *International Journal of Distributed Sensor Networks* 10.8, p. 291308. DOI: 10.1155/2014/291308. eprint: https://doi.org/10.1155/2014/291308. URL: https://doi.org/10.1155/2014/291308.

Khattab, Ahmed, Yasmine A. Fahmy, and Ahmed Abdel Wahab (2015). "High Accuracy GPS-Free Vehicle Localization Framework via an INS-Assisted Single RSU". In: *International Journal of Distributed Sensor Networks* 11.5, p. 795036. DOI: 10.1155/2015/795036. eprint: https://doi.org/10.1155/2015/795036. URL: https://doi.org/10.1155/2015/795036.

Kuang, Yan, Xiaobo Qu, and Shuaian Wang (2015). "A tree-structured crash surrogate measure for freeways". In: *Accident Analysis Prevention* 77, pp. 137–148. DOI: https://doi.org/10.1016/j.aap.2015.02.007. URL: https://www.sciencedirect.com/science/article/pii/S000145751500041X.

Parrado, Natalia and Yezid Donoso (2015). "Congestion Based Mechanism for Route Discovery in a V2I-V2V System Applying Smart Devices and IoT". In: *Sensors* 15, pp. 7768–7806. DOI: 10.3390/s150407768.

RTS/ITS (2015). "Intelligent Transport Systems (ITS); Mitigation techniques to avoid interference between European CEN Dedicated Short Range Communication (CEN DSRC) equipment and Intelligent Transport Systems (ITS) operating in the 5 GHz frequency range". In.

Cooper, Craig et al. (2016). "A Comparative Survey of VANET Clustering Techniques". In: *IEEE Communications Surveys Tutorials* PP, pp. 1–1. DOI: 10.1109/COMST.2016.2611524.

Olia, Arash et al. (2016). "Assessing the Potential Impacts of Connected Vehicles: Mobility, Environmental, and Safety Perspectives". In: *Journal of Intelligent Transportation Systems* 20.3, pp. 229–243. DOI: 10.1080/15472450.2015.1062728. eprint: https://doi.org/10.1080/15472450.2015.1062728. URL: https://doi.org/10.1080/15472450.2015.1062728.

Sharma, Vijay, Abhinav Vidwans, and Manish Gupta (2016). "AES based security clustering routing for VANET". In: *2016 International Conference on Signal Processing, Communication, Power and Embedded System (SCOPES)*, pp. 332–336. DOI: 10.1109/SCOPES.2016.7955846.

Silva, Cristiano et al. (2016). "Gamma Deployment: Designing the Communication Infrastructure in Vehicular Networks Assuring Guarantees on the V2I Inter-Contact Time". In: DOI: 10.1109/MASS.2016.041.

Tian, Daxin et al. (2016). "Modeling chain collisions in vehicular networks with variable penetration rates". In: *Transportation Research Part C: Emerging Technologies* 69, pp. 36–59. DOI: https://doi.org/10.1016/j.trc.2016.05.013. URL: https://www.sciencedirect.com/science/article/pii/S0968090X1630050X.

Togou, Mohammed Amine, Abdelhakim Senhaji Hafid, and Lyes Khoukhi (2016). "SCRP: Stable CDS-based Routing Protocol for Urban Vehicular Ad Hoc Networks". In: *IEEE Transactions on Intelligent Transportation Systems* 99. DOI: 10.1109/TITS.2015.2504129.

Alouache, Lylia et al. (2017). "Nouveau protocole robuste pour les communications dans l'IoV". In.

Cecchini, G. et al. (2017). "Performance comparison between IEEE 802.11p and LTE-V2V in-coverage and out-of-coverage for cooperative awareness". In: *2017 IEEE Vehicular Networking Conference (VNC)*, pp. 109–114.

Eggert, Julian and Tim Puphal (2017). "Continuous Risk Measures for ADAS and AD". In.

Frenzel, Lou (2017). "The Battle Over V2V Wireless Technologies". In.

Fyfe Martin Sayed, Tarek (2017). "Safety Evaluation of Connected Vehicles for a Cumulative Travel Time Adaptive Signal Control Microsimulation Using the Surrogate Safety Assessment Model". In: *Transportation Research Board 96th Annual Meeting*.

Gruyer, Dominique (2017). "Real-Time Architecture For Obstacle Detection , Tracking And Filtering : An Issue For The Autonomous Driving". In.

Gruyer, Dominique et al. (2017). "Real-Time Architecture For Obstacle Detection, Tracking And Filtering: An IssueFor The Autonomous Driving". In: *Journal of Intelligent Computing* 8.2, pp.33–48. URL: https://hal.archives-ouvertes.fr/hal-01651991.

Katrakazas, Christos, Mohammed Quddus, and Wen-Hua Chen (2017). *A new methodology for collision risk assessment of autonomous vehicles*. URL: https://hdl.handle.net/2134/24158.

Li, Yingshuai, Jian Lu, and Kuisheng Xu (2017). "Crash Risk Prediction Model of Lane-Change Behavior on Approaching Intersections". In: *Discrete Dynamics in Nature and Society* 2017, pp. 1–12. URL: https://EconPapers.repec.org/RePEc:hin:jnddns:7328562.

Mahmud, S. M. et al. (2017). "Application of proximal surrogate indicators for safety evaluation: A review of recent developments and research needs". In: *IATSS Research* 41. DOI: 10.1016/j.iatssr.2017.02.001.

Sethi, Vivek and Narottam Chand (2017). "A Destination Based Routing Protocol for Context Based Clusters in VANET". In: *CN* 09.03, pp. 179–191. DOI: 10.4236/cn.2017.93013. URL: http://www.scirp.org/journal/doi.aspx?DOI=10.4236/cn.2017.93013 (visited on 04/01/2020).

Silva, C. M. et al. (2017). "A Survey on Infrastructure-Based Vehicular Networks". In: *Mob. Inf. Syst.* 2017, 6123868:1–6123868:28.

Zheng, J., H. Tong, and Y. Wu (2017). "A Cluster-Based Delay Tolerant Routing Algorithm for Vehicular Ad Hoc Networks". In: *2017 IEEE 85th Vehicular Technology Conference (VTC Spring)*, pp. 1–5.

Ansari, Abdul Rahim et al. (2018). "Accurate 3D Localization Method for Public Safety Applications in Vehicular Ad-Hoc Networks". In: *IEEE Access* 6, pp. 20756–20763. DOI: 10.1109/ACCESS.2018.2825371.

Hallerbach, Sven et al. (2018). "Simulation-Based Identification of Critical Scenarios for Cooperative and Automated Vehicles". In: *SAE Technical Papers* 2018-01-1066. DOI: 10.4271/2018-01-1066.

Johnsson, Carl, Aliaksei Laureshyn, and Tim De Ceunynck (2018). "In search of surrogate safety indicators for vulnerable road users: a review of surrogate safety indicators". In: *Transport Reviews* 38.6, pp. 765–785. DOI: 10.1080/01441647.2018.1442888. eprint: https://doi.org/10.1080/01441647.2018.1442888. URL: https://doi.org/10.1080/01441647.2018.1442888.

Marchang, Jims, Benjamin Sanders, and Dany Joy (2018). "Adaptive V2V Routing with RSUs and Gateway Support to Enhance Network Performance in VANET". In: *International Conference on Wired/Wireless Internet Communication (WWIC)*. Ed. by Kaushik Roy Chowdhury et al. Vol. LNCS-10866. Wired/Wireless Internet Communications. Part 6: Vehicular and Content Delivery Networks. Boston, MA, United States: Springer International Publishing, pp. 298–310. DOI: 10.1007/978-3-030-02931-9_24. URL: https://hal.inria.fr/hal-02269734.

Mobileye, Intel (2018). "RSS: Responsibility-Sensitive Safety for Autonomous Vehicles". In: *arXiv preprint arXiv:1802.01781*.

Rahman, Md Sharikur et al. (2018). "Understanding the Highway Safety Benefits of Different Approaches of Connected Vehicles in Reduced Visibility Conditions". In: *Transportation Research Record* 2672.19, pp. 91–101. DOI: 10.1177/0361198118776113. eprint: https://doi.org/10.1177/0361198118776113. URL: https://doi.org/10.1177/0361198118776113.

RIVOIRARD, Lucas (2018). "Self-organization model for routing protocols in vehicular ad hoc network : application to extended perception and cooperative localization". Theses. Université de Lille. URL: https://hal.archives-ouvertes.fr/tel-02003878.

Rivoirard, Lucas et al. (2018). "Chain-Branch-Leaf: A clustering scheme for vehicular networks using only V2V communications". In: *Ad Hoc Networks* 68. Advances in Wireless Communication and Networking for Cooperating Autonomous Systems, pp. 70–84. DOI: https://doi.org/10.1016/j.adhoc.2017.10.007. URL: https://www.sciencedirect.com/science/article/pii/S1570870517301798.

Shi, X. et al. (2018). "Key risk indicators for accident assessment conditioned on pre-crash vehicle trajectory". In: *Accident Analysis Prevention* 117, pp. 346–356. DOI: https://doi.org/10.1016/j.aap.2018.05.007. URL: https://www.sciencedirect.com/science/article/pii/S000145751830191X.

Shin, Donghoon and Kyongsu Yi (2018). "Human Factor Considered Risk Assessment of Automated Vehicle Using Vehicle to Vehicle Wireless Communication". In: *International Journal of Automotive Engineering* 9.2, pp. 56–63. DOI: 10.20485/jsaeijae.9.2_56.

Tarko, Andrew P (2018). "Surrogate measures of safety". In: *Safe mobility: challenges, methodology and solutions*. Emerald Publishing Limited.

Wahid, Ishtiaq et al. (2018). "State of the Art Routing Protocols in VANETs: A Review". en. In: *Procedia Computer Science*. The 9th International Conference on Ambient Systems, Networks and Technologies (ANT 2018) / The 8th International Conference on Sustainable Energy Information Technology (SEIT-2018) / Affiliated Workshops 130, pp. 689–694. DOI: 10.1016/j.procs.2018.04.121. URL: http://www.sciencedirect.com/science/article/pii/S1877050918304836 (visited on 04/11/2020).

Wang, Junhua et al. (2018). "Dynamic Clustering and Cooperative Scheduling for Vehicle-to-Vehicle Communication in Bidirectional Road Scenarios". In: *IEEE Transactions on Intelligent Transportation Systems* 19.6, pp. 1913–1924. DOI: 10.1109/TITS.2017.2743821.

Yang, Huanhuan, Zongpu Jia, and Guojun Xie (2018). "Delay-Bounded and Cost-Limited RSU Deployment in Urban Vehicular Ad Hoc Networks". In: *Sensors* 18.9. DOI: 10.3390/s18092764. URL: https://www.mdpi.com/1424-8220/18/9/2764.

Zekri, Abdennour and Weijia Jia (2018). "Heterogeneous vehicular communications: A comprehensive study". en. In: *Ad Hoc Networks* 75-76, pp. 52–79. DOI: 10.1016/j.adhoc.2018.03.010. URL: http://www.sciencedirect.com/science/article/pii/S1570870518300672 (visited on 11/26/2020).

Chai, Chen et al. (2019). "Safety Evaluation of Responsibility-Sensitive Safety (RSS) on Autonomous Car-Following Maneuvers Based on Surrogate Safety Measurements". In: *2019 IEEE Intelligent Transportation Systems Conference (ITSC)*. Auckland, New Zealand: IEEE Press, 175–180. DOI: 10.1109/ITSC.2019.8917421. URL: https://doi.org/10.1109/ITSC.2019.8917421.

Charly, Anna and Tom V. Mathew (2019). "Estimation of traffic conflicts using precise lateral position and width of vehicles for safety assessment". In: *Accident Analysis Prevention* 132, p. 105264. DOI: https://doi.org/10.1016/j.aap.2019.105264. URL: https://www.sciencedirect.com/science/article/pii/S0001457519300740.

Chen, Yu and Yuren Chen (2019). "Reliability Evaluation of Sight Distance on Mountainous Expressway Using 3D Mobile Mapping". In: *2019 5th International Conference on Transportation Information and Safety (ICTIS)*, pp. 1–7. DOI: 10.1109/ICTIS.2019.8883801.

Correa, Alejandro et al. (2019). *TransAID Deliverable 5.2: V2X-based cooperative sensing and driving in Transition Areas*. Tech. rep. URL: https://elib.dlr.de/133911/.

ETSI (2019). *Analysis of the Collective Perception Service (CPS)*. en. URL: http://www.etsi.org/standards-search (visited on 12/2019).

Gruyer, Dominique and Mohamed-Cherif Rahal (2019). "Multi-Layer Laser Scanner Strategy for Obstacle Detection and Tracking". In: *2019 IEEE/ACS 16th International Conference on Computer Systems and Applications (AICCSA)*, pp. 1–8. DOI: 10.1109/AICCSA47632.2019.9035243.

Koopman, Philip, Beth Osyk, and Jack Weast (2019). "Autonomous Vehicles Meet the Physical World: RSS, Variability, Uncertainty, and Proving Safety". In: *Computer Safety, Reliability, and Security*. Ed. by Alexander Romanovsky, Elena Troubitsyna, and Friedemann Bitsch. Cham: Springer International Publishing, pp. 245–253. ISBN: 978-3-030-26601-1.

Lu, Zhaojun, Gang Qu, and Zhenglin Liu (2019). "A Survey on Recent Advances in Vehicular Network Security, Trust, and Privacy". In: *IEEE Transactions on Intelligent Transportation Systems* 20.2, pp. 760–776. DOI: 10.1109/TITS.2018.2818888.

National Highway Traffic Safety Administration, NHTSA (2019). *Automated Vehicles for Safety*. URL: www.nhtsa.gov/technology-innovation/automated-vehicles-safety.

Nguyen, B. L. et al. (2019). "Combining V2I with V2V Communications for Service Continuity in Vehicular Networks". In: *2019 IEEE Intelligent Transportation Systems Conference (ITSC)*, pp. 201–206.

Philipp, Andreas and Dan Goehring (2019). "Analytic Collision Risk Calculation for Autonomous Vehicle Navigation". In: *2019 International Conference on Robotics and Automation (ICRA)*, pp. 1744–1750.

Sathya Narayanan, P. and C. S. Joice (2019). "Vehicle-to-Vehicle (V2V) Communication using Routing Protocols: A Review". In: *2019 International Conference on Smart Structures and Systems (ICSSS)*, pp. 1–10. DOI: 10.1109/ICSSS.2019.8882828.

Senouci, Oussama, Zibouda Aliouat, and Saad Harous (2019). "MCA-V2I: A Multi-hop Clustering Approach over Vehicle-to-Internet communication for improving VANETs performances". en. In: *Future Generation Computer Systems* 96, pp. 309–323. DOI: 10.1016/j.future.2019.02.024. URL: http://www.sciencedirect.com/science/article/pii/S0167739X18329315 (visited on 04/11/2020).

Sharma, Sakshi and Nidhi (2019). "Vehicular Ad-Hoc Network: An Overview". In: *2019 International Conference on Computing, Communication, and Intelligent Systems (ICCCIS)*, pp. 131–134. DOI: 10.1109/ICCCIS48478.2019.8974524.

Tripp-Barba, Carolina et al. (2019). "Survey on Routing Protocols for Vehicular Ad Hoc Networks Based on Multimetrics". In: *Electronics* 8, p. 1177. DOI: 10.3390/electronics8101177.

Wang, Jiadai, Jiajia Liu, and Nei Kato (2019). "Networking and Communications in Autonomous Driving: A Survey". In: *IEEE Communications Surveys Tutorials* 21.2, pp. 1243–1274. DOI: 10.1109/COMST.2018.2888904.

Yuan, Jinghui et al. (2019). "Investigating drivers' mandatory lane change behavior on the weaving section of freeway with managed lanes: A driving simulator study". In: *Transportation Research Part F: Traffic Psychology and Behaviour* 62, pp. 11–32. DOI: https://doi.org/10.1016/j.trf.2018.12.007. URL: https://www.sciencedirect.com/science/article/pii/S1369847818303875.

Banikhalaf, M. and M. A. Khder (2020). "A Simple and Robust Clustering Scheme for Large-Scale and Dynamic VANETs". In: *IEEE Access* 8, pp. 103565–103575.

Bao, Xu et al. (2020). "Efficient clustering V2V routing based on PSO in VANETs". en. In: *Measurement* 152, p. 107306. DOI: 10.1016/j.measurement.2019.107306. URL: http://www.sciencedirect.com/science/article/pii/S0263224119311704 (visited on 06/04/2020).

Belmekki, Sabrine et al. (2020). "Toward the Integration of V2V Based Clusters in a Global Infrastructure Network for Vehicles". In: *Communication Technologies for Vehicles*. Ed. by Francine Krief et al. Cham: Springer International Publishing, pp. 113–122. ISBN: 978-3-030-66030-7.

ETSI (2020). *ETSI TS 103 300-2 V2.1.1 (2020-05) - Intelligent Transport System (ITS); Vulnerable Road Users (VRU) awareness; Part 2: Functional Architecture and Requirements definition; Release 2*. en. URL: https://standards.iteh.ai/catalog/standards/etsi/a5f082e2-8d86-48b5-89dd-68fe91b54283/etsi-ts-103-300-2-v2-1-1-2020-05 (visited on 11/22/2021).

European Telecommunications Standards Institute (ETSI) (2020). *Intelligent Transport System (ITS); Vulnerable Road Users (VRU) awareness; Part 2: Functional Architecture and Requirements definition; Release 2 DTS/ITS-00186*. ETSI Technical Specification 103 166. URL: https://www.etsi.org/deliver/etsi_ts/103100_103199/103166/02.01.00_20/ts_103166v020100p.pdf.

Herbert, M., Andras Varadi, and L. Bokor (2020). "Modelling and Examination of Collective Perception Service for V2X Supported Autonomous Driving". In: *ICAI*.

Huang, Chung-Ming, Shih-Yang Lin, and Zhong-You Wu (2020). "The k-hop-limited V2V2I VANET data offloading using the Mobile Edge Computing (MEC) mechanism". In: *Vehicular Communications* 26, p. 100268. DOI: https://doi.org/10.1016/j.vehcom.2020.100268. URL: https://www.sciencedirect.com/science/article/pii/S2214209620300395.

Kassir, Saadallah et al. (2020). "Performance Analysis of RSU-based Multihomed Multilane Vehicular Networks". In: *ArXiv* abs/2002.06481.

Leroy, Jérémy et al. (2020). "Five key components-based risk indicators ontology for the modelling and identification of critical interaction between human driven and automated vehicles." In: *3rd IFAC Conference on Cyber-Physical Human-Systems (CPHS)*. Shanghai, China.

Ma, Yongfeng et al. (2020). "Predicting Traffic Conflicts for Expressway Diverging Areas Using Vehicle Trajectory Data". In: *Journal of Transportation Engineering, Part A: Systems* 146.3, p. 04020003. DOI: 10.1061/JTEPBS.0000320. eprint: https://ascelibrary.org/doi/pdf/10.1061/JTEPBS.0000320. URL: https://ascelibrary.org/doi/abs/10.1061/JTEPBS.0000320.

Mahajan, Vishal, Christos Katrakazas, and Constantinos Antoniou (2020). "Prediction of Lane-Changing Maneuvers with Automatic Labeling and Deep Learning". In: *Transportation Research Record* 2674.7, pp. 336–347. DOI: 10.1177/0361198120922210. eprint: https://doi.org/10.1177/0361198120922210. URL: https://doi.org/10.1177/0361198120922210.

Mattas, Konstantinos et al. (2020). "Fuzzy Surrogate Safety Metrics for real-time assessment of rear-end collision risk. A study based on empirical observations". In: *Accident Analysis Prevention* 148, p. 105794. DOI: https://doi.org/10.1016/j.aap.2020.105794. URL: https://www.sciencedirect.com/science/article/pii/S0001457520316146.

Md Muzahid, Abu Jafar, Syafiq Fauzi Kamarulzaman, and Md Abdur Rahim (2020). "Learning-Based Conceptual framework for Threat Assessment of Multiple Vehicle Collision in Autonomous Driving". In: *2020 Emerging Technology in Computing, Communication and Electronics (ETCCE)*, pp. 1–6. DOI: 10.1109/ETCCE51779.2020.9350869.

Monkhouse, Helen E., Ibrahim Habli, and John McDermid (2020). "An enhanced vehicle control model for assessing highly automated driving safety". In: *Reliability Engineering System Safety* 202, p. 107061. DOI: https://doi.org/10.1016/j.ress.2020.107061. URL: https://www.sciencedirect.com/science/article/pii/S0951832020305627.

Thandavarayan, Gokulnath, Miguel Sepulcre, and Javier Gozalvez (2020). "Generation of Cooperative Perception Messages for Connected and Automated Vehicles". In: *IEEE Transactions on Vehicular Technology* 69.12, pp. 16336–16341. DOI: 10.1109/TVT.2020.3036165.

UIT, Union internationale des télécommunications secteur des radiocommunications de (2020). "Normes relatives aux interfaces radioélectriques pour les communications bidirectionnelles de véhicule à véhicule et de véhicule à infrastructure pour les applications des systèmes de transport intelligents". In: URL: https://www.mwrf.com/

technologies/systems/article/21848325/the-battle-over-v2v-wireless-technologies.

Um, Jin-Yeong (2020). "Performance Evaluation according to RSU Range in Vehicle-to-Vehicle Communications". In.

Chang, Huigang and Nianwen Ning (2021). "An Intelligent Multimode Clustering Mechanism Using Driving Pattern Recognition in Cognitive Internet of Vehicles". In: *Sensors* 21.22. DOI: 10.3390/s21227588. URL: https://www.mdpi.com/1424-8220/21/22/7588.

Debnath, Arindam et al. (2021). "Fuzzy logic-based VANET routing method to increase the QoS by considering the dynamic nature of vehicles". In: *Computing* 103.7, pp. 1391–1415. DOI: 10.1007/s00607-020-00890-x. URL: https://doi.org/10.1007/s00607-020-00890-x.

Jeffs, James (2021). *Autonomous Cars, Robotaxis Sensors 2022-2042*. URL: https://www.idtechex.com/en/research-report/autonomous-cars-robotaxis-and-sensors-2022-2042/832.

Jeong, Jaehoon et al. (2021). "A comprehensive survey on vehicular networks for smart roads: A focus on IP-based approaches". In: *Vehicular Communications* 29, p. 100334. DOI: https://doi.org/10.1016/j.vehcom.2021.100334. URL: https://www.sciencedirect.com/science/article/pii/S2214209621000036.

Leroy, Jérémy et al. (2021). "Adapted Risk Indicator For Autonomous Driving System With Uncertainties and Multi-Dimensional Configurations Modeling". In: *2021 IEEE International Intelligent Transportation Systems Conference (ITSC)*, pp. 2034–2041. DOI: 10.1109/ITSC48978.2021.9564857.

Muzahid, Abu, Syafiq Fauzi, and Md Abdur Rahim (2021). "Learning-Based Conceptual framework for Threat Assessment of Multiple Vehicle Collision in Autonomous Driving". In: DOI: 10.1109/ETCCE51779.2020.9350869.

Pinnow, Jack et al. (2021). "A review of naturalistic driving study surrogates and surrogate indicator viability within the context of different road geometries". In: *Accident Analysis Prevention* 157, p. 106185. DOI: https://doi.org/10.1016/j.aap.2021.106185. URL: https://www.sciencedirect.com/science/article/pii/S0001457521002165.

Rana, Md. Masud and Kamal Hossain (2021). "Connected and Autonomous Vehicles and Infrastructures: A Literature Review". In: *International Journal of Pavement Research and Technology*. DOI: 10.1007/s42947-021-00130-1. URL: https://doi.org/10.1007/s42947-021-00130-1.

Saleem, Yasir, Nathalie Mitton, and Valeria Loscri (2021). "A QoS-Aware Hybrid V2I and V2V Data Offloading for Vehicular Networks". In: *2021 IEEE 94th Vehicular Tech-*

nology Conference (VTC2021-Fall), pp. 1–5. DOI: 10.1109/VTC2021-Fall52928.2021.9625261.

Shan, Mao et al. (2021). "Demonstrations of Cooperative Perception: Safety and Robustness in Connected and Automated Vehicle Operations". In: *Sensors* 21.1. DOI: 10.3390/s21010200. URL: https://www.mdpi.com/1424-8220/21/1/200.

Wang, Chen et al. (2021). "A review of surrogate safety measures and their applications in connected and automated vehicles safety modeling". In: *Accident Analysis Prevention* 157, p. 106157. DOI: https://doi.org/10.1016/j.aap.2021.106157. URL: https://www.sciencedirect.com/science/article/pii/S0001457521001883.

Belmekki, Sabrine, Dominique Gruyer, and Charles Tatkeu (2022). "Chain Branch Leaf-Gateway, a Strategy for Dynamic Clustering and Optimal Coverage of Communication for Automated Mobility". In: *2022 IEEE 2nd International Conference on Digital Twins and Parallel Intelligence (DTPI)*, pp. 1–5. DOI: 10.1109/DTPI55838.2022.9998893.

Maaloul, Sassi et al. (2022). "Performance Analysis of Existing ITS Technologies: Evaluation and Coexistence". In: *Sensors* 22.24. DOI: 10.3390/s22249570. URL: https://www.mdpi.com/1424-8220/22/24/9570.

Trabelsi, Rim et al. (2022). "Recent Advances in Vision-Based On-Road Behaviors Understanding: A Critical Survey". In: *Sensors* 22.7. DOI: 10.3390/s22072654. URL: https://www.mdpi.com/1424-8220/22/7/2654.

Westhofen, Lukas et al. (2022). "Criticality Metrics for Automated Driving: A Review and Suitability Analysis of the State of the Art". In: *Archives of Computational Methods in Engineering* 30.1, pp. 1–35. DOI: 10.1007/s11831-022-09788-7. URL: https://doi.org/10.1007%2Fs11831-022-09788-7.

Aimonen, Petteri (25 November 2011). *The diagram explains the basic steps of Kalman filtering: prediction and update*. URL: https://commons.wikimedia.org/wiki/File:Basic_concept_of_Kalman_filtering.svg.

Abstract

Automated vehicles are rapidly developing to create fully connected transportation systems, reducing collisions, traffic congestion, fuel consumption, and offering increased flexibility. This requires data related to obstacle detection and the environment. The objective of this thesis is to improve communication between connected vehicles for safer and more efficient traffic and to examine the adaptability and suitability of the Chain Branch Leaf (CBL) communication model in cooperative systems. We also developed a new version of the CBL-G model to improve coverage. We studied this communication architecture to improve service quality by using information from surrounding vehicles and explored multi-level perception to estimate the four (extended) collision risks including local, extended local, extended branch, and global. For our future research, we will study situations such as road intersections and highway exits and develop risk indicators that cover all key elements.

Keywords:

Cooperative Systems, Automated vehicles, Vehicle-to-Vehicle communications, IEEE 802.11p, Vehicle-to-Infrastructure communications, Clustering, Gateway, Extended Perception, Multi-level Collision Risk, extended collision risks, uncertainties, multidimensional configurations.

Résumé

Les véhicules automatisés se développent rapidement pour créer des systèmes de transport entièrement connectés, réduisant les collisions, les embouteillages, la consommation de carburant et offrant une flexibilité accrue. Cela nécessite des données relatives à la détection d'obstacles et l'environnement. L'objectif de cette thèse est d'améliorer la communication entre véhicules connectés pour une circulation plus sûre et efficace et d'examiner l'adaptabilité et l'aptitude du modèle de communication de la feuille de branche de chaîne (Chain Branch Leaf-CBL) dans les systèmes coopératifs. Nous avons également développé une nouvelle version du modèle CBL-G pour améliorer la couverture. Nous avons étudié cette architecture de communication afin d'améliorer la qualité de service en utilisant les informations des véhicules environnants et avons exploré la perception multi-niveau pour estimer les quatre risques de collision (local, local étendu, branche étendue et global). Pour nos futures recherches, nous étudierons des situations comme les intersections routières et les sorties d'autoroutes et élaborerons des indicateurs de risque qui couvrent tous les éléments clés.

Mots clés:

Systèmes coopératifs, véhicules automatisés, communications véhicule-à-véhicule, IEEE 802.11p, communications véhicule-à-infrastructure, clustering, passerelle, perception étendue, risque de collision multi-niveau, incertitudes, configurations multidimensionnelles.